THE ADSORPTION OF COLLOIDAL MATERIAL TO HIGHLY POROUS ION-EXCHANGE RESINS.

BY

MICHAEL ALLAN BOWLEY

B.Sc. (Eng) (University of Cape Town)

Submitted to the University of Cape Town in fulfilment of the requirements for the degree of Master of Science in Engineering.

April 1985

ABSTRACT

Adsorptive filtration using highly porous adsorbents offers an alternative technique to the conventional practices of flocculation, coagulation and filtration, for the removal of colloidal matter from water.

Adsorptive filtration of colloidal particles from liquid streams by highly porous ion-exchange resins has been investigated using Amberlite IRA 938 resin, a well characterised synthetic model colloidal particle (Primal E1743) and a comprehensive variation of the fluid dynamic and electrostatic parameters expected to affect colloid adsorption to charged porous adsorbents.

These investigations carried out using a batch system, a recycle reactor (resin column) with an infinite recycle ratio, showed:-

Adsorption of colloidal particles to Amberlite IRA 938 resin is restricted to the readily accessible outside surface of the resin, unless very long contact times are allowed. The rate of colloid adsorption to the outer regions of the resin is determined by the transport of the colloidal particles across the hydrodynamic boundary layer surrounding the resin bead. Transport across its outer regions is influenced by the colloid concentration gradient and Brownian diffusion while transport over its inner regions is determined by electrostatic forces. At very high superficial fluid velocities in the resin bed, when the hydrodynamic boundary layer becomes thin, surface reaction (physisorption) may be rate limiting. Adsorption to highly porous Amberlite IRA 938 resin is enhanced by its extended rough surface.

A simple empirical model has been developed which describes the special case of colloid adsorption to highly porous adsorbents, such as Amberlite IRA 938 resin. The model is based on three parameters namely: hydrodynamic boundary layer thickness, the distance over which electrostatic forces are effective and the surface reaction rate (physisorption rate).

ACKNOWLEDGEMENTS

The author wishes to thank the following people and organisations for their assistance during his research studies:

1) Mr. B.A. Hendry for his supervision, and ceaseless interest in the project.

2) The Council for Scientific and Industrial Research, Foundation for Research Development for their financial assistance and encouragement.

3) Rohm and Haas for supplying resin samples.

4) The Electronmicroscope Unit at UCT for the training and use of their electronmicroscopes.

5) The Zoology Department at UCT for the use of their Coulter Counter.

6) Wood Science department at the University of Stellenbosch for the use of their Zeta-meter.

7) Mr. K. Wheeler and Mr. A. Barker for their assistance in constructing apparatus for this project.

8) The Water Research Commission and South African Pulp and Paper Industry for supporting water research in the Department of Chemical Engineering at UCT.

9) The post-graduate students in the Department of Chemical Engineering, for their friendship and support.

To my parents.

CONTENTS

LIST OF TABLES

LIST OF FIGURES

LIST OF ELECTRON MICROSCOPE PHOTOGRAPHS

NOMENCLATURE

A - Hamaker's constant (erg)

a - radius of collector particle (m, cm*)

a_h - radius of colloidal particle (m, cm*)

B - defined by equation 18 in Chapter 2.

C_a - particle concentation in the bulk suspension (particles/m^3)

C_c - particle concentration at the collector surface (particles/m^3)

C_{so} - readily available area (outside area) of collector (m^2)

C_{si} - interior surface area of collector (m^2)

D - diffusion coefficient of particles (m^2/s)

e_i - charge of ionic species i (esu)

k - mass transfer rate constant (m/s)

k_B - Boltzmann constant (J/K, erg/K*)

k_f, k_d - film mass transfer rate constant (m/s)

k_i - defined by equation 8 in Chapter 2.

k_r - surface reaction rate constant (m/s)

n_i - concentration of ionic species i (ions/cm^3)

$N_{\ell o}$ - London group given by equation 19 in Chapter 2.

Pe - Peclet number

Q - aspect ratio, ratio of collector and paticle radii

$-r_a$ - rate of particle removal (particles/$s.m^3$)

R - roughness term (dimensionless)

Re - Reynolds number

S - collector surface area (m^2)

T - absolute temperature (K)

U - superficial fluid velocity in packed bed (m/s)

V - volume of suspension (m^3)

V_{max} - maximum interaction potential energy (erg)

V_{smin} - value of interaction potential energy at the secondary minimum (erg)

x - separation distance between collector and particle (cm)

* These units must be used when calculating London - van der Waals and electrical double layer potential energies.

Greek Letters

α - defined by eqation 1 in Chapter 4.

ε - bed porosity term (dimensionless)

γ - fraction of solid in the bed ie.$(1 - \varepsilon)$

β - bed void fraction (dimensionless)

δ, δ_d - diffusion film thickness (m)

δ_ϕ - distance over which interaction forces are active (m)

ξ - dielectric constant (dimensionless)

η - fluid viscosity (kg/ms)

κ - Debye-Huckel reciprocal length (cm^{-1})

ρ - fluid density (kg/m^3)

Φ - interaction potential energy (erg)

Φ_A - London - van der Waals potential energy (erg)

Φ_R - Double layer potential energy (erg)

Ψ_i - surface potential of surface i (esu)

CHAPTER 1

INTRODUCTION

Many industrial processes require ultra high purity water. Contaminants in the raw water supply include dissolved ions or molecules and suspended matter. The latter may be divided into a settleable fraction, and colloidal and sub-colloidal fractions. It is often found that conventional methods of treatment using flocculation, settling and filtration do not completely remove the colloid size fraction and the clarified water still contains significant amounts of residual colloidal matter.

For example colloidal silica remaining in boiler feed water may cause deposits on the boiler tubes and turbine blades causing over-heating and damage (1). Colloidal matter in water used in semi-conductor components manufacture in the electronics industry has deleterious effects on the finished products (1,2). In seawater desalination by reverse osmosis, colloidal particles in the seawater which have passed through conventional pretreatment plants, still cause fouling of the reverse osmosis membranes. Membrane fouling can add over 40% (3) to the operating cost of a reverse osmosis plant and often results in an otherwise attractive desalination process being uneconomical. Similar situations arise with other reverse osmosis feed solutions and also with other membrane processes such as ultrafiltration. In these cases colloidal particles are usually regarded as a specific class of foulant distinct from microbiological films, organics forming gelled layers and metal hydroxides (4). However, a little reflection shows that colloids are implicated in all of these.

Failure of conventional treatment systems in the complete removal of deleterious colloidal particles from liquid streams, is due to the wide variety of colloidal particles, variation of their properties and the stochastic nature of the removal mechanisms of coagulation, flocculation and entrapment in flocc and on filter media.

Adsorptive processes utilising porous solids appear to offer a more positive removal mechanism as the particles are attracted to, and held to, the adsorbent surface by strong attractive forces. Once inside a porous adsorbent the attached particle is tightly held and not subject to shear or other removal mechanisms as in the case of non-porous, smooth media such as sand particles.

The removal of micro-particles from liquid streams by adsorbents in a packed bed configuration is generally termed adsorptive filtration (5).

1.1 ADSORPTIVE FILTRATION

There are three mechanisms by which particles can be filtered from liquids:

i) Surface straining filtration (Figure 1.1a)
ii) Depth straining filtration (Figure 1.1b)
iii) Adsorptive filtration (Figure 1.1c & 1.1d)

Adsorptive filtration can be further subdivided:

i) Adsorption on a smooth collector surface (Figure 1.1c)
ii) Adsorption onto the surface and inside the pores of a highly porous collector (Figure 1.1d)

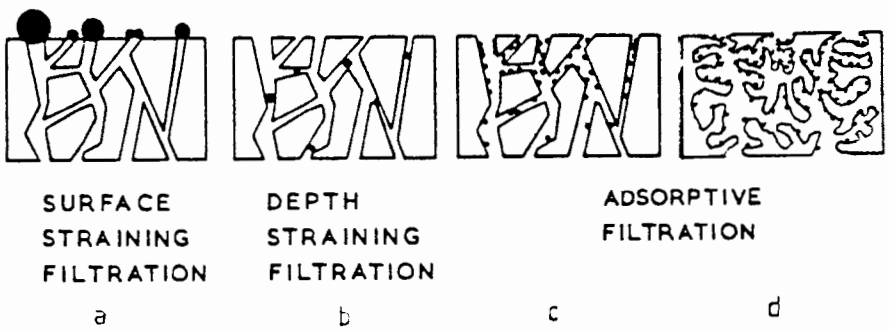

Figure 1.1 FILTRATION MECHANISMS

Colloids, generally defined as particles intermediate in size between true solutions and suspended matter(6,7,8), are too small to be removed by surface and depth straining (unless first

prevalence is expected to increase dramatically before the turn of the century.

DESALINATION PROCESSES

A number of different processes are presently available for seawater desalination. These processes can be divided into two groups based on the nature of energy input into the process, namely thermal processes and mechanical-electrical processes.

The thermal processes, multi-stage flash (MSF) and multiple effect evaporation (MEE) are commercially established forms of the distillation process whereby water vapour is evaporated from the saline water and pure water is obtained by condensing this vapour.

The mechanical-electrical processes are vapour compression evaporation (VCE), freezing and reverse osmosis (RO).

Vapour compression evaporation is another distillation process and is often termed mechanical compression evaporation, as the required energy is supplied by compression of steam produced from boiling brine in the unit. When the steam is compressed its temperature rises and the higher temperature is used to evaporate more water.

The freezing process relies on the fact that on cooling to its freezing point, a salt solution will deposit crystallites of pure water, which on separation from the mother liquor, washing and melting, yield good quality desalinated water.

Reverse osmosis desalination is based on the principle of natural osmosis, where pure water passes through a semi-permeable membrane from a dilute to a more concentrated salt solution. The technology uses semi-permeable membranes, through which water is forced in the reverse to the normal flow direction by an externally applied pressure. Thus the feed stream is split into a pure water stream (permeate) and a concentrate stream (brine) which contains most of the dissolved minerals, organics and

colloidal matter. The available driving force to effect the separation is the net difference in pressure between that applied and the osmotic pressure exerted by the fresh water. Seawater RO desalination plants are typically operated at pressures between 4 and 8 MPa.

Economic considerations

Many factors must be considered when evaluating desalination processes, these include the desalination duty required, plant availabilty and reliabilty, capital costs, and perhaps the most important, operating costs. A fairly recent analysis (610 of the role of energy in desalination of seawater indicated that the energy cost, as a percentage of the total desalination cost, varies from 27% for RO to about 65% for distillation processes (61). These figures clearly indicate the very substantial role that the cost of energy plays in the total cost of desalination and it is obvious that even comparatively small energy cost increases are reflected in increased desalination costs. This emphasises the importance of low energy systems.

REVERSE OSMOSIS DESALINATION OF SEAWATER

Reverse osmosis is the newest commercial process for desalting saline water. The first successful RO membranes were developed simultaneously at the Universities of Florida and California in the early 1960's. Since that time RO technology has progressed rapidly and is already the most frequently used desalination process for brackish water. The use of RO for seawater desalination is expected to follow the same trend.

The heart of the reverse osmosis technique is the semi-permeable membrane which determines both the salt rejection and flux of any RO system. The membranes most often used are cellulose acetate, polyamide, or thin film composite membranes.

A number of membrane configurations are available. The most popular are tubular, spiral wrapped and hollow fibre membranes.

Tubular membranes are cast on the inside of paper or fabric tubes and are usually supported by a suitably corrosion resistant perforated metal tube. Pressurised feed water is introduced into the end of a tube, and the product water permeates through the membrane and is collected on the outside. The reject or concentrate exits from the end of the tube. Tubular configurations are the least space efficient and have membrane surface area to volume ratios of approximately 100.

Spiral wrapped membranes consist of a number of rolled membrane envelopes housed in a pressure vessel. The membranes, in each envelope, are separated by a spacer, through which the permeate flows along the spiral to a central collection tube while the feed water flows axially across the membrane surfaces. A typical surface area to volume ratio for this configuration is 300.

Hollow fibre membranes, typically consist of fine hairlike extruded tubes of polyamide with outside diameters of 85 microns and capillary diameters of 42 microns. A skein of about a million of these fibres is folded back upon itself and the ends are encapsulated in a resin tube sheet. The bundle is contained in a cylindrical pressure vessel through which feed water flows; the product water passes through the walls of the fibres and flows out through the encapsulated ends. This configuration is extremely compact and has surface area to volume ratios of approximately 5000.

Reverse osmosis systems compared to other desalination processes are simple. They consist essentially of suitable high pressure pumps, cartridge filters to remove particulate matter from the feed, the membranes in their pressure vessels and the necessary piping, flow measurement devices and control valves to achieve the prescribed operating conditions.

It is apparent that with such a simple system the only real problems must be centered on the membranes. This is born out in practice and we find that fouling and membrane life are the main problem areas.

Reverse osmosis membrane fouling

Membrane fouling is an extremely complex phenomena for which there is no simple definition. Perhaps the most informative and broadly applicable definition is given by Eykamp (62);

> "Fouling is a condition in which a membrane undergoes plugging or coating by some element in the stream being treated, in such a way that its output or flux is reduced and in such a way that the foulant is not in dynamic equilibrium with the stream being ultrafiltrated. In other words, something has occurred that makes the micro-environment near the membrane a nonsteady state situation."

Fouling of a membrane is caused by one or a combination of the following factors, membrane scaling, metal oxide fouling, device plugging, biological fouling and colloidal fouling (4).

Membrane scaling is caused by the precipitation of salts dissolved in the seawater. As the brine stream is concentrated due to the loss of water during the RO process, the dissolved salts in the brine stream can exceed their solubility limits and can precipitate on the membrane surface. In seawater the major scalants are calcium carbonate and calcium sulphate. Carbonate scaling can be prevented by pH controll while calcium sulphate scaling can be prevented with the use of antiscalants such as sodium hexametaphosphate.

Metal oxide fouling occurs as a result of corrosion of metal pieces of equipment in the RO system. This problem can be reduced by the use of plastic and other corrosion resistant materials.

Device plugging is caused by particles too large (eg. larger than 1/5 minimum channel) to pass through the feed-brine passage which are trapped in the permeator. This problem is usually avoided by the use of cartridge filters in the feed line.

Biological fouling is caused by biological attack of the RO

membrane. Prevention of biological attack on the membrane is usually accomplished by regular cleaning with the use of chlorine or other disinfectants. This however, has a detrimental effect on some types of membranes (e.g. polyamide membranes) and consequently a chlorine absorption stage has to be included in the process to protect the membranes.

Colloidal fouling is caused by the entrapment of colloids, particles intermediate in size between true solutions and suspended matter, on the membrane surface. Colloidal fouling is thought to occur by the destabilisation of colloidal particles at the reverse osmosis membrane surface.

The membrane concentrates both dissolved solids and colloidal particulates on the one side of the membrane while passing pure water through to be collected on the other side. At steady state, solute does not accumulate on the membrane, so solute transport by diffusion away from the membrane surface must occur simultaneously with convective diffusion towards the membrane. For reverse diffusion to occur a concentration gradient, with a higher solute concentration at the membrane surface than in the bulk, must exist. This phenomena is termed concentration polarisation.

As colloidal particles approach the membrane surface and enter the boundary layer of higher salt concentration, their diffuse boundary layers shink, resulting in a decrease in repulsive forces and the potential energy barrier between the particles. This allows the colloidal particles to approach each other more closely so that London - van der Waals forces, which are strongly distance dependent, can coagulate the particles. The larger coagulated particles then deposit on the membrane surface causing the reverse osmosis system to produce less purified water (permeate).

A further two theories on the mechanism of reverse osmosis fouling by particulates have been postulated. The simpler to the two theories postulates that colloids having low mobilities, (colloids have diffusion coefficients 2 to 3 orders of magnitude lower than inorganic salts), retrodiffuse from the membrane

surface much more slowly than ionic species and so tend to build up in the boundary layer at the membrane surface.

The second theory presented by Green and Belfort (63) combines lateral migration theory, standard filtration theory and particle trajectory analysis, and suggests that fouling occurs when the membrane permeation velocity (J) exceeds the radially directed particle lift velocity (L).

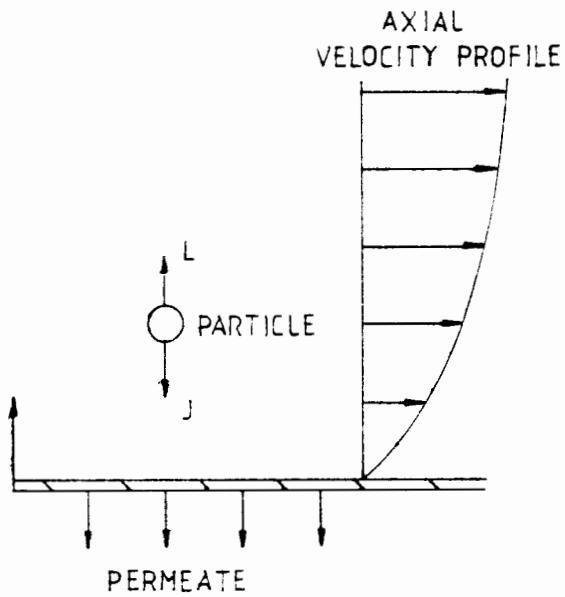

A schematic diagram of the forces on a particle flowing over a porous membrane.

This theory apparently presents the first quantitative model of colloidal fouling of reverse osmosis membranes, and predicts the minimum average axial velocity (Vc) required to prevent fouling, (no fouling when L> or =J). The critical velocity needed to sustain any given flux without fouling is given by

$$Vc \propto J^{\frac{1}{2}}$$

Pretreatment processes

The recognised technique for controlling colloidal fouling is pretreatment of the feed water to reduce the concentration of

these impurities. This is usually undertaken using a number of stages which include sedimentation, coagulation and filtration. This technique is however unreliable as most of the small colloidal particles, responsible for most of the colloidal fouling (20), pass through this process (6). The complex nature of the pretreatment required for seawater RO desalination is brought out by the typical pretreatment process described below.

A typical pretreatment plant for a multi-million liter per day reverse osmosis seawater desalination plant functions as follows. The feed, after passing through trash rakes and travelling screens, is chlorinated to kill micro-organisms and bacteria. The chlorinated feed is then treated with sulphuric acid to reduce its pH to 6.0 - 6.5, about 10ppm of a carbonate scale suppressent such as hexametaphosphate and a flocculating agent such as ferric chloride or aluminium sulphate are added at the clarifier. In most cases the treated water then flows through a series of filters. The first filter is typically, a sand filter, while the second is a polishing filter, usually a diatomaous earth or cartridge filter, that removes some the fine particles. Finally if the membrane is chlorine sensitive, the feed is treated with sodium bisulfite or activated carbon to remove any traces of remaining chlorine (64,65,66,67,68).

Membrane fouling can add over 40 % to the operating costs (excluding amortisation) of a seawater RO desalination plants (3). This is because the membranes are considered equipment consumables as they have a limited life, typically three years, as their pure water flux decreases due to fouling.

There is therefore strong motivation to investigate alternative processes or to simplify and improve existing pretreatment processes and so lengthen the life of the RO membranes and reduce operating costs of RO processes.

Current RO pretreatment processes using coagulation and filtration have been found to be expensive, complex and inadequate or unreliable in many situations. This is due to the variety of potential foulants, variation of their properties and the stochastic nature of the removal mechanisms of colloidal and

particulate foulants in these processes. Adsorptive processes utilising porous adorbents appear to offer a more positive removal mechanism and a simple reliable process. A preliminary study of the removal of particulates from seawater by adsorptive filtration using two macroporous basic anion exchanges, during 1982, proved extemely encouraging (see Appendix G).

This stimulated interest in the adsorption of colloidal materials to highly porous adsorbents and led to the fundamental investigation into the fluid dynamic and electrostatic factors which affect colloid adsorption to highly porous ion-exchange resin, dealt with in this thesis.

CURRENT USES OF ION-EXCHANGE RESINS IN ADSORPTIVE PROCESSES

Research has show that highly macro-porous resins can be used effectively for removing non-reactive silica, high molecular weight humic matter, radioactive "crud", and also for rendering water sterile and pyrogen free (13,15,16).

Non-reactive silica

The use of Amberlite IRA 938 resin to remove non-reactive colloidal silica from water in the electronics industry is receiving growing acceptance.

Non-reactive silica occurs as a colloid in association with organic material and various metal cations. This complex, shown in the figure below, is often referred to as the Universal Colloid and typically contains silica, iron(III) oxide, aluminium oxide, magnesium oxide, calcium oxide and naturally occuring organic acids (2).

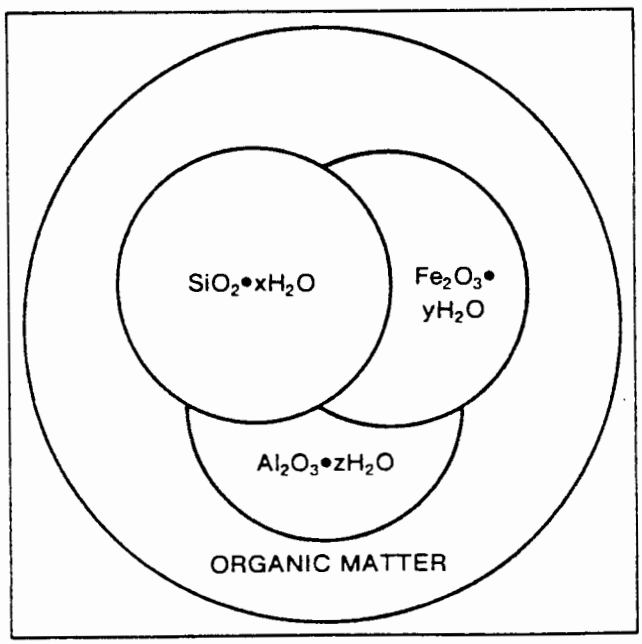

The universal colloid.

Colloidal silica is removed from Manchester Corporation Water Works water by Amberlite IRA 938 resin (16). On this plant it was found that 110 liters of wet settled resin produced over 180 000 liters of specification water, from 0.3 ppm silica feed water per regeneration (70% of the non-reactive silica is retained on a 0.1 micron membrane filter, but passes through a 1.2 micron membrane filter). Typical silica loadings on the resin were 1.2 - 1.9 grams silica per liter of wet settled resin.

The resin was initially regenerated using warm dilute hydrochloric acid followed by warm sodium hydroxide, however this did not remove the organic contaminants, thus the resin was further treated with a warm solution of 10% w/w sodium chloride and 5% w/w sodium hydroxide (16).

Bacteria, viruses and pyrogenic substances.

The use of ion-exchange resins for the removal and/or concentration of bacteria, viruses and pyrogenic substances from blood and saline solutions started in the 1950's (69). It was found that virus particles could be removed from both plasma and tissue extracts and in some instances the virus particles could be eluted from the resins without loss in activity (70). Further it does appear that viruses are primarily adsorbed by anion exchange resins and that they desorb using various electrolyte buffers.

A recent study (71) of the applicability of ion-exchange resins to the treatment of waste streams containing high molecular weight organics and viruses, showed that weak base resins have a significantly superior sorption capacity to traditional adsorbents such as activated carbon. Two model species were studied; bovine serum albumin (molecular weight 69000) as the model organic molecule and bacterial virus MS2 (diameter 0.025 microns) as the model virus.

Continuous flow studies were conducted with the weak anion resin Duolite A-7 in columns 19.8 cm in length and 1.5 cm in diameter and at flow rates of approximately 11.5 BV/hr. Column experiments

showed that Duolite A-7 resin has a breakthrough capacity of approximately $2*10^{-2}$ g/g for bovine serum albumin and that more than 90% of the sorbed protein can be obtained by caustic regeneration.

Column studies with the MS2 bacterial virus, fed at a concentration of 10^9/ml, indicated that virus removal is greater than 99% for the first 30 BV and then only decreases to 95% removal after a further 23 BV.

Further interesting points which emerged from this study were that resin capacity is strongly dependent on the ionic strength and pH of the bulk solution. The highest resin capacities were found to be at low ionic strength and neutral pH values.

In a recent article entitled "Removal of Bacteria Water by adhesion to Cross-Linked Poly(Vinylpyridinium Halide)" (72), column studies showed that 97 - 100% of viable cells could be eliminated from suspensions of bacteria (10^5 - 10^8 cells per ml) when the flow rate was 0,8 to 1,4 bed volumes per hour. Mechanistic studies demonstrated that the resin irreversibly captured the bacteria alive during the treatment.

Amberlite IRA 900 resin compared poorly with the above resin, adsorbing bacteria 3 to 10 times more slowly than the cross-linked poly(vinylpyridinium halide) resin. Unfortunately Amberlite IRA 938 resin was not used during these experiments, however it is expected to be more effective than Amberlite IRA 900 (72).

Amberlite IRA 938 resin has been used to prepare sterile and biologically pure water (69). In this investigation the effectiveness of Amberlite IRA 938 resin in the removal of pyrogenic substances was tested (pyrogens are macro-molecules of the order 10^6 molecular weight). Column studies showed that 0.2 Kg of mixed Amberlite 200 and Amberlite IRA 938 ion exchange resins produced at least 100 liters of sterile water from contaminated feed water (10 ng/cm^3 of international reference pyrogens) at flow rates of 50 liters per hour.

A P P E N D I X G

THE DETECTION AND CHARACTERIZATION OF COLLOIDAL MATTER INVOLVED IN SEAWATER REVERSE OSMOSIS MEMBRANE FOULING.
(Progress Report 10th June 1983.)

OBJECTIVES OF RESEARCH

The short term objective of this research involved the detection and characterisation of colloidal matter involved in seawater reverse osmosis membrane fouling. The ultimate long term objective is, however, to develop an efficient pretreatment process for seawater reverse osmosis desalination based on adsorptive processes. This would replace currently used coagulation/filtration processes which have been found to be inadequate or unreliable in some situations.

The short term objective is the development of a convenient colloidal particle analysis technique which gives both particle sizes and particle size distributions.

Once the short term objective has been achieved, the particle analysis technique will be used to measure and compare the removal of particulates from seawater by various macroreticular ion-exchange resins and related adsorbents, with conventional pretreatment processes.

The removal of particulates from seawater using two macroreticular strongly basic anion exchangers was studied during 1982. The results were extremely encouraging.

TABLE OF CONTENTS

INTRODUCTION

Desalination of seawater by reverse osmosis is becoming an increasingly attractive means of producing fresh water. The reverse osmosis process has the inherent problem of the semi-permeable membranes, housed in a sealed pressure vessel, being easily fouled by a variety of impurities. This calls for an effective pretreatment of seawater to remove these impurities prior to desalination by reverse osmosis.

One of the main problems in current pretreatment processes of coagulation and filtration, is the incomplete removal of colloidal matter which may be either organic or inorganic. It was therefore decided to develop a convenient colloidal particle analysis technique for seawater. After a considerable literature survey, the approach decided upon was a combination of two currently used particle size analysis and identification techniques : gravimetric size distribution analysis using membrane filters and electron microscopy. It is hoped should time permit to extend the above analysis and use macroreticular resins to perform a classification of colloidal matter into hydrophobic and hydrophibic groups and subsequently into cationic, anionic and neutral subgroups.

The use of a gravimetric analysis technique using membrane filters was studied in a final year student project in the Department of Chemical Engineering during 1981 and many of the problems of accuracy and sensitivity associated with this technique have been overcome. Thus optimum techniques for removing extractables present in membrane filters, drying and weighing the filters were studied.

Gravimetric analysis can be undertaken in two ways, various pore size filters can be used in series or parallel. Generally, however, the series technique is favoured as large particles can often mask the mass of smaller particles, if trapped on the same membrane.

Feed is passed through a series of preweighed filters, and after rinsing

and drying the mass of particles trapped on a particular filter is found. Thus the process is analogous to a screen analysis. The membrane pore sizes to be used in the preliminary investigation are as follows: 8,0μ to remove all macro particles, followed by 1,2μ, 0,45μ, 0,10μ and 0,025μ (each of these membranes is a factor of four smaller than the previous pore size).

After gravimetric analysis the membrane filters are studied using the electron-microscope, in this way the number and nature of the particles in each size range can be determined.

Once the above techniques have been developed to the desired degree of proficiency, the emphasis of the research will shift to monitoring the colloidal quality of seawater and evaluating the performance of ion-exchange resins as a pretreatment method to reduce fouling of reverse osmosis membranes.

During 1982 the removal of particulates from seawater by two macroreticular strongly basic anion exchangers was studied. Results showed that Amberlite IRA 904 is virtually incapable of reducing the Silt Density Index (SDI-index which the reverse osmosis industry was to evaluate the fouling nature of a water, see discussion for details of test) of the seawater, while the Amberlite IRA 938 resin reduced the SDI consistently to less than 70%. Specifications for different membrane types vary from a SDI of 45% to 65%.

Electron-microscope studies of the Amberlite IRA 938 resin beads showed that colloidal particles of less than 1μ seem to be adsorbed onto the resin surface. The pores of this resin consist of ± 70000 Å spaces between microspheres created during the manufacture of the resins, the particulates were adsorbed onto the surface of these internal microspheres.

Thus it would be valuable to evaluate each resin performance both with

the standard SDI test and a gravimetric analysis with its complimentary electron microscopy. In this manner the size and nature of the colloidal material removed by the resin may be determined.

This information on resin performance, will help in resin selection and the attainment of the long term objective of the research, the establishing of an ion-exchange pretreatment system for weawater desalination by reverse osmosis.

LITERATURE SURVEY

Colloidal particles are typically in the size range 0,001μ to 10μ (2). However, certain references (1, 3) consider colloids to lie between 0,001μ and 1μ. In this study, particles in the first mentioned size range will be referred to as colloidal. The larger particles are expected to be removed easily by filtration effects, while those in the quoted range, it is hoped, can be removed by macroreticular ion-exchange resins or related adsorbents.

Colloidal particle size distribution analysis techniques

Sedimentation as a technique for determining size distribution of particulates has been used by numerous researchers. However, only recently have the extremely long sedimentation times, due to colloids being retarded from settling by Brownian motion (particles of less than 10μ will settle at a rate of less than 10^{-4}m/s) (2), been overcome to some extent. Krischkes and Gast (4) refined sedimentation techniques and named this technique "Automatic Particle Size Analysis by Manometric Measurement under Gravity". With this method they can determine particle sizes down to 0,5μ with a 24 hour experiment. This figure is comparable with figures given by other researchers which quote minimum determinable particle sizes of 0,5μ (5), 0,4μ (6) and 0,3μ (7).

The intensity of light scattering is also routinely used for particle size analysis (i.e. turbidimetry and nephelometry). Both of the above methods need calibration against a standard ; turbidimetry measures the degree of decrease of the intensity of the incident light, nephelometry measures the degree of scattering of the incident light.

Turbidimeters are subject to the following inherent problem, in that a small number of large particles can give the same turbidity as a large number of small particles and thus particle size is not easily determinable.

Nephelometers can give particle size measurements since particle size affects

the angle at which the incident light is scattered. Typically nephelometers operate over a particle size range from 0,001µ to 10µ (8).

More recently nephelometry has been refined into what is termed "Quasielastic light Scattering". This technique allows extremely rapid measurement and has a relatively wide particle size range, 0,005µ to 2µ (9).

Particle counting is another recognised technique for determining size distributions. Particle counting can be undertaken in two ways i.e. electron-microscopy or the use of a particle counting instrument such as a "Coulter Counter". Beard and Tanka (10) who studied the use of particle counters stated that particle counters are extremely useful tools in the quantification and size distribution analysis of suspended matter. A typical particle size range of a "Coulter Counter" is 0,4µ to 800µ, "Nano-Sizers" typically cover 0,04µ to 3µ (these particle counters are currently availbale form Coulter Electronics South Africa (Pty) Ltd.).

Electron-microscope studies are undertaken in two ways scanning electron microscopy (SEM) and transmission electron microscopy (TEM). Researchers using these methods usually trap colloids on a suitable membrane filter and then count the number of colloids per given area. This type of study collects all colloids larger than the membrane filter pore size and gives little information on the size distribution of the colloids. Electron-microscopy is generally used over the size range 0,002µ to 0,15µ (11).

Light microscopes are also occasionally used, however, it is difficult to distinguish between particles whose size is less than 3µ (12). ASTM (American Standard Test Methods) has a general technique for counting and sizing particulate contanimants applicable to a variety of fluids, typically 5µ to 100µ, using a variable magnification light microscope (13).

Membrane filtration is a technique which is often used in conjunction with microscope studies. Colloidal particles are trapped on varying sizes of membrane filters and then counted using the ASTM technique (13). ASTM

also has a specialised technique for particulate contamination analysis in aerospace fluids using membrane filters (14), which is expected to be applicable to a variety of fluids. However, no information is available on its applications.

Membrane filtration is also used in gravimetric analyses. This method entails using membrane filters as sieves in series or parallel. Typically feed is passed through a series of preweighed filters and after drying the mass of the colloidal material trapped on the particular filter is found (15, 16).

The choice membrane filter and the volume of feed to be filtered has been found to be important in size separation of marine particles. Sheldon (23) found that the average minimum sizes of particles retained by metal membranes (Silas Flotronics) and perforated polycarbonate membranes (General Electric Nuclepore) were similar to the stated pore sizes when relatively small seawater samples with moderate concentrations of particles were filtered. However, cellulose ester membranes and Glass-fibre filters retained particles much smaller than the stated pore size even with small samples with low particle concentrations.

Danielsson (17) concluded that membrane filters are generally unsuitable for the separation of suspended matter as effective pore size is influenced by the amount of particles on the membrane surface due to the formation of a filtration cake.

Field-Flow Fractionation (FFF) is becoming increasingly popular as a size distribution analysis technique. FFF separations take place in an open flow channel over which a field is applied perpendicular to the flow. FFF may be broken down into 5 subtechniques according to the applied field, namely sedimentation FFF, electrical FFF, thermal FFF, flow FFF and steric FFF. The advantages of this method include flexibiltiy due to the variety of fields available and high resolution. Separation of macromolecules, colloids and particulate species over an effective molecular weight range

10^3 to 10^{18} is typical (18, 19).

The concentration of impurities by progressive freezing is exceedingly useful ; however, it is most often used in conjunction with size distribution analysis technique. The use of freezing is based on the fact that when ice is crystallised from an aqueous solution or suspension, the crystal is built up by more pure water, leaving the impurities in the remaining liquid (20). Ullman (21) noted that freeze concentration applies equally well whether the particle be Brownian or non-Brownian in size. Halde's (20) results showed that the coarser the particles the more easily they can be separated.

Thus by varying freezing rates one can remove varying sizes of particles (i.e. fast freezing only large particles are separated, small particles remain in liquid matrix, remove large particles, melt the ice and freeze at slower rate, slightly smaller particles will be separated etc.).

DISCUSSION

This section of the report will discuss the development of the gravimetric analysis and define the Silt Density Index test.

The Gravimetric Analysis

The membranes selected for the gravimetric analysis were millipore MF-type membrane filters. These filters are composed of cellulose acetate and cellulose nitrate and are recommended for all analytical applications (21). (At the time Millipore MF-type membrane filters were chosen, the article by Sheldon (23), on particle retensions on various membrane filters, had not yet been uncovered. However, most of the experience obtained with Millipore filters is directly applicable to Nucleopore membranes ; the membranes to be used in preference of Millipore membranes).

MF-Type filter materials is quality control tested for bubble point (± 10% to the rated pore size), porosity (70-80% void volume depending on pore size), extractables content and thickness (135µ at ± 10%). However, two of the above specifications have been found to be erroneous. Sheldon (23) found that the effective pore sizes were substantially lower than those quoted by the manufacturer, effective pore sizes found by Sheldon are shown in the following table. Further, it has been found that extractables exceeded the claimed specifications in the smaller pore size membranes. Care in their use is therefore necessary.

The following table shows the important characteristics of MF-type filters over the relevant pore size range (22).

The first problem encountered with the gravimetric analysis technique is that of extractables in the membranes. This was illustrated by the research done during 1981. Filtering 250ml of tap water through a 0,05µ filter, decreased the overall dried weight of the filter by 0,1mg (0,2% of the membrane mass), while filtering 400ml and 1500ml of tap water increased the dried weights by 0,1mg and 0,6mg respectively.

Pore Size (µ)	Pore size variation (µ)	Medium Pore size (µ) (Sheldon)	Porosity %	Extractables mon %
8,0	± 1,4	0,88	84	6,0
5,0	± 1,2	0,77	84	6,0
3,0	± 0,9	0,65	83	6,0
1,2	± 0,3	0,55	82	5,0
0,8	± 0,05	0,55	82	4,0
0,65	± 0,03	-	81	3,0
0,45	± 0,04	0,45	79	2,5
0,30	± 0,02	-	77	2,0
0,22	± 0,02	-	75	2,0
0,10	± 0,008	-	74	1,5
0,05	± 0,003	-	72	1,5
0,025	± 0,002	-	70	1,5

After many trials during 1981, the method established for removing the extractables is as follows :

1) Wash/soak the membrane in 50ml of clean water (e.g. reverse osmosis or ultrafilter permeate) at 60°C for 30 minutes.
2) Filter 200ml of clean water through the membrane filter (water at 60°C).
3) Dry the membrane at 80°C for 1 hour (supported on glass beads).

As the temperature of the water in the washing and filtering steps of the above process appears to have a marked influence on the rate at which the extractables are removed (requires ± 100ml at 100°C, ± 200ml at 60°C and ± 500ml at 20°C) the temperature of the water used has been raised to 70°C (maximum recommended temperature 75°C).

A further safeguard against errors due to extractables has been included in the analysis technique. Two identical filters are placed in the filtration apparatus. The samples pass through both filters, but all contaminants are retained on the upper filter. Thus the difference in dried weights between the two filters should be due to contaminant material.

A problem which was experienced in 1981 and has been reported by many other researchers (17, 23), is the problem of cake or gel filtration. Gel filtration caused particles smaller than the nominal pore size to be trapped on the membrane. This problem can be reduced by the use of a stirred cell which ensures that there is a high tangential shear at the membrane surface. This prevents the deposition and settling of colloids on the surface of the membrane, maintaining them in suspension in the liquid above the filter surface.

This has been achieved by designing a special stirred filtration cell, (Figure 1) which has a magnetic stirrer which is suspended ± 1mm above the membrane surface.

The problem of gel filtration and the reduction of effective pore size of filters, will be further reduced once Nucleopore membrane filters are used. Sheldon (23) claims that Nucleopore membrane filters, filter to the point of overloading without changing their effective pore size, unlike Millipore and Flotronics membrane filters.

Another problem encountered when applying gravimetric size analysis techniques to seawater is the low and variable concentration of colloids in seawater. This is shown by the following results obtained at Swakopmund, South West Africa.

Raw seawater collected from the surf-zone.

Particle size (μ)	Average concentration (mg/ℓ)	Concentration Range (mg/ℓ)
≧ 8μ	26,9	111,0 - 8,4
≧ 8μ ≧ 1,2μ	6,1	14,9 - 1,0
≧ 1,2μ ≧ 0,45μ	8,1	20,0 - 1,2
≧ 0,45μ ≧ 0,10μ	4,1	16,3 - 1,0

(These results were obtianed using Millipore membrane filters and therefore could be misleading. The concentrations of the larger colloids could be overstated, while the concentrations of the smaller colloids

are likely to be understated.)

The low concentration of colloids calls for large volumes of water to be filtered if errors are to be kept to a minimum. The balance available is accurate to 0,1mg, therefore to get a maximum error of 5% a minimum mass of 2mg must be trapped on each membrane filter. This calls for sample volumes up to 5ℓ. The volume of the stirred cell is 100ml. The additional storage capacity is provided by a dispensing pressure vessel, with a volume of 5ℓ. A regulated clean air pressure line is connected to the vessel and the water is pushed through a tube to the filtration cell.

The air which pressurises the reservoir is derived from the laboratory supply and is cleaned by a dust separator, a mist eliminator and finally be a membrane filter (0,025µ), thus all contaminants in this stream are eliminated. The air pressure to the reservoir is also regulated to the desired pressure and thus the filtration rate in the filtration cell can be varied as required. The filtrate is stored in a sealed vessel for repetition with a filter of smaller pore size.

The final problem encountered was the removal of salt solution trapped in the membranes during the seawater filtration. It appears that this problem can be overcome by filtering approximately 150ml of clean water, (e.g. reverse osmosis or ultrafilter permeate) through the membrane filter.

The analysis technique as it is at present is analogous to a screen analysis. It involves passing seawater through a series of prepared and preweighed membrane filters and after drying the mass of particles trapped on each filter is found. The filters are then studied under the electron microscope, in order to determine the number and nature of the colloids in each size range.

A summary of the technique applicable to Millipore membrane filters is as follows :

1. Wash/soak the membrane filters in 50ml of pure water at 70°C for 30 min.
2. Filter 200ml of pure water at 70°C.
3. Dry the membrane filters at 80°C for 1hr, support on glass beads (6mm ∅).
4. Weigh the membrane filters immediately after drying.
5. Wet the filters with pure water by putting them into a pure water water-bath.
6. Place two membrane filters, of the same pore size, on top of one another on the stainless steel support plate in the filtration cell and assemble cell.
7. Put 5ℓ seawater sample in cleaned pressure vessel.
8. Connect piping from reservoir to filtration cell.
9. Set pressure regulator to the required pressure.
10. Open bleed screw on filtration cell.
11. Switch on pressure.
12. Shut bleed screw once the filtration cell is 4/5 full of water.
13. Switch on magnetic stirrer to the required speed.
14. Collect filtrate in the filtrate reservoir.
15. Once 5ℓ has been filtered, switch off pressure and depressurise Amicon pressure vessel and add pure water to wash salt out of membranes.
16. Go back to steps 10 to 13.
17. Discard filtrate.
18. Switch off pressure and depressurise vessel.
19. Dismantle filtration cell.
20. Remove membrane filters carefully and dry on beads as support for 1 hour at 80°C.
21. Weigh the membrane filter.
22. Store membrane in sealed petri-dish for later examination under the electron-microscope.
23. Repeat process for next size membrane filter, putting the filtrate in the dispensing pressure vessel.

Silt Density Index

The membrane industry has adapted a test called the Silt Density Index to evaluate the degree of potential colloidal fouling a water will inflict on a reverse osmosis membrane.

To determine a Silt Density Index, feed water is passed through a 0,45µ filter under a controlled pressure of 30psig (210 KPa). One measures the time to collect the first 500ml of filtrate and then after a further 5,10 or 15 minutes one again measures the time to collect a further 500ml.

The Silt Density Index is then calculated as follows (24) :

$$SDI = \frac{P_{30}}{T} = \frac{(1 - \frac{t_i}{t_f})}{} \times 100$$

where SDI = Silt Density Index

P_{30} = % pluggage at 30 psig feed pressure

T = total test time in minutes

t_i = initial time required to obtain sample

t_f = time required to obtain final sample

Various problems with this test have been described by different workers. Scheppers and Verdouw (24) point out that no linear relationship exists between the index and the concentration of colloidal and suspended matter. Reed and Belfort(25) identified the problem of the SDI test not modelling tangentral (shear) flow across the membrane surface.

The major problem perceived by this author is the fact that particles smaller than 0,45µ can significantly foul reverse osmosis membranes, and thus the test does not give a good indication of a waters potential fouling ability.

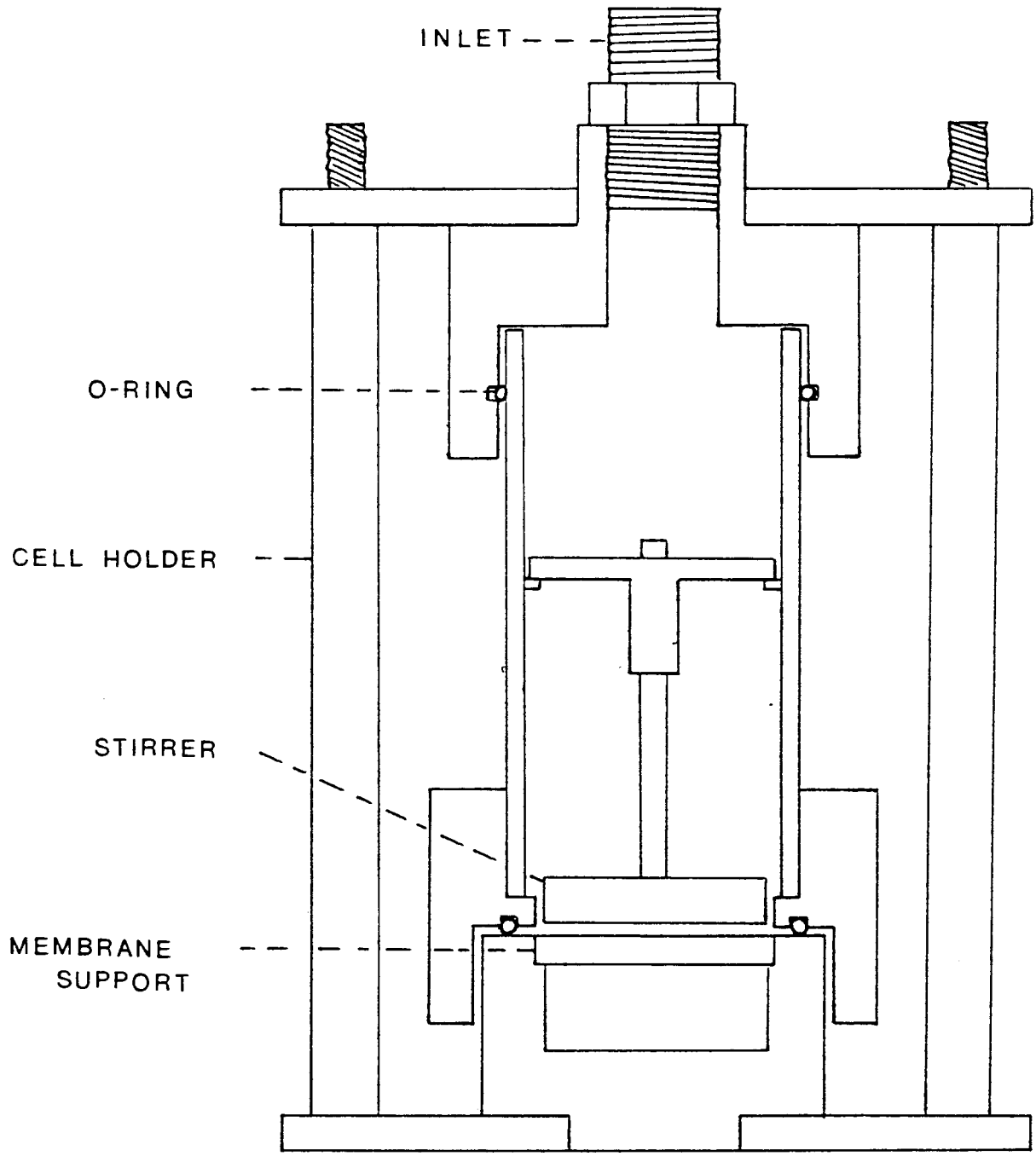

STIRRED CELL

REFERENCES

1. Riddick, T.M., "Zeta Potential and its Application to Different Waters". Jour. Amer. Water Works Assoc., 53, 1007 (1961)

2. Stumm, W., "Chemical Interaction in particle separation". Environmental Science & Technology, 11, 1066 (1977)

3. Morris, J.C. and McKay, G., "Principles of Colloidal Behaviour and Application to Water Estimation". Prac. Budolfs Research Conference, New Brunswick, N.Z. (1960)

4. Krischken, P. and Gost, T., "Automatic Particle Size Analysis by Manometric Measurement under Gravity". Gen. Chem. Eng., 3, 372 (1980)

5. Dayan, N. and Gallily, I.J., Applied Meteorol., 13, 78 (1974)

6. Dupack, A. and Vaughan, O.H., Applied Opt., 17, 374 (1978)

7. Stahloffer, W., Orbruster, L., Gekhort, T. and Grein, E., Atmos. Environ., 9, 851 (1975)

8. Beyer, G.L., "Turbidmetry and Hephelometry" in E.C.T. 1st ed., Vol. 14, pp. 373-380

9. McConnell, M.L., "Particle Size Determination by Quasielastic Light Scattering", Analytical Chemistry, 53, 1007 (1981)

10. Beard II, J.D. and Tanaka, T.S., "A Comparison of particle Counting and Nephelometry", Jour. Amer. Water Works Assn., October (1977), pp. 533

11. Eversole, J.D., Broida, H.P., Phys. Rev. B., 15, 1644 (1977)

12. Gathman, S.G., Jour. Appl. Meteorol., 14, 1293 (1975)

13. American National Standard, "Microscopical sizing and counting particles from aerospace fluids on membrane filters", ASTM F312-69 (1976)

14. American National Standard, "Processing aerospace liquid samples for particulate contamination analysis using membrane filters", ASTM F311-78

15. Benedict, A., "Development of a technique for gravimetric size analysis of colloidal particles in water and waste water, using Millipore membrane filters", Department of Chemical Engineering, University of Cape Town, (1981) (Student Project Report)

16. "Gravimetric Analysis", Millipore Bulletin EU 004, (1978)

17. Danielsson, L.G., "On the use of filters for distinguising between dissolved and particulate fractions in natural waters", Water Research, 16, 179, (1982)

18. Giddings, J.C., Graff, K.A. Caldwell, K.D. and Myers, M.N., "Field-Flow fractionation ; promising approach for the separation and characterisation of macromolecules", Department of Chemistry, University of Utah Salt Lake City, Utah 84112

19. Giddings, J.C., Myers, M.N., Caldwell, K.D. and Fisher, S.R., "Analysis of Biological Macromolecules and Particles by Field-Flow Fractionation". Methods of Biochemical Analysis, 26, 79

20. Halde, R., "Concentration of impurities by progressive freezing". Water Research, 14, 575 (1980)

21. Millipore Laboratory Products Catalogue, Millipore Corp. pp. 30 (1982)

22. Millipore Laboratory Products Catalogue, Millipore Corp. pp. 36 (1982)

23. Sheldon, R.W., "Size Separation of Marine Seston by Membrane and Glass-Fibre Filters". Limnology and Oceanography, 17, 494 (1972)

24. Schippers, J.C. and Verdouw, J., "The Modified Fouling Index, a method of determining the fouling characteristics of water", Desalination, 32, 137 (1980)

25. Reed, R.H. and Belford, G., "Characterisation of fouling potential for pressure-driven membrane processes : A New Simulated Flow Cell", Wat. Sci. Tech., 14, 499, (1982)

Test 2

Resin size - 600-425 microns

Resin volume - 40 ml (free settled volume)

35.4 ml (tapped volume)

NaOH concentration - 1.00 N

Volume of NaOH added (ml)	pH
1.2	4.47
3.4	4.48
5.2	4.49
7.2	4.57
8.2	4.62
9.2	4.71
10.2	4.80
11.2	4.98
11.7	5.27
11.9	6.10
12.1	9.42
12.8	11.61
15.2	12.41

$$\text{Capacity of the resin} = \frac{\text{NaOH (ml)} * \text{NaOH (N)}}{\text{resin (ml - fsv)}}$$

$$= \frac{11.95 * 1.00}{40}$$

$$= 0.30 \text{ meq/ml of resin}$$

CALCULATION OF INTERACTION POTENTIAL ENERGIES

The total interaction potential energy between a particle and collector, as a function of separating distance in an ionic medium is the sum of the London - van der Waals potential and the electrical double layer potentials. The formulae and calculation procedures used are identical to those in references 39 and 41.

The London - van der Waals potential is given by;

$$\Phi_A(x) = \frac{A_{132}}{6}\left[\ln\frac{(x+2a_h)}{x} - \frac{2a_h(x+a_h)}{x(x+2a_h)}\right]$$

where a_h is the particle radius (cm)

x the separation distance (cm)

and A_{123} the Hamakers constant for the system.

where A_{11}, A_{22} and A_{33} are the individual Hamaker constants for the collector, particle and medium.

The electrical double layer potential can be calculated using the linearised solution of the Poisson - Boltzman equation,

$$\Phi(x) = \pm\frac{\xi a_h}{4}\left[(\Psi_1+\Psi_2)^2\ln(1 \pm e^{-\kappa x}) + (\Psi_1-\Psi_2)^2\ln(1 \mp e^{-\kappa x})\right]$$

where ξ is the dielectric constant of the medium

Ψ_1 and Ψ_2 are the surface potentials of the particle, collector (esu)

κ is the Debye - Huckel reciprocal length and is given by;

$$\kappa = \sqrt{\frac{4\pi}{\xi k_B T}\sum_i n_i e_i^2}$$

where n_i is the number of ion of species i per unit volume

e_i is the charge on the species i

k_B is the Boltzman constant

and T the absolute temperature.

Taking the Amberlite IRA 938 - Primal E1743 system at pH of 7 as an example,

Zeta potential of resin	=	77.4 mv
Zeta potential of Primal E1743	=	-37.9 mv
Radius of Primal E1743 particles	=	$0.275 * 10^{-4}$ cm
Ionic strength of the medium	=	$3 * 10^{-5}$ M **
Dielectric costant of medium	=	80.1 at 20° C (ref. 57)
Hamakers constant for the resin	=	$6.4 * 10^{-13}$ erg
Hamakers constant for the particle	=	$6.4 * 10^{-13}$ erg
Hamakers constant of the medium	=	$4.38 * 10^{-13}$ erg

Hamakers constants for the system were taken Visser (56). The values for the ion-exchange resin and Primal E1743 spheres were average values for polymers/resins. The Hamaker constant for most polymers fell into the range 6 to $8 * 10^{-13}$.

** This figure was assumed for all experiments conducted at neutral pH and is based on conductivity measurements of the water and suspensions used in the experiments.

The following are calculated total interaction potential energies for the above system at various separation distances;

Distance (cm)	Total Interaction potential energy (erg)	Total Interaction Potential energy (Φ/k_BT)
$1 * 10^{-8}$	$- 5.171 * 10^{-10}$	- 12570
$1 * 10^{-7}$	$- 3.227 * 10^{-10}$	- 7841
$5 * 10^{-7}$	$- 1.943 * 10^{-10}$	- 4721
$1 * 10^{-7}$	$- 1.417 * 10^{-10}$	- 3444
$5 * 10^{-6}$	$- 3.970 * 10^{-11}$	- 965
$1 * 10^{-6}$	$- 1.352 * 10^{-11}$	- 329
$5 * 10^{-5}$	$- 9.946 * 10^{-15}$	- 0.240
$1 * 10^{-4}$	$-4.039 * 10^{-17}$	-0.001

CALCULATION OF ZETA POTENTIALS

1 Apparatus

The zeta potential of the particles was measured using a zeta-meter. A zeta-meter consists of a stereoscopic microscope with occular micrometer: 15x WF eye pieces; 2, 4, 6 and 8x (adjusted manification) objectives; and a special stage. An illuminator, producing a thin beam of intense blue-white light with heat absorbing filter is used; a d.c. power supply continuously variable from 0 to 500 volts; a clear plastic electrophoresis cell equipped with platinumiridium electrodes; a cell holder consisting of a thick and highly reflective mirror for reflecting the light (45 degrees) upward through the cell tube; and an interrupted-type cumulative reading electrical timer, reading in tenths of seconds.

2 Formulae and Calculation Procedures (Zeta meter manual ref. 58)

The Helmholtz-Smoluchowski formula, conventionally employed for determining the zeta potential of normally encountered colloids, is as follows;

$$Zp = \frac{EM * 4 * PI * z}{Dt}$$

where Zp is zeta potential (esu)

EM is electrophoretic mobility (cm/sec per esu/cm)

z is the viscosity of the medium (poise)

Dt is the dielectric constant of the suspending medium.

PI is the mathematical constant

Converting the above equation to more convenient units,

$$Zp = \frac{113000 * z * EM}{Dt}$$

where Zp is the zeta potential (mv)

z is the viscosity of the medium (poise)

EM is electrophoretic mobility (microns/sec per volt/cm)

For a suspending medium of water at 20° C,

$$\frac{11300 * z}{Dt} = 14.1$$

therefore $Zp = 14.1 * EM$

Taking Primal E1743 spheres, in distilled water at a pH of 7 and temperature of 18° C, as an example the zeta potential can be calculated as follows;

Volts = 150

Occular magnification = 8x (micrometer scale 120 microns)

Average time to cross one micometer division = 2.32 sec

$$EM = \frac{microns * cm}{volt * sec}$$

$$= \frac{120 * 10}{200 * 2.32}$$

$$= 2.586$$

therefore $Zp = 2.586 * 14.1$

But the temperature at which the zeta potential was measured was 18° C, therefore the zeta potential must be corrected for this temperature difference. The figure of 14.1 was based on a temperature of 20° C. The dielectric constant and viscosity must be adjusted.

$$Zp = 2.586 * 14.1 * 1.04$$

$$= - 37.9$$ (the negative sign indicates that the colloid is negatively charged)

ZETA-METER DATA

Sample	pH	Temp. °C	SC micro-mhos	V	Av. Time sec	Micro-meter scale	ZP mv	ZP corrected for temp. mv
Primal E1743	7	18	8,0	200	2,37	120 microns	-36,4	-37,9
					2,43			
					2,28			
					2,38			
					2,50			
					2,14			
					2,28			
					2,24			
Primal E1743	4	18	84	150	3,88	120 microns	-28,2	-29,3
					3,96			
					3,49			
					3,77			
					4,22			
					4,30			
					4,40			
					4,21			
					4,05			

ZETA-METER DATA

Sample	pH	Temp. °C	SC micro-mhos	V	Av. Time sec	Micro-meter scale	ZP mv	ZP corrected for temp. mv
Primal E1743	10	18	67	150	2,90	120 microns	-39,3	-40,9
					3,00			
					2,77			
					3,10			
					2,87			
					2,78			
					2,70			
					2,88			
Primal E1743	7	18	30	100	4,20	120 microns	-37,9	-39,4
Electrolyte strength 10 ppm NaCl					4,45			
					4,33			
					4,78			
					4,58			
					4,64			
					4,47			
					4,30			

ZETA-METER DATA

Sample	pH	Temp. °C	SC micro-mhos	V	Av. Time sec	Micro-meter scale	ZP mv	ZP corrected for temp. mv
Primal E1743	7	18	300	100	3,65	120 microns	-44,8	-46,4
Electrolyte strength 110 ppm NaCl					3,59			
					3,99			
					3,90			
					3,52			
					3,78			
					4,07			
					3,74			
					3,78			
Primal E1743	7	18	2250	100	4,10	120 microns	-46,1	-47,9
Electrolyte strength 1000 ppm NaCl					3,72			
					3,91			
					4,19			
					3,62			
					3,64			
					4,11			

ZETA-METER DATA

Sample	pH	Temp. °C	SC micro-mhos	V	Av. Time sec	Micro-meter scale	ZP mv	ZP corrected for temp. mv
Amberlite IRA 938 resin	7	18	12	150	1,57	120 microns	74,4	77,4
					1,56			
					1,48			
					1,53			
					1,50			
					1,53			
					1,50			
Amberlite IRA 938 resin	4	18	75	150	2,36	120 microns		51,4
					2,23		49,4	
					2,22			
					2,35			
					2,36			
					2,28			
					2,25			

ZETA-METER DATA

Sample	pH	Temp. °C	SC micro-mhos	V	Av. Time sec	Micro-meter scale	ZP mv	ZP corrected for temp. mv
Amberlite IRA 938 resin	10	18	150	150	1,38	120 microns	87,0	90,5
					1,35			
					1,25			
					1,30			
					1,30			
					1,27			
					1,28			
					1,26			
Amberlite IRA 938 resin	7	18	130	100	2,97	120 microns	57,7	60,0
Electrolyte strength 50 ppm NaCl					2,97			
					2,90			
					3,03			
					2,86			
					2,93			
					3,03			
					2,85			

ZETA-METER DATA

Sample	pH	Temp. °C	SC micro-mhos	V	Av. Time sec	Micro-meter scale	ZP mv	ZP corrected for temp. mv
Amberlite IRA 938 resin	7	18	510	100	3,50	120 microns	49,7	51,7
Electrolyte strength 200 ppm NaCl					3,53			
					3,48			
					3,35			
					3,23			
					3,25			
					3,44			
					3,46			
Amberlite IRA 938 resin	7	18	2200	100	3,90	120 microns	43,4	45,1
Electrolyte strength 2200 ppm NaCl					4,25			
					3,98			
					3,94			
					4,33			
					3,56			
					3,54			
					3,76			

A P P E N D I X E

THE EFFECT OF COLLOIDAL PARTICLE SIZE ON ADSORPTION RATE

TITLE : THE EFFECT OF COLLOIDAL PARTICLE SIZE OF ADSORPTION RATE

RUN NO. : 1a

RESIN : Amberlite IRA 938

RESIN BEAD SIZE : 508 microns

COLLOID : silicon dioxide - (0.012 microns)

FLOW RATE : 22 ml/min

pH : 7 +- 1.5

IONIC STRENGTH : distilled water

TIME (min)	COLLOID CONCENTRATION (NTU)	-ln(C/Co)
0	0.93	0.000
5	0.84	0.102
10	0.78	0.176
15	0.71	0.270
20	0.65	0.358
25	0.59	0.455
30	0.54	0.544
35	0.50	0.621
40	0.45	0.725
50	0.38	0.895

Straight line curve fit - least square method.

$y = a + bx$

Regression coefficient R = 1.000
a = 0.003
b = 0.018

TITLE : THE EFFECT OF COLLOIDAL PARTICLE SIZE ON ADSORPTION RATE

RUN NO. : 1b

RESIN : Amberlite IRA 938

RESIN BEAD SIZE : Amberlite IRA 938

COLLOID : silicon dioxide - (0.012 microns)

FLOW RATE : 22 ml/min

pH : 7 +- 1.5

IONIC STRENGTH : distilled water

TIME (min)	COLLOID CONCENTRATION (NTU)	-ln(C/Co)
0	0.90	0.000
5	0.81	0.105
10	0.75	0.182
15	0.69	0.266
20	0.61	0.389
25	0.58	0.439
30	0.53	0.530
35	0.48	0.629
40	0.46	0.671
45	0.41	0.786
55	0.34	0.973

Straight line curve fit - least square method.

$y = a + bx$

Regression coefficient $R = 0.997$
$a = 0.012$
$b = 0.017$

TITLE : THE EFFECT OF COLLOIDAL PARTICLE SIZE ON ADSORPTION RATE

RUN NO. : 2a

RESIN : Amberlite IRA 938

RESIN BEAD SIZE : 508 microns

COLLOID : silicon dioxide - (0.5 microns)

FLOW RATE : 22 ml/min

pH : 7 +- 1.5

IONIC STRENGTH : distilled water

TIME (min)	COLLOID CONCENTRATION (NTU)	-ln(C/Co)
0	1.01	0.000
5	0.99	0.020
10	0.96	0.051
20	0.91	0.104
30	0.85	0.172
40	0.80	0.233
50	0.76	0.284
60	0.72	0.338
70	0.67	0.410
80	0.64	0.456
90	0.59	0.538
100	0.55	0.608
110	0.51	0.683
120	0.48	0.744
130	0.44	0.831
140	0.41	0.902
155	0.37	1.004
170	0.33	1.119

Straight line curve fit - least square method.

$y = a + bx$

Regression coefficient $R = 0.997$

$a = -0.031$

$b = 0.006$

TITLE : THE EFFECT OF COLLOIDAL PARTICLE SIZE ON ADSORPTION RATE

RUN NO. : 2b

RESIN : Amberlite IRA 938

RESIN BEAD SIZE : 508 microns

COLLOID : silicon dioxide - (0.5 microns)

FLOW RATE : 22 ml/min

pH : 7 +- 1.5

IONIC STRENGTH : distilled water

TIME (min)	COLLOID CONCENTRATION (NTU)	-ln(C/Co)
0	0.98	0.000
10	0.93	0.052
20	0.88	0.108
30	0.83	0.166
40	0.79	0.216
50	0.74	0.281
60	0.69	0.351
70	0.64	0.426
80	0.60	0.491
90	0.56	0.560
100	0.53	0.615
110	0.50	0.673
120	0.47	0.735
130	0.43	0.824
140	0.40	0.896

Straight line curve fit - least square method.

$y = a + bx$

Regression coefficient $R = 0.998$

$a = -0.20$

$b = 0.006$

TITLE : THE EFFECT OF COLLOIDAL PARTICLE SIZE ON ADSORPTION RATE

RUN NO. : 3a

RESIN : Amberlite IRA 938

RESIN BEAD SIZE : 508 microns

COLLOID : silicon dioxide - (1.2 microns)

FLOW RATE : 22 ml/min

pH : 7 +- 1.5

IONIC STRENGTH : distilled water

TIME (min)	COLLOID CONCENTRATION (NTU)	-ln(C/Co)
0	0.96	0.000
5	0.91	0.053
10	0.85	0.122
15	0.80	0.182
20	0.75	0.247
25	0.71	0.302
30	0.67	0.360
35	0.63	0.421
40	0.60	0.470
45	0.56	0.539
55	0.50	0.652
66	0.44	0.780
75	0.39	0.901
85	0.35	1.009
95	0.32	1.099
105	0.28	1.232
115	0.25	1.345

Straight line curve fit - least square method.

$y = a + bx$

Regression coefficient $R = 1.000$
$a = 0.007$
$b = 0.012$

TITLE : THE EFFECT OF COLLOIDAL PARTICLE SIZE ON ADSORPTION RATE

RUN NO. : 3b

RESIN : Amberlite IRA 938

RESIN BEAD SIZE : 508 microns

COLLOID : silicon dioxide - (1.2 microns)

FLOW RATE : 22 ml/min

pH : 7 +- 1.5

IONIC STRENGTH : distilled water

TIME (min)	COLLOID CONCENTRATION (NTU)	-ln(C/Co)
0	0.99	0.000
5	0.94	0.52
10	0.89	0.106
15	0.84	0.164
20	0.80	0.213
25	0.75	0.278
30	0.70	0.347
35	0.65	0.421
40	0.57	0.550
55	0.51	0.663
65	0.45	0.788
75	0.41	0.882
85	0.37	0.984
95	0.34	1.069
105	0.30	1.194
115	0.27	1.299

Straight line curve fit - least square method.

$y = a + bx$

Regression coefficient $R = 0.998$

$a = 0.006$

$b = 0.012$

TITLE : THE EFFECT OF COLLOIDAL PARTICLE SIZE ON ADSORPTION RATE

RUN NO. : 4a

RESIN : Amberlite IRA 938

RESIN BEAD SIZE : 508 microns

COLLOID : silicon dioxide - (4 microns)

FLOW RATE : 22 ml/min

pH : 7 +- 1.5

IONIC STRENGTH : distilled water

TIME (min)	COLLOID CONCENTRATION (NTU)	-ln(C/Co)
0	0.88	0.000
5	0.77	0.134
10	0.67	0.273
15	0.58	0.417
20	0.52	0.526
25	0.47	0.627
30	0.42	0.740
35	0.38	0.840
40	0.32	0.981
45	0.29	1.110
55	0.23	1.342

Straight line curve fit - least square method.

$y = a + bx$

Regression coefficient R = 0.998
a = 0.025
b = 0.024

TITLE : THE EFFECT OF COLLOIDAL PARTICLE SIZE ON ADSORPTION RATE

RUN NO. : 4b

RESIN : Amberlite IRA 938

RESIN BEAD SIZE : 508 microns

COLLOID : silica dioxide - (4 microns)

FLOW RATE : 22 ml/min

pH : 7 +- 1.5

IONIC STRENGTH : distilled water

TIME (min)	COLLOID CONCENTRATION (NTU)	-ln(C/Co)
0	0.97	0.000
5	0.85	0.132
10	0.75	0.257
15	0.67	0.370
20	0.58	0.514
25	0.51	0.643
30	0.45	0.768
35	0.40	0.886
40	0.35	1.019
45	0.31	1.141
50	0.28	1.243

Straight line curve fit - least square method.

$y = a + bx$

Regression coefficient $R = 1.000$
$a = 0.006$
$b = 0.025$

TITLE : THE EFFECT OF COLLOIDAL PARTICLE SIZE ON ADSORPTION RATE

RUN NO. : 5a

RESIN : Amberlite IRA 938

RESIN BEAD SIZE : 508 microns

COLLOID : silica dioxide - (8 microns)

FLOW RATE : 22 ml/min

pH : 7 +- 1.5

IONIC STRENGTH : distilled water

TIME (min)	COLLOID CONCENTRATION (NTU)	-ln(C/Co)
0	0.74	0.000
2.5	0.65	0.130
5.0	0.57	0.261
7.5	0.52	0.353
10	0.45	0.497
15	0.37	0.693
20	0.27	1.008
25	0.23	1.169
30	0.18	1.414

Straight line curve fit - least square method.

$y = a + bx$

Regression coefficient R = 0.998
a = 0.012
b = 0.047

TITLE : THE EFFECT OF COLLOIDAL PARTICLE SIZE ON ADSORPTION RATE

RUN NO. : 5b

RESIN : Amberlite IRA 938

RESIN BEAD SIZE : 508 microns

COLLOID : silica dioxide - (8 microns)

FLOW RATE : 22 ml/min

pH : 7 +- 1.5

IONIC STRENGTH : distilled water

TIME (min)	COLLOID CONCENTRATION (NTU)	-ln(C/Co)
0	0.90	0.000
2.5	0.79	0.130
5.0	0.69	0.266
7.5	0.62	0.373
10.0	0.54	0.511
12.5	0.49	0.608
15	0.45	0.693
20	0.35	0.944
25	0.28	1.168
30	0.22	1.409

Straight line curve fit - least square method.

$y = a + bx$

Regression coefficient R = 0.999
a = 0.021
b = 0.046

A P P E N D I X F

THE NEED TO INVESTIGATE ALTERNATIVE WATER RESOURCES

DESALINATION PROCESSES

REVERSE OSMOSIS DESALINATION OF SEAWATER

CURRENT USES OF ION-EXCHANGE RESINS IN ADSORPTIVE PROCESSES

THE NEED TO INVESTIGATE ALTERNATIVE WATER RESOURCES

Fresh water, like other natural resources, is becoming a scarce commodity, in a developing Southern Africa. Rapid population growth and industrial expansion are putting ever increasing demands on local and regional water supplies. Calculations indicate that the Republic's water balance will become critical shortly after the turn of the century and that the water demand will exceed the estimated total resource (59).

The South Western Cape, although having a relatively high rainfall in South African terms, is no exception to the problems of rapidly increasing population and industrial expansion. It has been estimated that the water demand by the year 2010 will be 2173 million m^3 per annum for urban and industrial use and a further 1124 million m^3 per annum will be required for agriculture (60). This gives a total demand of 3297 million m^3 per annum which is just about equal to the estimated total resource for the region 3330 million cubic meters per annum. This shows that in an overall regional context, no uncoventional resources need be introduced before 2010; thereafter however alternative sources for supplementing the regions fresh water will have to be provided (60).

The South Western Cape has however a vast untapped water resource; the sea.

Desalination of seawater for the South Western Cape has not received much attention, as this process has traditionally been both energy and cost intensive. The practical applicability of desalination is directly related to the unit cost of the product water and the reliability of the desalination process. Up to the present the main deterrent to large scale use of desalination processes has been their inability to compete on a cost basis with conventional sources of supply.

Desalination of seawater is however becoming popular in areas where alternative supplies are simply not available or are very costly. Such conditions do occur in Southern Africa and their

TITLE : THE EFFECT OF SURFACE CHARGE ON ADSORPTION RATE

RUN NO. : 19a

RESIN : Amberlite IRA 938

RESIN BEAD SIZE : 508 microns

COLLOID : Primal E1743

FLOW RATE : 70 ml/min

pH : 7 +- 1.5

IONIC STRENGTH : 1000 ppm NaCl

TIME (min)	COLLOID CONCENTRATION (abs)	-ln(C/Co)
0	0.820	0.000
1	0.750	0.089
2	0.687	0.177
3	0.628	0.267
4	0.575	0.355
5	0.525	0.446
6	0.482	0.531
7	0.443	0.616
8	0.407	0.700
9	0.373	0.788
11	0.313	0.963
13	0.267	1.122
15	0.225	1.293
17	0.190	1.462
19	0.163	1.616
21	0.137	1.789

Straight line curve fit - least square method.

$y = a + bx$

Regression coefficient R = 1.000
a = 0.014
b = 0.085

TITLE : THE EFFECT OF SURFACE CHARGE ON ADSORPTION RATE

RUN NO. : 20a

RESIN : Amberlite IRA 938

RESIN BEAD SIZE : 508 microns

COLLOID : Primal E1743

FLOW RATE : 70 ml/min

pH : 7 +- 1.5

IONIC STRENGTH : 2500 ppm NaCl

TIME (min)	COLLOID CONCENTRATION (abs)	-ln(C/Co)
0	0.755	0.000
1	0.690	0.090
2	0.630	0.181
3	0.577	0.269
4	0.530	0.354
5	0.485	0.443
6	0.443	0.533
7	0.405	0.623
8	0.370	0.713
9	0.340	0.798
11	0.283	0.981
13	0.237	1.159
15	0.200	1.328
17	0.167	1.509
19	0.140	1.685
21	0.117	1.865

Straight line curve fit - least square method.

$y = a + bx$

Regression coefficient R = 1.000
a = 0.002
b = 0.089

TITLE : THE EFFECT OF SURFACE CHARGE ON ADSORPTION RATE

RUN NO. : 21a

RESIN : Amberlite IRA 938

RESIN BEAD SIZE : 508 microns

COLLOID : Primal E1743

FLOW RATE : 70 ml/min

pH : 7 +- 1.5

IONIC STRENGTH : 3000 ppm NaCl

TIME (min)	COLLOID CONCENTRATION (abs)	-ln(C/Co)
0	0.810	0.000
1	0.741	0.089
2	0.680	0.175
3	0.625	0.259
4	0.577	0.339
5	0.530	0.424
6	0.490	0.503
7	0.449	0.590
8	0.414	0.671
9	0.380	0.757
11	0.322	0.922
13	0.272	1.091
15	0.230	1.259
17	0.195	1.424
19	0.165	1.591
21	0.139	1.763

Straight line curve fit - least square method.

$y = a + bx$

Regression coefficient R = 1.000
a = 0.005
b = 0.084

AMBERLITE IRA 938 AND IT'S CATION AND UNCHARGED EQUIVALENTS

1 The properties of Amberlite IRA 938

Physical form	Uniform yellow sperical particles shipped in the chloride form in a moist condition.
Structure	Crosslinked macroreticular, styrene-divinylbenzene.
Functional group	$-N-(CH_3)$
Moisture content	72 - 78 %
Swelling	Approximately 10 % upon conversion from the choride to the hydroxide form.
Densities (g/cm^3)	
Skeletal	1.203
Apparent	0.555
Porosity (cm^3 pores/g) (dry resin)	0.972
Pore diameter (Å)	
Mean	70 000 Å
Range	25 000 to 250 000 Å
Surface area (m^2)	7.3
Anion exchange capacity (dry)	3.8 meq/g (choride form)*

* As capacity in terms of meq/g dry resin is not particularly appropriate when dealing with organic and colloidal matter, Dr. Kunin gives a figure of 100mg/g of resin for organic and colloidal matter, but stresses this capacity is dependent on the nature of the organic and colloidal matter.

2 The properties of the Unfunctionalised and Cation resin

The unfunctionalised precusor of Amberlite IRA 938 resin and the cation resin prepared from the latter have the same specifications as Amberlite IRA 938 resin, except for the following:

Unfunctionalised resin

Appearance	white
Functional group	none
Ion-exchange capacity	zero

Cation resin

Appearance	light brown
Functional group	$-SO_3$
Cation exchange capacity	0.30 meq/g (hydrogen form)

3 Procedure to sulphonate the co-polymer of Amberlite IRA 938

i) Charge 100 parts by weight of co-polymer into a mixture of 2500 parts sulphuric acid (95-98%) and 100 parts ethylene dichloride.

ii) Distill off the ethylene dichoride while heating the mixture to a temperature of 120°C. Agitate the slurry gently.

iii) Hold the temperature at 120° C for three hours.

iv) Add water dropwise keeping the temperature below 120° C (heat is evolved on addition of water) untill complete dilution.

v) After cooling, wash the filtered resin beads repeatedly with water to remove soluable materials.

vi) The resin is now in the hydrogen form, if the sodium form is required place the filtered resin in water and neutralise the slurry with NaOH while agitating.

3 The capacity of the sulphonated co-polymer

The capacity of the sulphonated resin was determined using pH titrations. A measured volume of resin, in the hydrogen form, was placed in 50 ml of distilled water was titrated against 1 N NaOH. The pH of the slurry was monitored using digital pH meter.

Test 1

Resin size - 600-425 microns

Resin volume - 40 ml (free settled volume)

35.6 ml (tapped volume)

NaOH concentration - 1.00 N

Volume of NaOH added (ml)	pH
5.0	4.38
8.0	4.50
10.0	4.63
11.0	4.75
11.5	4.97
12.0	5.20
12.5	9.40
13.0	11.30
13.3	11.94
15.0	12.46

$$\text{Capacity of the resin} = \frac{\text{NaOH (ml)} * \text{NaOH (N)}}{\text{resin (ml - fsv)}}$$

$$= \frac{12.4 * 1.00}{40}$$

$$= 0.31 \text{ meq/ml of resin}$$

TITLE : THE EFFECT OF SURFACE CHARGE ON ADSORPTION RATE

RUN NO. : 7a

RESIN : Amberlite IRA 938

RESIN BEAD SIZE : 508 microns

COLLOID : titanium dioxide

FLOW RATE : 70 ml/min

pH : 7 +- 1.5

IONIC STRENGTH : distilled water

Titanium dioxide did not adsorb to Amberlite IRA 938 resin at this pH.

TITLE : THE EFFECT OF SURFACE CHARGE ON ADSORPTION RATE

RUN NO. : 8a

RESIN : Amberlite IRA 938

RESIN BEAD SIZE : 508 microns

COLLOID : titanium dioxide

FLOW RATE : 70 ml/min

pH : 4 +- 0.2

IONIC STRENGTH : distilled water

Titanium dioxide did not adsorb to Amberlite IRA 938 resin at this pH.

TITLE : THE EFFECT OF SURFACE CHARGE ON ADSORPTION RATE

RUN NO. : 9a

RESIN : Amberlite IRA 938

RESIN BEAD SIZE : 508 microns

COLLOID : titanium dioxide

FLOW RATE : 70 ml/min

pH : 10 +- 0.2

IONIC STRENGTH : distilled water

TIME (min)	COLLOID CONCENTRATION (abs)	-ln(C/Co)
0	0.910	0.000
2	0.795	0.135
4	0.697	0.267
6	0.610	0.400
8	0.535	0.531
10	0.473	0.654
12	0.417	0.780
14	0.370	0.900
18	0.293	1.133
22	0.233	1.362
26	0.187	1.582
30	0.150	1.803

Straight line curve fit - least square method.

$y = a + bx$

Regression coefficient R = 0.999
a = 0.035
b = 0.060

TITLE : THE EFFECT OF SURFACE CHARGE ON ADSORPTION RATE

RUN NO. : 10a

RESIN : cation form

RESIN BEAD SIZE : 508 microns

COLLOID : silicon dioxide

FLOW RATE : 70 ml/min

pH : 7 +- 1.5

IONIC STRENGTH : distilled water

Silicon dioxide did not adsorb to cation resin at this pH.

TITLE : THE EFFECT OF SURFACE CHARGE ON ADSORPTION RATE

RUN NO. : 11a

RESIN : cation form

RESIN BEAD SIZE : 508 microns

COLLOID : Primal E1743

FLOW RATE : 70 ml/min

pH : 7 +- 1.5

IONIC STRENGTH : distilled water

Primal E1743 did not adsorb to the cation resin at this pH.

TITLE : THE EFFECT OF SURFACE CHARGE ON ADSORPTION RATE

RUN NO. : 12a

RESIN : cation form

RESIN BEAD SIZE : 508 microns

COLLOID : titanium dioxide

FLOW RATE : 70 ml/min

pH : 7 +- 1.5

IONIC STRENGTH : distilled water

Titanium dioxide did not adsorb to the cation resin at neutral pH, however some adsorption was measured at pH values less than 5.

TITLE : THE EFFECT OF SURFACE CHARGE ON ADSORPTION RATE

RUN NO. : 13a

RESIN : uncharged

RESIN BEAD SIZE : 508 microns

COLLOID : silicon dioxide

FLOW RATE : 70 ml/min

pH : 7 +- 1.5

IONIC STRENGTH : distilled water

TIME (min)	COLLOID CONCENTRATION (abs)	-ln(C/Co)
0	1.01	0.000
2	0.98	0.030
4	0.95	0.061
8	0.89	0.126
12	0.84	0.184
16	0.80	0.233
20	0.75	0.298
24	0.71	0.352
29	0.67	0.410
34	0.63	0.472
44	0.57	0.572
54	0.52	0.664

Straight line curve fit - least square method.

$y = a + bx$

Regression coefficient $R = 0.991$
$a = 0.024$
$b = 0.013$

TITLE : THE EFFECT OF SURFACE CHARGE ON ADSORPTION RATE

RUN NO. : 14a

RESIN : uncharged

RESIN BEAD SIZE : 508 microns

COLLOID : Primal E1743

FLOW RATE : 70 ml/min

pH : 7 +- 1.5

IONIC STRENGTH : distilled water

TIME (min)	COLLOID CONCENTRATION (abs)	-ln(C/Co)
0	0.850	0.000
2	0.792	0.071
4	0.735	0.145
6	0.682	0.220
8	0.630	0.300
10	0.578	0.386
12	0.532	0.469
14	0.487	0.557
16	0.447	0.643
18	0.400	0.754
20	0.360	0.859
22	0.322	0.971
24	0.285	1.100
26	0.248	1.232
28	0.215	1.375
30	0.184	1.530

Straight line curve fit - least square method.

$y = a + bx$

Regression coefficient $R = 0.986$
$a = 0.084$
$b = 0.050$

TITLE : THE EFFECT OF SURFACE CHARGE ON ADSORPTION RATE

RUN NO. : 14b

RESIN : uncharged

RESIN BEAD SIZE : 508 microns

COLLOID : Primal E1743

FLOW RATE : 70 ml/min

pH : 7 +- 1.5

IONIC STRENGTH : distilled water

TIME (min)	COLLOID CONCENTRATION (abs)	-ln(C/Co)
0	0.800	0.000
2	0.745	0.071
4	0.690	0.148
6	0.640	0.223
8	0.590	0.304
10	0.545	0.384
12	0.500	0.470
14	0.457	0.560
16	0.415	0.656
18	0.375	0.758
20	0.336	0.868
22	0.300	0.981
24	0.265	1.105
26	0.233	1.234
28	0.202	1.376
30	0.163	1.591

Straight line curve fit - least square method.

$y = a + bx$

Regression coefficient $R = 0.983$
$a = 0.089$
$b = 0.051$

TITLE : THE EFFECT OF SURFACE CHARGE ON ADSORPTION RATE

RUN NO. : 15a

RESIN : uncharged

RESIN BEAD SIZE : 508 microns

COLLOID : titanium dioxide

FLOW RATE : 70 ml/min

pH : 7 +- 1.5

IONIC STRENGTH : distilled water

TIME (min)	COLLOID CONCENTRATION (abs)	-ln(C/Co)
0	0.400	0.000
2	0.378	0.057
4	0.356	0.117
6	0.336	0.174
8	0.316	0.236
10	0.299	0.291
12	0.283	0.346
14	0.268	0.400
18	0.242	0.503
22	0.220	0.598
26	0.201	0.688
30	0.185	0.771
34	0.170	0.856

Straight line curve fit - least square method.

$y = a + bx$

Regression coefficient $R = 0.996$
$a = 0.020$
$b = 0.026$

TITLE : THE EFFECT OF SURFACE CHARGE ON ADSORPTION RATE

RUN NO. : 16a

RESIN : Amberlite IRA 938

RESIN BEAD SIZE : 508 microns

COLLOID : Primal E1743

FLOW RATE : 70 ml/min

pH : 7 +- 1.5

IONIC STRENGTH : 0 ppm NaCl

TIME (min)	COLLOID CONCENTRATION (abs)	-ln(C/Co)
0	0.703	0.000
1	0.637	0.099
2	0.565	0.219
3	0.510	0.321
4	0.457	0.431
5	0.410	0.539
6	0.370	0.642
7	0.330	0.756
8	0.295	0.868
9	0.265	0.976
11	0.210	1.208
13	0.166	1.443
15	0.133	1.665
17	0.105	1.901
19	0.083	2.137
21	0.065	2.381

Straight line curve fit - least square method.

$y = a + bx$

Regression coefficient $R = 1.000$
$a = -0.023$
$b = 0.113$

TITLE : THE EFFECT OF SURFACE CHARGE ON ADSORPTION RATE

RUN NO. : 17a

RESIN : Amberlite IRA 938

RESIN BEAD SIZE : 508 microns

COLLOID : Primal E1743

FLOW RATE : 70 ml/min

pH : 7 +- 1.5

IONIC STRENGTH : 20 ppm NaCl

TIME (min)	COLLOID CONCENTRATION (abs)	-ln(C/Co)
0	0.743	0.000
1	0.675	0.096
2	0.615	0.189
3	0.565	0.274
4	0.515	0.367
5	0.472	0.454
6	0.432	0.542
7	0.393	0.637
8	0.360	0.725
9	0.331	0.809
11	0.275	0.994
13	0.230	1.173
15	0.190	1.364
17	0.157	1.554
19	0.130	1.743
21	0.110	1.910

Straight line curve fit - least square method.

$y = a + bx$

Regression coefficient R = 1.000
a = 0.000
b = 0.091

TITLE : THE EFFECT OF SURFACE CHARGE ON ADSORPTION RATE

RUN NO. : 18a

RESIN : Amberlite IRA 938

RESIN BEAD SIZE : 508 microns

COLLOID : Primal E1743

FLOW RATE : 70 ml/min

pH : 7 +- 1.5

IONIC STRENGTH : 250 ppm NaCl

TIME (min)	COLLOID CONCENTRATION (abs)	-ln(C/Co)
0	0.760	0.000
1	0.695	0.089
2	0.635	0.180
3	0.585	0.262
4	0.535	0.351
5	0.490	0.439
6	0.450	0.524
7	0.412	0.612
8	0.380	0.693
9	0.348	0.781
11	0.293	0.953
13	0.246	1.128
15	0.207	1.301
17	0.175	1.469
19	0.145	1.657
21	0.122	1.829

Straight line curve fit - least square method.

$y = a + bx$

Regression coefficient R = 1.000
a = 0.002
b = 0.087

63. Green, G. and Belfort, G. "Fouling of ultrafiltration membranes: Lateral migration and the particle trajectory model". Desalination, 35, 129 (1980).

64. Tidball, R.A. et al. "Operating experience with seawater reverse osmosis plants in the Middle East". Desalination, 29, 319 (1979).

65. Du Pont Design Manual, Technical Bulletin 440 4/6/77, Du Pont Company, Wilmington, DE.

66. Quinn, R.M., "Design and operation of an 800 000 GPD reverse osmosis seawater system". Idea Congress Nice, France. Oct 22-26 (1979).

67. Office of Water Research and Technology U.S. Department of the Interior, Washington D.C., Final report field test evaluation of seawater reverse osmosis and electrodialysis pilot plants at the Wrightsville Beach Test Facility. Contacts no. 14-30-3175 and 14-34-0001-6512, p.43-54 (1976)

68. Al-Gholaikah, A. et al. "The worlds first large seawater reverse osmosis desalination plant at Jeddah, Kingdom of Saudi Arabia". Sixth International Symposium of Fresh Water from the Sea, Las Palmas, Gran Canaria, Spain. Sept (1978).

69. Saunders, L. et al., "Prepartion of biologically pure water by ion-exchange". Conference, Imperial College of Science and Technology London, S.W.7. July 16-18 (1969).

70. Kunin, R., "Ion-exchange technology in medicine and the pharmaceutical industry, Part iv". Amberhilites, Rohm and Haas Company, Philadephia, Pensylvania. 145 (1975)

71. Foster, D.H. et al. "Application of weak base ion-exchange resins for the removal of proteins". Environmental Science and Technology, 11, 1, 55 (1977).

72. Kawabata, N. et al., "Removal of bacteria from water by the adhesion to cross-linked poly(vinylpyridinium halide)". Applied and Enviromental Microbiology, 46, 1, 203 (1983).

73. Levenspiel, O. Chemical Reaction Engineering. 2nd Edt., John Wiley and Sons, New York, p 361-365 (1972).

BIBLIOGRAPHY

1) Verwey, E.J.W. and Overbeek, J.G., Theory of the stability of lyophobic colloids. Elsevier, New York (1948).

2) Kruyt, H.R. (editor), Colloid Science. Volume 1. Elsevier, Amsterdam (1952).

3) Levich, V.G., Physicochemical Hydrodynamics. Prentice-Hall, Englewood Cliffs, N.J. (1962).

4) Bitton, G. and Marshall, K. (editors), Adsorption of micro-organisms to surfaces. John Wiley and Sons, New York (1980).

5) Crank, J., McFarlane, N.R., Newby, J.C., Patterson, G.D. and Pedley, J.B. Diffusion processes in environmental systems. MacMillan Press, Hong Kong (1981).

6) Levenspiel, O. Chemical Reaction Engineering. 2nd edition, Wiley International Edition (1972).

7) Levenspiel, O. The chemical reactor omnibook. OSU book stores, Corvopllis (1979).

8) Helfferich, F.G. Ion Exchange. McGraw-Hill, New York (1962).

9) Liberti, L. and Helfferich, F.G. (editors) Mass transfer and kinetics of ion exchange. Martinus Nijhoff Publishers, The Hague (1983).

10) Naden, D. and Streat, M. Ion Exchange Technology. Ellis Horwood Limited, Chichester (1984).

A P P E N D I X A

ADSORPTION ISOTHERMS (PRIMAL E1743 - AMBERLITE IRA 938)

RESIN REGENERATION/CLEANING

THE EFFECT OF SURFACE COVERAGE/RESIN LOADING ON ADSORPTION RATE

ADSORPTION ISOTHERMS FOR THE PRIMAL E1743 - AMBERLITE IRA 938 RESIN SYSTEM

1 Gram resin samples were placed into bottles containing 300 ml of distilled water. Varying amounts of model colloid (Primal E1743) were then added to each bottle.

Time (days)	Sample No.	Suspension concentration (mg/l)	Resin loading (mg/g dry resin)
0	1	34,7	0
	2	69,5	0
	3	104	0
	4	139	0
	5	174	0
	6	174	0
	7	217	0
	8	260	0
	9	261	0
	10	296	0
	11	322	0
	12	348	0
20	1	0,27	12,2
	2	0,65	24,6
	3	3,2	35,6
	4	13,8	44,6
	5	22,5	53,0
	6	28,7	51,6
	7	43,2	60,8
	8	62,5	70,5
	9	67,7	67,7
	10	86,0	73,5
	11	104	76,3
	12	109	83,7
40	7	5,0	74,2
	11	44,3	97,2
90	3	1,18	36,6
	4	1,24	49,0
	6	1,45	61,4
	8	15,2	87,1
110	7	0,4	75,8
	11	0,7	112

RESIN REGENERATION/CLEANING

1 Gram resin samples each loaded with between 25 and 45 mg of model colloid (Primal E1743), were used in the regeneration techniques studied.

1 Chemical Regeneration

Regeneration using hot HCl and NaOH. A minimal amount of the colloid was released during the first five minutes of the experiment while hot HCl was pumped through the system. The colloid was released slowly while the hot NaOH was cycled through the resin bed.

Resin loading at start of regeneration = 25 mg/g

Time (hrs)	Colloid concentration (absorbance 4 cm cell)	% Regeneration
0	0	0
2	0,85	11
3	1,18	15
3,5	1,33	17
4	1,43	18
7,5	1,81	23
11	2,10	27
14	2,37	30
20	2,63	35

2 Ultrasonic regeneration

The resin column was submerged in a temperature controlled ultrasonic bath. Distilled water was pumped through the resin bed and the colloid particle concentration in the effluent water was monitored.

Resin loading at start of regeneration = 45mg/g

Time (min)	Colloid concentration (absorbance 4 cm cell)	Time	Abs (cont'd)
0	0	95	0,42
12	0	100	0,41
15	0,48	105	0,38
20	1,65	110	0,41
25	1,90	115	0,44
30	1,63	120	0,46
35	1,43	125	0,50
40	1,16	130	0,61
45	1,09	135	0,47
50	1,06	140	0,40
55	0,90	145	0,42
60	0,80	150	0,40
65	0,74	155	0,38
70	0,63	160	0,36
75	0,50	165	0,34
80	0,48	170	0,30
85	0,50	175	0,29
90	0,43	180	0,29

TITLE : THE EFFECT OF SURFACE COVERAGE/LOADING ON ADSORPTION RATE

RUN NO. : 1

RESIN : Amberlite IRA 938

RESIN BEAD SIZE : 508 microns

COLLOID : Primal E1743

FLOW RATE : 45 ml/min

pH : 7 +- 1.5

IONIC STRENGTH : distilled water

WEIGHT OF COLLOID ADSORBED PRIOR TO START OF RUN = 0 mg

TIME (min)	COLLOID CONCENTRATION (abs)	-ln(C/Co)
0	1.17	0.000
2.5	1.12	0.044
5.0	1.07	0.089
7.5	1.03	0.126
10.0	0.99	0.167
15	0.92	0.240
20	0.84	0.331
25	0.78	0.406

Straight line curve fit - least square method.

$y = a + bx$

Regression coefficient R = 0.999
a = 0.004
b = 0.0162

THE WEIGHT OF COLLOID ADSORBED PRIOR TO START OF RUN = 25 mg

TIME (min)	COLLOID CONCENTRATION (abs)	-ln(C/Co)
0	1.75	0.000
5	1.69	0.035
10	1.63	0.071
15	1.58	0.102
20	1.53	0.134
25	1.48	0.168
30	1.43	0.202
35	1.39	0.230

Straight line curve fit - least square method.

$y = a + bx$

Regression coefficient R = 0.999
a = 0.002
b = 0.0066

THE WEIGHT OF COLLOID ADSORBED PRIOR TO START OF RUN = 37 mg

TIME (min)	COLLOID CONCENTRATION (abs)	-ln(C/Co)
0	1.10	0.000
10	1.06	0.037
20	1.02	0.075
30	0.99	0.105
40	0.95	0.147
50	0.93	0.168
60	0.89	0.212
70	0.86	0.246

Straight line curve fit - least square method.

$y = a + bx$

Regression coefficient R = 0.998
a = 0.002
b = 0.0035

THE WEIGHT OF COLLOID ADSORBED PRIOR TO START OF RUN = 55 mg

TIME (min)	COLLOID CONCENTRATION (abs)	-ln(C/Co)
0	1.44	0.000
20	1.39	0.035
40	1.35	0.065
60	1.31	0.095
80	1.27	0.126
100	1.23	0.158

Straight line curve fit - least square method.

$y = a + bx$

Regression coefficient R = 1.000
a = 0.002
b = 0.0016

THE WEIGHT OF COLLOID ADSORBED PRIOR TO START OF RUN = 67 mg

TIME (min)	COLLOID CONCENTRATION (abs)	-ln(C/Co)
0	1.02	0.000
40	0.98	0.046
80	0.94	0.082
120	0.91	0.114
160	0.87	0.159
200	0.83	0.206

Straight line curve fit - least square method.

$y = a + bx$

Regression coefficient R = 0.996
a = 0.001
b = 0.0010

THE WEIGHT OF COLLOID ADSORBED PRIOR TO START OF RUN = 73 mg

TIME (min)	COLLOID CONCENTRATION (abs)	-ln(C/Co)
0	1.40	0.000
40	1.35	0.036
80	1.30	0.074
120	1.26	0.105
160	1.21	0.146
200	1.17	0.180

Straight line curve fit - least square method.

$y = a + bx$

Regression coefficient $R = 0.999$
$a = 0.000$
$b = 0.0009$

A P P E N D I X B

THE EFFECT OF RESIN BEAD SIZE ON ADSORPTION RATE

CALCULATION OF RESIN BEAD SURFACE AREAS

TITLE : THE EFFECT OF RESIN BEAD SIZE ON ADSORPTION RATE

RUN NO. : 1a

RESIN : Amberlite IRA 938

RESIN BEAD SIZE : 508 microns

COLLOID : Primal E1743

FLOW RATE : 45 ml/min

pH : 7 +- 1.5

IONIC STRENGTH : distilled water

TIME (min)	COLLOID CONCENTRATION (abs)	-ln(C/Co)
0	0.908	0.000
1.25	0.790	0.139
2.5	0.692	0.272
5.0	0.632	0.362
7.5	0.409	0.798
10.0	0.315	1.059
12.5	0.242	1.322
15.0	0.188	1.575
17.5	0.145	1.835
20.0	0.110	2.111
22.5	0.087	2.345
25.0	0.066	2.622
27.5	0.052	2.860
30.0	0.040	3.122
32.5	0.032	3.346
35.0	0.024	3.633

Straight line curve fit - least square method.

$y = a + bx$

Regression coefficient $R = 0.999$
$a = -0.008$
$b = 0.104$

TITLE : THE EFFECT OF RESIN BEAD SIZE ON ADSORPTION RATE

RUN NO. : 1b

RESIN : Amberlite IRA 938

RESIN BEAD SIZE : 508 microns

COLLOID : Primal E1743

FLOW RATE : 45 ml/min

pH : 7 +- 1.5

IONIC STRENGTH : distilled water

TIME (min)	COLLOID CONCENTRATION (abs)	-ln(C/Co)
0	0.745	0.000
1.25	0.665	0.114
2.5	0.597	0.221
5.0	0.485	0.429
7.5	0.388	0.652
10.0	0.308	0.883
12.5	0.241	1.129
15.0	0.185	1.393
17.5	0.140	1.672
20.0	0.104	1.969
22.5	0.076	2.283
25.0	0.058	2.553
27.5	0.043	2.852
30.0	0.033	3.117
32.5	0.026	3.355

Straight line curve fit - least square method.

$y = a + bx$

Regression coefficient $R = 0.997$
$a = -0.094$
$b = 0.105$

TITLE : THE EFFECT OF RESIN BEAD SIZE ON ADSORPTION RATE

RUN NO. : 1c

RESIN : Amberlite IRA 938

RESIN BEAD SIZE : 508 microns

COLLOID : Primal E1743

FLOW RATE : 45 ml/min

pH : 7 +- 1.5

IONIC STRENGTH : distilled water

TIME (min)	COLLOID CONCENTRATION (abs)	-ln(C/Co)
0	0.810	0.000
1.25	0.701	0.145
2.5	0.615	0.275
5.0	0.470	0.544
7.5	0.360	0.811
10.0	0.279	1.066
12.5	0.214	1.331
15.0	0.165	1.591
17.5	0.127	1.853
20.0	0.097	2.122
22.5	0.074	2.393
25.0	0.058	2.637
27.5	0.045	2.890
30.0	0.031	3.263
32.5	0.027	3.401

Straight line curve fit - least square method.

$y = a + bx$

Regression coefficient R = 0.999
a = 0.010
b = 0.106

TITLE : THE EFFECT OF RESIN BEAD SIZE ON ADSORPTION RATE

RUN NO. : 2a

RESIN : Amberlite IRA 938

RESIN BEAD SIZE : 697 microns

COLLOID : Primal E1743

FLOW RATE : 45 ml/min

pH : 7 +- 1.5

IONIC STRENGTH : distilled water

TIME (min)	COLLOID CONCENTRATION (abs)	-ln(C/Co)
0	0.863	0.000
1.25	0.800	0.076
2.50	0.733	0.163
3.75	0.670	0.253
5.0	0.610	0.347
7.5	0.505	0.536
10.0	0.420	0.720
12.5	0.348	0.908
15.0	0.290	1.091
17.5	0.249	1.243
20.0	0.215	1.390
22.5	0.192	1.503
25.0	0.173	1.607
27.5	0.159	1.692
30.0	0.148	1.763
35.0	0.130	1.893

Straight line curve fit - least square method.

$y = a + bx$

Regression coefficient $R = 0.975$
$a = 0.090$
$b = 0.058$

TITLE : THE EFFECT OF RESIN BEAD SIZE ON ADSORPTION RATE

RUN NO. : 2b

RESIN : Amberlite IRA 938

RESIN BEAD SIZE : 697 microns

COLLOID : Primal E1743

FLOW RATE : 45 ml/min

pH : 7 +- 1.5

IONIC STRENGTH : distilled water

TIME (min)	COLLOID CONCENTRATION (abs)	-ln(C/Co)
0	0.905	0.000
1.25	0.830	0.087
2.5	0.775	0.155
5.0	0.670	0.301
7.5	0.579	0.447
10.0	0.501	0.591
12.5	0.432	0.740
15.0	0.374	0.884
17.5	0.322	1.033
20.0	0.278	1.180
22.5	0.239	1.331
25.0	0.205	1.485
27.5	0.176	1.637
30.0	0.151	1.791
32.5	0.129	1.948
35.0	0.110	2.107

Straight line curve fit - least square method.

$y = a + bx$

Regression coefficient R = 1.000
a = -0.002
b = 0.060

TITLE : THE EFFECT OF RESIN BEAD SIZE ON ADSORPTION RATE

RUN NO. : 2c

RESIN : Amberlite IRA 938

RESIN BEAD SIZE : 697 microns

COLLOID : Primal E1743

FLOW RATE : 45 ml/min

pH : 7 +- 1.5

IONIC STRENGTH : distilled water

TIME (min)	COLLOID CONCENTRATION (abs)	-ln(C/Co)
0	0.890	0.000
1.25	0.820	0.082
2.5	0.767	0.149
5.0	0.665	0.291
7.5	0.575	0.437
10.0	0.500	0.577
12.5	0.433	0.720
15.0	0.378	0.856
17.5	0.328	0.998
20.0	0.285	1.139
22.5	0.247	1.282
25.0	0.214	1.425
27.5	0.187	1.560
30.0	0.162	1.704
32.5	0.143	1.828
35.0	0.123	1.979
40.0	0.094	2.248

Straight line curve fit - least square method.

$y = a + bx$

Regression coefficient R = 1.000
a = 0.012
b = 0.056

TITLE : THE EFFECT OF RESIN BEAD SIZE ON ADSORPTION RATE

RUN NO. : 3a

RESIN : Amberlite IRA 938

RESIN BEAD SIZE : 374 microns

COLLOID : Primal E1743

FLOW RATE : 45 ml/min

pH : 7 +- 1.5

IONIC STRENGTH : distilled water

TIME (min)	COLLOID CONCENTRATION (abs)	-ln(C/Co)
0	0.985	0.000
1.25	0.813	0.192
2.5	0.677	0.375
5.0	0.470	0.740
7.5	0.329	1.097
10.0	0.229	1.459
12.5	0.159	1.824
15.0	0.107	2.220
17.5	0.077	2.549
20.0	0.054	2.904
22.5	0.049	3.204
25.0	0.024	3.715

Straight line curve fit - least square method.

$y = a + bx$

Regression coefficient R = 0.999
a = 0.007
b = 0.146

TITLE : THE EFFECT OF RESIN BEAD SIZE ON ADSRPTION RATE

RUN NO. : 3b

RESIN : Amberlite IRA 938

RESIN BEAD SIZE : 374 microns

COLLOID : Primal E1743

FLOW RATE : 45 ml/min

pH : 7 +- 1.5

IONIC STRENGTH : distilled water

TIME (min)	COLLOID CONCENTRATION (abs)	-ln(C/Co)
0	0.523	0.000
1.25	0.433	0.189
2.5	0.360	0.373
5.0	0.257	0.711
7.5	0.175	1.095
10.0	0.123	1.447
12.5	0.085	1.817
15.0	0.059	2.182
17.5	0.041	2.546
20.0	0.029	2.892
22.5	0.021	3.215

Straight line curve fit - least square method.

$y = a + bx$

Regression coefficient R = 1.000
a = 0.009
b = 0.144

TITLE : THE EFFECT OF RESIN BEAD SIZE ON ADSORPTION RATE

RUN NO. : 4a

RESIN : Amberlite IRA 938

RESIN BEAD SIZE : 919 microns

COLLOID : Primal E1743

FLOW RATE : 45 ml/min

pH : 7 +- 1.5

IONIC STRENGTH : distilled water

TIME (min)	COLLOID CONCENTRATION (abs)	-ln(C/Co)
0	0.915	0.000
2.5	0.868	0.056
5.0	0.823	0.109
7.5	0.783	0.159
10.0	0.747	0.206
12.5	0.713	0.253
15.0	0.680	0.300
17.5	0.647	0.350
20.0	0.620	0.392
22.5	0.593	0.437
25.0	0.565	0.485
27.5	0.543	0.525
30.0	0.520	0.568
32.5	0.498	0.612
35.0	0.475	0.659
37.5	0.455	0.702
40.0	0.430	0.758

Straight line curve fit - least square method.

$y = a + bx$

Regression coefficient $R = 0.999$

$a = 0.016$

$b = 0.019$

TITLE : THE EFFECT OF RESIN BEAD SIZE ON ADSORPTION RATE

RUN NO. : 5a

RESIN : Amberlite IRA 938

RESIN BEAD SIZE : 231 microns

COLLOID : Primal E1743

FLOW RATE : 45 ml/min

pH : 7 +- 1.5

IONIC STRENGTH : distilled water

TIME (min)	COLLOID CONCENTRATION (abs)	-ln(C/Co)
0	0.265	0.000
0.5	0.233	0.129
1.0	0.203	0.267
1.5	0.176	0.409
2.0	0.154	0.543
2.5	0.135	0.674
3.0	0.118	0.809
3.5	0.105	0.926
4.0	0.091	1.069
4.5	0.080	1.198
5.5	0.060	1.485
6.5	0.045	1.773
7.5	0.034	2.053
8.5	0.025	2.361
9.5	0.019	2.635

Straight line curve fit - least square method.

$y = a + bx$

Regression coefficient $R = 1.000$

$a = 0.019$

$b = 0.277 = 0.308*$

(* 0.9 grams of dry resin was used and therefore the slope of the curve scaled up accordingly.)

CALCULATION OF RESIN BEAD SURFACE AREAS

The resin was screened, as explained in Section 3.3, and the following resin size distribution resulted;

Resin size (microns)	percent by weight
> 1000	0.5
1000 < 850	1.6
850 < 600	19.7
600 < 425	60.2
425 < 300	15.0
300 < 150	2.5
< 150	0.5

A graph of percent oversize versus log particle size was then plotted. Using this plot the six resin sizes were subdivided into 50 and 25 microns size intervals as follows;

Resin size (microns)	% cumulative oversize	Area (1)	Volume (2)	No. of beads	Surface area (3)
1000-950	0.9	2.99	4.85	1970	5.890
950-900	1.5	2.69	4.14	3462	9.313
900-850	2.1	2.41	3.51	4083	9.840
					25.04
850-800	4.2	2.14	2.94	1391	2.977
800-750	7.0	1.89	2.44	2224	4.203
750-700	10.0	1.65	2.00	2904	4.792
700-650	15.6	1.43	1.61	6741	9.640
650-600	21.8	1.23	1.28	9405	11.57
					33.18
600-550	34.0	1.04	0.995	7797	8.109
550-500	53.0	0.866	0.758	15932	13.80
500-450	76.5	0.709	0.561	26568	18.84
450-425	82.0	0.600	0.437	7958	4.775
					45.52

425-400	87.0	0.533	0.366	34771	18.53
400-350	93.0	0.422	0.276	55386	23.37
350-300	97.0	0.332	0.180	56688	18.82
					60.72
300-250	98.0	0.238	0.109	140244	33.38
250-200	98.8	0.159	0.060	205190	32.63
200-150	99.5	0.096	0.010	380806	36.64
					102.6

(1) - is the outside surface area (* 10^{-6} m^2) of a single resin bead of average size in the fraction.

(2) - is the volume (* 10^{-4} cm^3) of a single resin bead of average size in the resin fraction.

(3) - is the overall surface area (* 10^{-3} m^2) for the particular resin size fraction.

In each 50 or 25 micron resin size fraction an average surface area and volume for a single resin bead was calculated. Using these figures, the published density of the resin (0.157 g/cm^3), and the cumulative percent oversize a surface area for a size fraction can be calculated as follows;

$$\text{no. of beads} = \frac{\text{volume occupied by the resin}}{\text{volume of one bead}}$$

1 gram of resin occupies = $1/0.157$ cm^3

$= 6.37$ cm^3

porosity in a bed of spheres = 0.4

therefore volume occupied by the resin = $0.6 * 6.37$

$= 3.82$ cm^3

Using the 1000-950 size interval as an example,

no. of beads in a 1g bed of resin = $3.82 / 4.85 * 10^{-4}$

= 7876 beads

But the 1000-950 size interval only accounts for 25% of the resin in the 1000-850 sieve size fraction,

therefore surface area attributed to this size fraction is

= 0.25 * area of one bead * 7876

= $5.890 * 10^{-3}$ m^2

Adding the surface areas for each 25 or 50 micron size interval gives the overall surface area for the particular sieve size fraction.

The weighted average resin bead size for a sieve size fraction was calculated using the average particle diameters for the 25 or 50 micron size intervals and the percent cumulative oversize as follows;

Weighted particle size =

the sum of (average particle size * fraction of the sieve sample)

Taking the 1000-850 sieve size fraction as an example.

Weighted particle size = [(975 * 25)+(925 * 37.5)+(875 * 37.5)]

= 919 microns

A P P E N D I X C

THE EFFECT OF SUPERFICIAL FLUID VELOCITY ON ADSORPTION RATE

TITLE : THE EFFECT OF FLOW RATE ON ADSORPTION RATE

RUN NO. : 1a

RESIN : Amberlite IRA 938

RESIN BEAD SIZE : 508 microns

COLLOID : Primal E1743

FLOW RATE : 43 ml/min

pH : 7 +- 1.5

IONIC STRENGTH : distilled water

TIME (min)	COLLOID CONCENTRATION (abs)	-ln(C/Co)
0	0.855	0.000
1.25	0.685	0.097
2.5	0.628	0.184
3.75	0.585	0.255
5.0	0.535	0.344
6.25	0.500	0.412
7.5	0.460	0.495
10.0	0.390	0.661
12.5	0.330	0.828
15.0	0.278	0.999
17.5	0.233	1.176
20.0	0.190	1.380
22.5	0.160	1.552
25.0	0.130	1.759
30.0	0.108	1.945
35.0	0.070	2.378

Straight line curve fit - least square method.

$y = a + bx$

Regression coefficient $R = 0.998$

$a = 0.002$

$b = 0.068$

TITLE : THE EFFECT OF FLOW RATE ON ADSORPTION RATE

RUN NO. : 1b

RESIN : Amberlite IRA 938

RESIN BEAD SIZE : 508 microns

COLLOID : Primal E1743

FLOW RATE : 80 ml/min

pH : 7 +- 1.5

IONIC STRENGTH : distilled water

TIME (min)	COLLOID CONCENTRATION (abs)	-ln(C/Co)
0	0.719	0.000
1.25	0.579	0.217
2.50	0.419	0.540
3.75	0.374	0.654
5.00	0.294	0.894
6.25	0.249	1.060
7.50	0.204	1.260
8.75	0.164	1.478
11.25	0.104	1.933
13.75	0.069	2.344
16.25	0.044	2.794
18.75	0.029	3.211

Straight line curve fit - least square method.

$y = a + bx$

Regression coefficient R = 0.999
a = 0.024
b = 0.169

TITLE : THE EFFECT OF FLOW RATE ON ADSORPTION RATE

RUN NO. : 1c

RESIN : Amberlite IRA 938

RESIN BEAD SIZE : 508 microns

COLLOID : Primal E1743

FLOW RATE : 117 ml/min

pH : 7 +- 1.5

IONIC STRENGTH : distilled water

TIME (min)	COLLOID CONCENTRATION (abs)	-ln(C/Co)
0	0.660	0.000
0.5	0.590	0.112
1.0	0.535	0.210
1.5	0.485	0.308
2.5	0.400	0.501
3.5	0.325	0.708
4.5	0.270	0.894
5.5	0.225	1.076
6.5	0.183	1.283
7.5	0.150	1.482
8.5	0.125	1.664
10.5	0.085	2.050
12.5	0.060	2.398
14.5	0.045	2.686
16.5	0.035	2.937

Straight line curve fit - least square method.

$y = a + bx$

Regression coefficient $R = 0.997$
$a = 0.055$
$b = 0.183$

TITLE : THE EFFECT OF FLOW RATE ON ADSORPTION RATE

RUN NO. : 2a

RESIN : Amberlite IRA 938

RESIN BEAD SIZE : 508 microns

COLLOID : Primal E1743

FLOW RATE : 46 ml/min

pH : 7 +- 1.5

IONIC STRENGTH : distilled water

TIME (min)	COLLOID CONCENTRATION (abs)	-ln(C/Co)
0	0.730	0.000
2.5	0.615	0.171
5.0	0.525	0.330
7.5	0.455	0.473
10.0	0.385	0.640
12.5	0.330	0.794
15.0	0.280	0.958
20.0	0.202	1.285
25.0	0.140	1.651
30.0	0.095	2.039
35.0	0.065	2.419
40.0	0.043	2.832

Straight line curve fit - least square method.

$y = a + bx$

Regression coefficient R = 0.998
a = -0.048
b = 0.070

TITLE : THE EFFECT OF FLOW RATE ON ADSORPTION RATE

RUN NO. : 2b

RESIN : Amberlite IRA 938

RESIN BEAD SIZE : 508 microns

COLLOID : Primal E1743

FLOW RATE : 77 ml/min

pH : 7 +- 1.5

IONIC STRENGTH : distilled water

TIME (min)	COLLOID CONCENTRATION (abs)	-ln(C/Co)
0	0.820	0.000
1	0.775	0.195
2	0.590	0.329
3	0.507	0.481
4	0.435	0.634
5	0.370	0.796
6	0.317	0.950
7	0.270	1.111
8	0.225	1.293
9	0.195	1.436
10	0.170	1.574
12	0.122	1.905
14	0.090	2.209
17	0.060	2.615

Straight line curve fit - least square method.

$y = a + bx$

Regression coefficient R = 0.999
a = 0.024
b = 0.155

TITLE : THE EFFECT OF FLOW RATE ON ADSORPTION RATE

RUN NO. : 2c

RESIN : Amberlite IRA 938

RESIN BEAD SIZE : 508 microns

COLLOID : Primal E1743

FLOW RATE : 98 ml/min

pH : 7 +- 1.5

IONIC STRENGTH : distilled water

TIME (min)	COLLOID CONCENTRATION (abs)	-ln(C/Co)
0	0.770	0.000
1	0.640	0.185
2	0.550	0.336
3	0.465	0.504
4	0.390	0.680
5	0.328	0.853
6	0.280	1.012
7	0.237	1.176
8	0.200	1.348
9	0.171	1.511
10	0.144	1.677
12	0.104	2.002
14	0.075	2.329

Straight line curve fit - least square method.

$y = a + bx$

Regression coefficient $R = 1.000$
$a = 0.011$
$b = 0.166$

TITLE : THE EFFECT OF FLOW RATE ON ADSORPTION RATE

RUN NO. : 3a

RESIN : Amberlite IRA 938

RESIN BEAD SIZE : 508 microns

COLLOID : Primal E1743

FLOW RATE : 65 ml/min

pH : 7 +- 1.5

IONIC STRENGTH : distilled water

TIME (min)	COLLOID CONCENTRATION (abs)	-ln(C/Co)
0	0.780	0.000
1	0.702	0.105
2	0.642	0.195
3	0.590	0.279
4	0.545	0.359
5	0.500	0.445
6	0.460	0.528
7	0.425	0.607
8	0.390	0.693
9	0.360	0.773
10	0.330	0.866
12	0.277	1.035
14	0.235	1.200
16	0.200	1.361
18	0.165	1.553
20	0.138	1.732

Straight line curve fit - least square method.

$y = a + bx$

Regression coefficient $R = 1.000$
$a = 0.015$
$b = 0.085$

TITLE : THE EFFECT OF FLOW RATE ON ADSROPTION RATE

RUN NO. : 3b

RESIN : Amberlite IRA 938

RESIN BEAD SIZE : 508 microns

COLLOID : Primal E1743

FLOW RATE : 81 ml/min

pH : 7 +- 1.5

IONIC STRENGTH : distilled water

TIME (min)	COLLOID CONCENTRATION (abs)	-ln(C/Co)
0	0.800	0.000
1	0.681	0.161
2	0.597	0.293
3	0.550	0.375
4	0.465	0.543
5	0.405	0.681
6	0.355	0.812
7	0.310	0.948
8	0.270	1.086
10	0.205	1.362
12	0.155	1.641
14	0.115	1.940
16	0.085	2.242

Straight line curve fit - least square method.

$y = a + bx$

Regression coefficient $R = 0.999$
$a = -0.009$
$b = 0.139$

TITLE : THE EFFECT OF FLOW RATE ON ADSORPTION RATE

RUN NO. : 3c

RESIN : Amberlite IRA 938

RESIN BEAD SIZE : 508 microns

COLLOID : Primal E1743

FLOW RATE : 98 ml/min

pH : 7 +- 1.5

IONIC STRENGTH : distilled water

TIME (min)	COLLOID CONCENTRATION (abs)	-ln(C/Co)
0	0.755	0.000
1	0.625	0.189
2	0.533	0.348
3	0.455	0.506
4	0.385	0.673
5	0.325	0.843
6	0.275	1.010
7	0.232	1.180
8	0.195	1.354
9	0.165	1.521
10	0.137	1.707
12	0.095	2.073
14	0.067	2.422
16	0.047	2.777

Straight line curve fit - least square method.

$y = a + bx$

Regression coefficient $R = 1.000$

$a = -0.012$

$b = 0.173$

TITLE : THE EFFECT OF FLOW RATE ON ADSORPTION RATE

RUN NO. : 3d

RESIN : Amberlite IRA 938

RESIN BEAD SIZE : 508 microns

COLLOID : Primal E1743

FLOW RATE : 132 ml/min

pH : 7 +- 1.5

IONIC STRENGTH : distilled water

TIME (min)	COLLOID CONCENTRATION (abs)	-ln(C/Co)
0	0.710	0.000
0.5	0.643	0.099
1.5	0.528	0.296
2.5	0.433	0.495
3.5	0.358	0.685
4.5	0.300	0.861
5.5	0.246	1.060
6.5	0.205	1.242
7.5	0.171	1.424
8.5	0.141	1.617
10.5	0.096	2.001
12.5	0.066	2.376
14.5	0.046	2.737
16.5	0.031	3.131

Straight line curve fit - least square method.

$y = a + bx$

Regression coefficient R = 1.000
a = 0.013
b = 0.189

TITLE : THE EFFECT OF FLOW RATE ON ADSORPTION RATE

RUN NO. : 4a

RESIN : Amberlite IRA 938

RESIN BEAD SIZE : 508 microns

COLLOID : Primal E1743

FLOW RATE : 55 ml/min

pH : 7 +- 1.5

IONIC STRENGTH : distilled water

TIME (min)	COLLOID CONCENTRATION (abs)	-ln(C/Co)
0	0.850	0.000
1	0.775	0.092
2	0.714	0.175
3	0.658	0.256
4	0.609	0.334
5	0.557	0.422
6	0.516	0.500
7	0.475	0.581
8	0.438	0.663
9	0.404	0.744
10	0.373	0.824
12	0.316	0.991
14	0.268	1.155

Straight line curve fit - least square method.

$y = a + bx$

Regression coefficient R = 1.000
a = 0.008
b = 0.082

TITLE : THE EFFECT OF FLOW RATE ON ADSRPTION RATE

RUN NO. : 4b

RESIN : Amberlite IRA 938

RESIN BEAD SIZE : 508 microns

COLLOID : Primal E1743

FLOW RATE : 66 ml/min

pH : 7 +- 1.5

IONIC STRENGTH : distilled water

TIME (min)	COLLOID CONCENTRATION (abs)	-ln(C/Co)
0	0.830	0.000
1	0.726	0.134
2	0.648	0.248
3	0.578	0.362
4	0.509	0.490
5	0.453	0.605
6	0.402	0.725
7	0.356	0.847
8	0.315	0.969
9	0.279	1.090
10	0.245	1.220
12	0.191	1.470
14	0.146	1.740

Straight line curve fit - least square method.

$y = a + bx$

Regression coefficient $R = 1.000$
$a = -0.004$
$b = 0.123$

TITLE : THE EFFECT OF FLOW RATE ON ADSORPTION RATE

RUN NO. : 4c

RESIN : Amberlite IRA 938

RESIN BEAD SIZE : 508 microns

COLLOID : Primal E1743

FLOW RATE : 86 ml/min

pH : 7 +- 1.5

IONIC STRENGTH : distilled water

TIME (min)	COLLOID CONCENTRATION (abs)	-ln(C/Co)
0	0.810	0.000
1	0.678	0.176
2	0.575	0.342
3	0.487	0.508
4	0.414	0.672
5	0.360	0.811
6	0.298	1.000
7	0.253	1.164
8	0.214	1.330
9	0.182	1.492
10	0.155	1.657
12	0.111	1.987

Straight line curve fit - least square method.

$y = a + bx$

Regression coefficient R = 1.000
a = 0.007
b = 0.165

TITLE : THE EFFECT OF FLOW RATE ON ADSORPTION RATE

RUN NO. : 4d

RESIN : Amberlite IRA 938

RESIN BEAD SIZE : 508 microns

COLLOID : Primal E1743

FLOW RATE : 128 ml/min

pH : 7 +- 1.5

IONIC STRENGTH : distilled water

TIME (min)	COLLOID CONCENTRATION (abs)	-ln(C/Co)
0	0.882	0.000
1	0.725	0.196
2	0.606	0.375
3	0.503	0.562
4	0.417	0.750
5	0.345	0.938
6	0.286	1.126
7	0.237	1.314
8	0.197	1.501
9	0.163	1.686
10	0.136	1.873
12	0.093	2.245

Straight line curve fit - least square method.

$y = a + bx$

Regression coefficient $R = 0.999$
$a = 0.003$
$b = 0.187$

A P P E N D I X D

THE EFFECT OF SURFACE CHARGE ON ADSORPTION RATE

AMBERLITE IRA 938 AND IT'S CATION AND UNCHARGED EQUIVALENTS

CALCULATION OF INTERACTION POTENTIAL ENERGIES

CALCULATION OF ZETA POTENTIALS

TITLE : THE EFFECT OF SURFACE CHARGE ON ADSORPTION RATE

RUN NO. : 1a

RESIN : Amberlite IRA 938

RESIN BEAD SIZE : 508 microns

COLLOID : silicon dioxide

FLOW RATE : 70 ml/min

pH : 7 +- 1.5

IONIC STRENGTH : distilled water

TIME (min)	COLLOID CONCENTRATION (NTU)	-ln(C/Co)
0	0.91	0.000
2	0.73	0.220
4	0.59	0.433
6	0.48	0.640
8	0.40	0.822
10	0.32	1.045
12	0.26	1.253
14	0.21	1.466
16	0.18	1.620
18	0.16	1.738

Straight line curve fit - least square method.

$y = a + bx$

Regression coefficient $R = 0.997$
$a = 0.033$
$b = 0.099$

TITLE : THE EFFECT OF SURFACE CHARGE ON ADSORPTION RATE

RUN NO. : 1b

RESIN : Amberlite IRA 938

RESIN BEAD SIZE : 508 microns

COLLOID : silicon dioxide

FLOW RATE : 70 ml/min

pH : 7 +- 1.5

IONIC STRENGTH : distilled water

TIME (min)	COLLOID CONCENTRATION (abs)	-ln(C/Co)
0	0.76	0.000
2	0.61	0.220
4	0.49	0.439
6	0.41	0.617
8	0.34	0.804
10	0.27	1.035
12	0.22	1.240
14	0.18	1.440
16	0.15	1.623
18	0.13	1.766

Straight line curve fit - least square method.

$y = a + bx$

Regression coefficient R = 0.999
a = 0.023
b = 0.099

TITLE : THE EFFECT OF SURFACE CHARGE ON ADSORPTION RATE

RUN NO. : 2a

RESIN : Amberlite IRA 938

RESIN BEAD SIZE : 508 microns

COLLOID : silicon dioxide

FLOW RATE : 70 ml/min

pH : 4 +- 0.2

IONIC STRENGTH : distilled water

Silicon dioxide did not adsorb to Amberlite IRA 938 resin at this pH.

TITLE : THE EFFECT OF SURFACE CHARGE ON ADSORPTION RATE

RUN NO. : 3a

RESIN : Amberlite IRA 938

RESIN BEAD SIZE : 508 microns

COLLOID : silicon dioxide

FLOW RATE : 70 ml/min

pH : 10 +- 0.2

IONIC STRENGTH : distilled water

TIME (min)	COLLOID CONCENTRATION (abs)	-ln(C/Co)
0	0.98	0.000
2	0.83	0.166
4	0.73	0.295
6	0.63	0.442
8	0.55	0.578
10	0.48	0.714
12	0.42	0.847
14	0.38	0.947
16	0.33	1.088
18	0.30	1.184

Straight line curve fit - least square method.

$y = a + bx$

Regression coefficient R = 0.997
a = 0.034
b = 0.066

TITLE : THE EFFECT OF SURFACE CHARGE ON ADSORPTION RATE

RUN NO. : 3b

RESIN : Amberlite IRA 938

RESIN BEAD SIZE : 508 microns

COLLOID : silicon dioxide

FLOW RATE : 70 ml/min

pH : 10 +- 0.2

IONIC STRENGTH : distilled water

TIME (min)	COLLOID CONCENTRATION (abs)	-ln(C/Co)
0	0.97	0.000
2	0.82	0.168
4	0.71	0.312
6	0.61	0.464
8	0.54	0.586
10	0.48	0.704
12	0.42	0.837
14	0.37	0.964
16	0.33	1.078
18	0.29	1.207
20	0.26	1.317

Straight line curve fit - least square method.

$y = a + bx$

Regression coefficient R = 0.998
a = 0.045
b = 0.065

TITLE : THE EFFECT OF SURFACE CHARGE ON ADSORPTION RATE

RUN NO. : 4a

RESIN : Amberlite IRA 938

RESIN BEAD SIZE : 508 microns

COLLOID : Primal E1743

FLOW RATE : 70 ml/min

pH : 7 +- 1.5

IONIC STRENGTH : distilled water

TIME (min)	COLLOID CONCENTRATION (abs)	-ln(C/Co)
0	0.660	0.000
2	0.517	0.244
4	0.415	0.464
6	0.333	0.684
8	0.270	0.894
10	0.217	1.112
12	0.177	1.316
14	0.145	1.516
16	0.120	1.705
18	0.100	1.887

Straight line curve fit - least square method.

$y = a + bx$

Regression coefficient $R = 0.999$

$a = 0.039$

$b = 0.105$

TITLE : THE EFFECT OF SURFACE CHARGE ON ADSORPTION RATE

RUN NO. : 5a

RESIN : Amberlite IRA 938

RESIN BEAD SIZE : 508 microns

COLLOID : Primal E1743

FLOW RATE : 70 ml/min

pH : 4 +- 0.2

IONIC STRENGTH : distilled water

TIME (min)	COLLOID CONCENTRATION (abs)	-ln(C/Co)
0	0.825	0.000
1	0.750	0.095
2	0.675	0.201
4	0.555	0.396
6	0.453	0.599
8	0.367	0.810
10	0.300	1.012
12	0.245	1.214
14	0.202	1.407
16	0.167	1.597
18	0.140	1.774

Straight line curve fit - least square method.

$y = a + bx$

Regression coefficient R = 1.000
a = 0.003
b = 0.100

TITLE : THE EFFECT OF SURFACE CHARGE ON ADSORPTION RATE

RUN NO. : 6a

RESIN : Amberlite IRA 938

RESIN BEAD SIZE : 508 microns

COLLOID : Primal E1743

FLOW RATE : 70 ml/min

pH : 10 +- 0.2

IONIC STRENGTH : distilled water

TIME (min)	COLLOID CONCENTRATION (abs)	-ln(C/Co)
0	0.725	0.000
2	0.615	0.165
4	0.518	0.336
6	0.438	0.504
8	0.373	0.665
10	0.316	0.830
12	0.268	0.996
14	0.230	1.148
16	0.200	1.288
18	0.170	1.450
20	0.146	1.603

Straight line curve fit - least square method.

$y = a + bx$

Regression coefficient $R = 0.999$
$a = 0.015$
$b = 0.080$

potential energy curves for the Primal E1743 and silicon dioxide - Amberlite IRA 938 resin system at three different pH values. The effect of the increase in the attractive force between the colloid and the resin, due to the changes in zeta potential between pH 7 and pH 10 shown in Table 4.8, is completely masked by the effect of the increase in the total ionic strength of the solution due to the chemicals added to adjust the pH. Figure 4.13 shows, however, that there is still a significant difference in the strength of the attractive forces operating at the two pH values and accordingly the adsorption rate at a pH of 10 should be faster than that at a pH of 4. This however was not indicated in the measured rates. Similarly according to Figure 4.14 the adsorption rate of silicon dioxide to Amberlite IRA 938 resin should not have been zero at a pH of 4.

The above discrepancies could possibly arise from inaccuracies in the values of the zeta potentials used in the calculations. The uncertainty in the zeta potentials of the Primal E1743 particles is however believed to be less than 15%. The measured values are presented in Appendix D. The zeta potential of silicondioxide and titanium dioxide were taken from the literature (54,55) and may not accurately reflect the particular materials used in these experiments. Further, the inconsistencies could arise from errors in the calculation of the total interaction potential energies, which arise from the uncertainty in the values of the Hamaker constants and the application of the linearised solution of the Poisson - Boltzmann equation, beyond its normal range of applicability: the equation only holds exactly for zeta potentials below 25mv.

The effect of surface charge on the adsorption is well illustrated in Figure 4.15 which shows the variation of interaction potential energy with pH for the titanium dioxide - Amberlite IRA 938 resin system. At a pH of 4 there is a potential energy barrier, due to the repulsive coulombic forces, which must be overcome if adsorption is to occur. A colloidal particle has to have an approach distance of less than 25 Angstroms from the resin surface before London - van der Waals attractive forces overcome the coulombic forces and adsorption can occur.

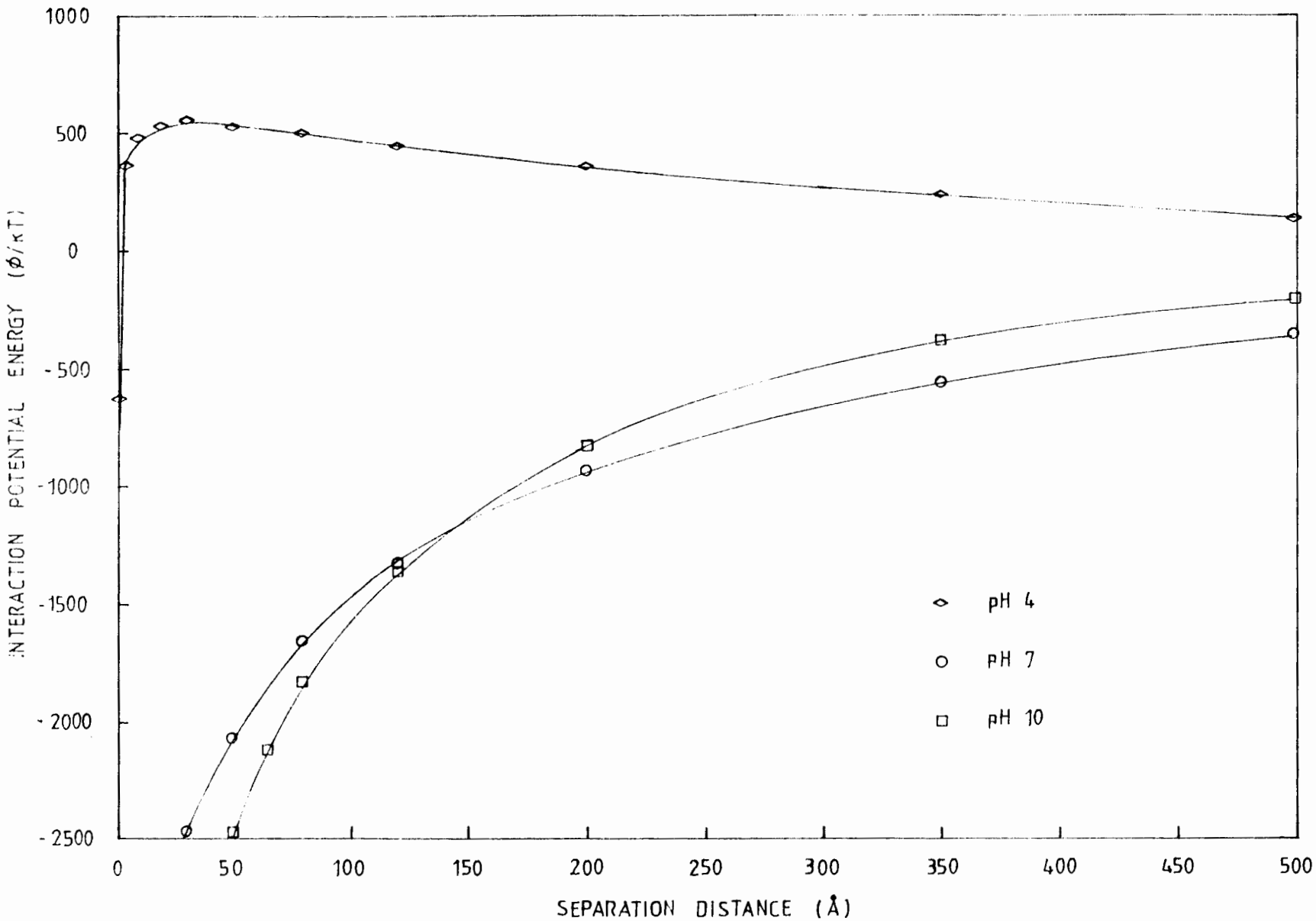

Figure 4.15 THE EFFECT OF pH ON THE INTERACTION POTENTIAL ENERGY CURVES FOR THE AMBERLITE IRA 938 RESIN - TITANIUM DIOXIDE SYSTEM.

Calculation of the adsorption rate using the approaches of Prieve and Ruckenstein (40,41) and Kim and Ragagopalan (11) presented in Section 2.4 both indicate that the dimensionless potential energy barrier (V_{max}) value of 545 (see Appendix D for calculation method) is about 2 orders of magnitude too large to allow any significant adsorption. The observed adsorption rate of zero, therefore is quite reasonable.

At low separation distances the forces of attraction at a pH of 10, due to coulombic forces (see Figure 4.15), are stronger than at a pH of 7. However as the separation distance increases the effect of increased ionic strength at the higher pH of 10 decreases the attractive forces between the particle and the resin. The two curves therefore cross and the attractive forces at a pH of 7 become stronger than those at a pH of 10.

4.5 ADSORPTION MODEL

4.5.1 Qualitative model

Having discussed the role of each parameter affecting adsorption of colloidal particles to Amberlite IRA 938 resin, the phenomena observed experimentally can be summarised and explained by the following "qualitative model".

Colloidal particles are in constant motion in the liquid phase and exist as stable individual particles capable of diffusion by stochastic processes under either a concentration gradient or an electrostatic force field. Inertia and interception effects are insignificant in the particle size range of interest in this study.

A stagnant boundary layer surrounding the resin beads with an electrostatic sub-layer intruding part of the way from the resin into the boundary layer can be envisaged. The thickness of the stagnant boundary layer depends upon:

i) Superficial fluid velocity in the resin bed.
ii) Surface roughness of the resin.

The distance the electrostatic sub-layer intrudes into the stagnant boundary layer depends on:

i) Zeta potentials of the resin and colloid.
ii) pH of the colloid suspension.
iii) Ionic strengh of the colloid suspension.

Particles diffuse across the the stagnant boundary layer, reach the electrostatic sub-layer and are accelerated towards the resin surface. As the particles approach the resin surface they are slowed by hydrodynamic retardation. On reaching the resin surface physisorption occurs.

Adsorption of colloidal particles to Amberlite IRA 938 resin first occurs at the outermost surfaces of the resin. The adsorption zone then moves into the resin and leaves behind a covered/converted resin outer region. Thus at any time there exists a clean/unreacted core of resin which shrinks in size during the adsorption process. However, in most cases the adsorption zone is less than 50 microns thick because colloid diffusion in the resin pores is very slow. At high resin loading pore diffusion is adsorption rate controlling.

At low resin loading, adsorption occurs only on the outermost surfaces of the resin and consequently the thickness of the hydrodynamic boundary layer is important. Thus adsorption at high and low flow rates should be considered further.

At low flow rates the stagnant boundary layer surrounding the resin beads is thick compared to the electrostatic sublayer, therefore adsorption is film diffusion controlled.

At high flow rates the stagnant boundary layer becomes very thin, colloid movement to the resin surface is rapid and consequently the particles arrive at the resin surface faster than they can be removed by physisorption. Film diffusion control tends to give way to surface reaction control.

Adsorption to the resin can be enhanced, retarded or prevented by the surface charge on the resin and colloidal particle. Like

charges retard or prevent adsorption while opposite charges can enhance the adsorption rate to the resin. The degree to which surface forces enhance or retard the adsorption is largely dependent on the ionic strength of the solution. Coulombic/double -layer forces act over large distances at low ionic strengths and thus adsorption rates are highest at low ionic strengths.

4.5.2 Numerical Model

The adsorption of colloidal particles to a collector surface against a potential energy barrier, has been well covered by Prieve and Ruckenstein and Kim and Rajagopalan (see Section 2.4). From their investigations it appears that significant adsorption against a potential energy barrier, is likely to occur only if the potential energy barrier is small and in this case adsorption rates appear to be adequately modelled by their equations (8 and 14 in Section 2.6).

However, the numerical solution to the problem of predicting the enhanced adsorption rates of colloidal particles to the surface of Amberlite IRA 938 resin requires the calculation of an "effective" diffusion film thickness.

The "effective" diffusion film is described by the dimensionless parameter:

$$\alpha = \delta_d/\delta_\phi \qquad - 1$$

where δ_d is the diffusion film thickness and δ_ϕ is the distance over which the London - van der Waals and Double layer forces are active.

As α becomes large, the adsorption rate becomes film diffusion controlled and as α becomes small, the adsorption rate becomes surface reaction controlled.

4.5.2.1 Case of low surface coverage

Adsorption to the outer surface of the resin, as explained in section 4.4.4, can be considered to be controlled by two resistances or rate controlling steps in series. Further the adsorption rate, assuming very low surface coverage, can be modelled using first order kinetics, where the rate constant is made up of two terms.

$$- r_a = \frac{1}{V} kC_a \qquad \text{where } C_{so} \text{ is a constant}$$

$$\text{and} \quad k = \left[\frac{1}{k_f} + \frac{1}{k_r}\right]^{-1} \qquad - 2$$

k_f is the film mass transfer rate constant and is determined by the thickness of the diffusion boundary layer. k_r is the reaction rate constant and is determined by the speed of the physisorption step.

Most convective diffusion equations are based on three parameters;

i) the concentration difference,
ii) the thickness of the diffusion film, and
iii) the particle diffusion coefficient.

$$- r_a = \frac{D(C_a - C_c)S}{\delta} \qquad - 3$$

As explained in section 2.4, C_c can be assumed to be zero for film diffusion controlled adsorption, and if S, the available surface area of the collector, is almost constant the equation becomes:

$$- r_a \propto \frac{DC_a}{\delta} \qquad - 4$$

Combining equations 2 and 4, for the film diffusion controlled situation (ie. $k_r << k_f$), one finds that the film mass transfer rate is related to the diffusion coefficient of the particles and the diffusion film thickness.

$$k_f \propto D/\delta \qquad - 5$$

The "effective" diffusion boundary layer covering a collector

surface can be significantly thinner than the diffusion boundary layer thickness, δ_d , as the zone of interaction forces, δ_ϕ , lies within the diffusion boundary layer. The movement of colloidal particles in the zone of interaction forces is not governed by Brownian diffusion, but by the London - van der Waals and coulombic forces.

In this work the limit of the zone of interaction forces, δ_ϕ , is defined as that distance between a particle and collector that produces a dimensionless interaction potential energy, $\Phi/k_BT \cong -10$. (This gives rise to a force that produces particle velocities approximately equal to Brownian diffusion velocities.)

The "effective" distance across which diffusion takes place has been defined as follows;

$$\delta_{eff} = \delta_d\left(\frac{\alpha}{\alpha+1}\right) \qquad - 6$$

$$\text{where} \quad \alpha = \frac{\delta_d}{\delta_\phi}$$

This is an empirical equation based on equations presented by Ruckenstein and Prieve and Spielman and Friedlander. In the extreme case of very low ionic strength and very high superficial velocities where δ_d and δ_ϕ can be of similar magnitude and δ_{eff} is a fraction of δ_d , this equation appears to be inaccurate (ie. if $\delta_d \cong \delta_\phi$ then $\alpha \cong 1$, which would give $\delta_{eff} \cong \frac{1}{2}\delta_d$). However to refine it further for this extreme case a more rigorous treatment of the roles of the steep and flat portions of the interaction potential energy curves in the acceleration of the particles would be required.

Φ can be calculated by summing the coulombic, $\Phi_R(x)$, and London - van der Waals, $\Phi_A(x)$, interaction potential energies for various separation distances, between the colloid and resin surface, using the following equations,

$$\Phi_A(x) = \frac{A_{132}}{6}\left[\ln\frac{(x+2a_h)}{x} - \frac{2a_h(x+a_h)}{x(x+2a_h)}\right] \qquad - 7$$

where x is the separation distance between the resin and colloid, a_h the radius of the particle and A_{132} the Hamakers constant for the system.

$$\Phi_R(x) = \pm \frac{\xi a_h}{4} \left[(\Psi_1 + \Psi_2)^2 \ln(1 \pm e^{-\kappa x}) + (\Psi_1 - \Psi_2)^2 \ln(1 \mp e^{-\kappa x}) \right] \quad - 8$$

where ξ is the dielectric constant of the medium, κ the Debye-Huckel reciprical length and Ψ_1, Ψ_2 the surface potentials of the resin and particles respectively.
(See Appendix D for calculation procedures of $\Phi_A(x)$ and $\Phi_R(x)$.)

δ_d, the characteristic thickness of the diffusion layer, is calculated using a correlation based on the Levich relation,

$$\delta_d \cong a(D/Ua)^{\frac{1}{3}} \quad - 9$$

This relation, discussed in section 4.4.3, overestimates the thickness of the diffusion boundary layer. This inaccuracy probably arises from the fact that the above relation was derived for smooth spheres. Amberlite IRA 938 resin is highly macroporous and consequently has a rough surface.

Equation 8 was therefore modified by the addition of a "roughness term" as follows:

$$\delta_d \cong Ra(D/Ua)^{\frac{1}{3}}$$

$$R = 0{,}58\ Re^{-2{,}76} \quad - 10$$

The roughness term, R, was determined using the results in Appendix C and is therefore an empirical relation.

Using equations 2,5,6,7,8 and 10 one can predict the adsorption rate of colloidal particles to Amberlite IRA 938 for any given set of conditions (ie. flow rate , ionic strength, bulk solution/ suspension pH and zeta potential of the colloidal species).

In Figure 4.16 the experimental results of adsorption rate versus flow rate for the Primal E1743 - Amberlite IRA 938 resin system, are compared with the predicted results using the above approach. It is apparent that for the conditions used in the calculations, the numerical model adequately models the adsorption process.

Figure 4.17 compares predicted and experimental results of adsorption rate as a function of ionic strength. The predicted

rates are slighly higher but the trends in the two curves are identical.

The offset is considered of small significance considering the scatter in the experimental adsorption rates at low flow rates, shown in Figure 4.16. Should the empirical roughness factor, have been based on either of the extreme adsorption rates (envelope limits) shown in Figure 4.16 instead of an average adsorption rate, the predicted results in Figure 4.17 would have been represented by either of the dashed curves.

4.5.2.2 Case of high total surface coverage

This case was not studied, as high surface coverages were impossible to attain in reasonable contact times and thus would be of little practical use. For example it took 3.12 days to get a total coverage of 3.5% in the column studies and 104 days to get similar coverages in the equilibrium studies on the tumbler wheel. This case was therefore not considered important, however the mechanisms of pore diffusion in the resin beads and a rate expression for high surface coverages are discussed in sections 4.2.5 and 4.2.6 respectively.

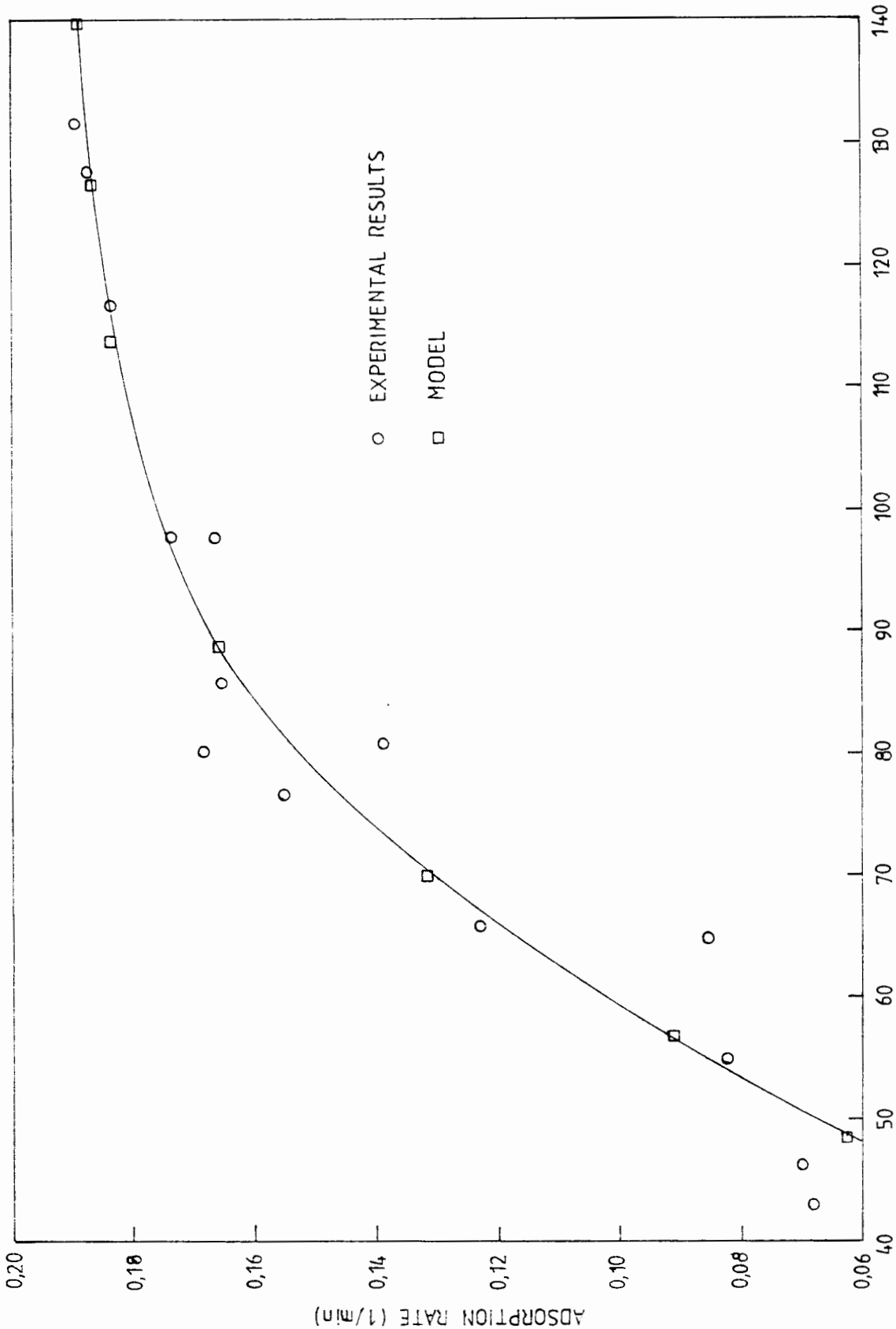

Figure 4.16 A COMPARISON BETWEEN PREDICTED AND MEASURED ADSORPTION RATES AS AFFECTED BY FLOW RATE.

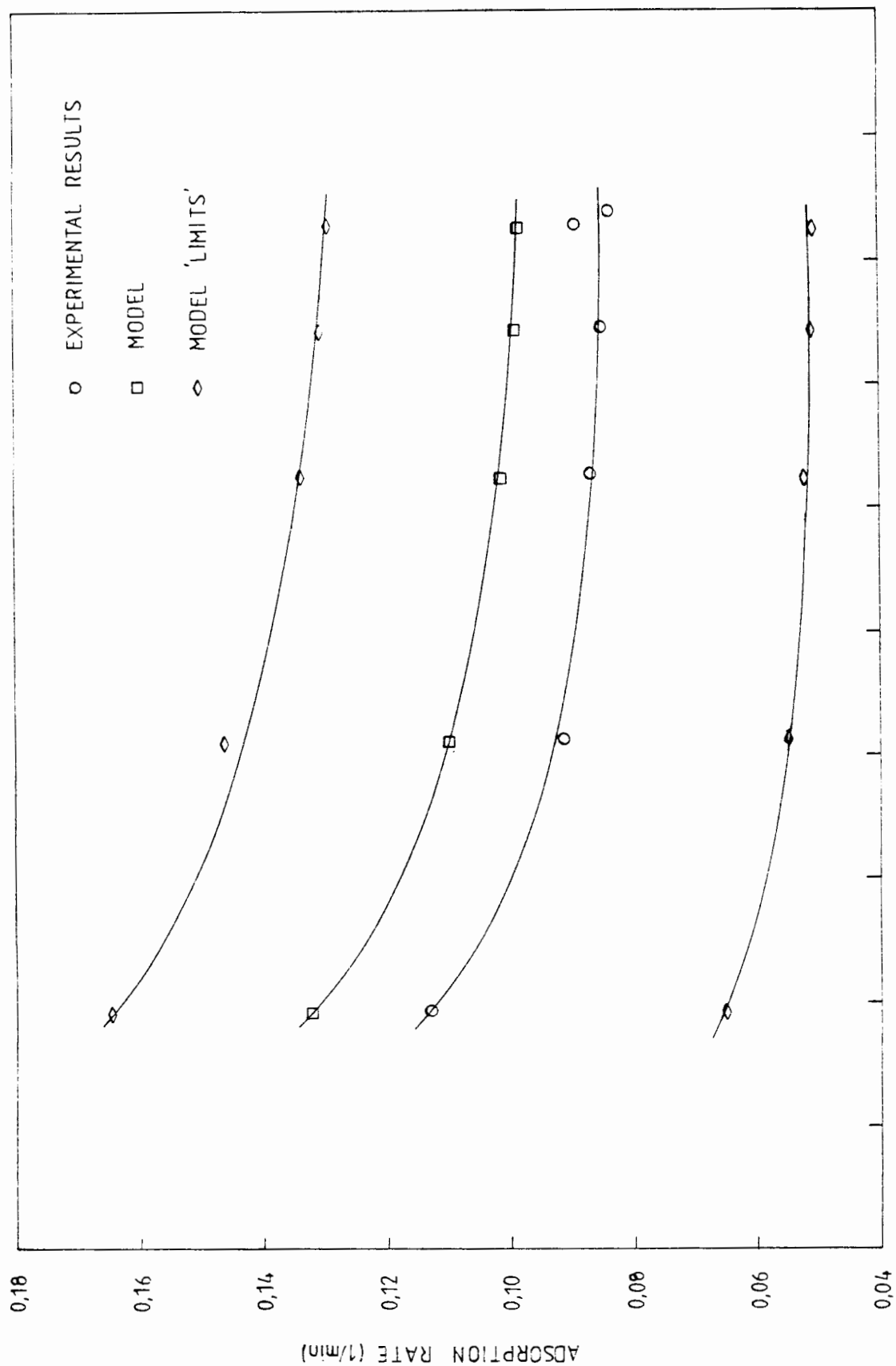

Figure 4.17 A COMPARISON BETWEEN PREDICTED AND MEASURED ADSORPTION RATES AS EFFECTED BY IONIC STRENGTH.

CHAPTER 5

CONCLUSIONS

Adsorptive filtration using highly porous ion-exchange resins or other similar materials offers a useful technique for removal of colloidal matter from water. This technique offers an efficient alternative to the current practices of flocculation, coagulation and filtration.

In certain colloid - resin collector systems adsorption is irreversible, resulting in potentially complete removal of colloidal impurities from water. Nevertheless techniques such as chemical regeneration and ultrasonic cleaning are feasible methods of regeneration of the ion-exchange resins used for this purpose.

Adsorption in other colloid - resin collector systems may be reversible. The adsorption is mainly dependent upon the surface charges on the resin and the colloid.

Colloid adsorption in the systems;

i) Primal E1743 - Amberlite IRA 938 resin
ii) Silicon dioxide - Amberlite IRA 938 resin
iii) Natural seawater colloids - Amberlite IRA 938 resin

is restricted to the resin outer shell or readily accessible surface, unless very long contact times are allowed, when the whole interior of the resin bead can be utilised. It is likely that the above is true for most colloid - collector systems using higly porous resin. Pore diffusion is very slow, but may be speeded if the adsorption vessel is placed in an ultasonic bath.

The rate of adsorption depends largely on the colloid particle transport mechanisms. Two regions and their corresponding transport mechanisms need to be considered:

i) Hydrodynamic boundary layer - surrounds the resin beads.
ii) Pores - within the resin beads.

The hydrodynamic boundary layer can be further subdivided into two regions. Colloid transport over its outer region is affected by the colloid concentration gradient and Brownian diffusion. Over the inner regions, adjacent to the resin surface, colloid transport is influenced by electrostatic forces.

When the electrostatic force is attractive, due to oppositely charged colloid and collector, the adsorption rate is enhanced and visa versa.

The extent to which the electrostatic forces intrude into the hydrodynamic boundary layer depends on the colloid and resin surface charges and the solution pH and ionic strength.

pH affects the surface charges on the resin collector and colloid particles and consequently affects the strength of adsorptive forces between them.

Ionic strength determines the thickness of the electrical double layer adjacent to the resin and colloidal particles, in accordance with the theory presented in section 2.2. Increased ionic strength shrinks the thickness of the electrical double layer and reduces the distance over which coulombic forces are active. Colloid adsorption rate to the resin is therefore reduced.

Colloid transport within the resin bead (pores) is governed by Knudsen diffusion and surface "hopping". These transport mechanisms are so slow that the internal porosity (surface area) of the resin can be ignored for practical applications.

The highly porous resin beads of Amberlite IRA 938 present an extended surface (ie. the resin has irregular projections) to the bulk fluid. The resin bead therefore, does not have a simple spherical boundary. An effective exterior surface area for the highly porous beads has been defined and calculated, in this work, by comparing measured adsorption rates for rough beads (Amberlite IRA 938) with those of otherwise identical smooth beads (Amberlite IRA 904).

Adsorption rate has been found to be first order with respect to

this effective exterior surface area.

Unlike the deeper internal resin porosity, porosity near the resin boundary affects the resin surface roughness in addition to enhancing the resin outside surface area, and thus affects the fluid flow close to the resin surface.

This effect can be explained if localised turbulence at and within the extended resin surface is assumed. This work defined and included a roughness factor in rate models to correlate the observed data for Amberlite IRA 938 resin.

At high superficial fluid velocities in a packed resin bed, the resin surface roughness causes considerable reduction in the hydrodynamic boundary layer thickness and consequently the colloid transport across this layer is rapid and mainly dependent on the electrostatic region. Thus at high flow rates the comparatively slow physisorption step can become adsorption rate limiting.

Colloid adsorption to Amberlite IRA 938 resin can only be understood and modelled if both the physical characteristics and the electrostatic forces of the system are considered.

In conclusion a simple model has been presented which fits the special case of colloid adsorption to highly porous ion-exchange resins such as Amberlite IRA 938. This model is based on three terms:

i) The thickness of the hydrodynamic boundary layer surrounding the highly porous Amberlite IRA 938 resin beads - this can be predicted by the incorporation of a roughness factor into the correlation derived by Levich for the hydrodynamic boundary layer surrounding smooth spheres.

ii) The extent to which the interaction forces intrude into the hydrodynamic boundary layer - this can be estimated by calculating the London - van der Waals and coulombic interaction potential energies between the resin and colloid. The equations used in the calculation of these interaction energies incorporate the following measured

values for the system; zeta potentials of the colloid and resin, colloid and resin particle size and the total ionic strength of the suspension.

iii) The surface reaction rate (physisorption rate) - this rate is estimated by extrapolation of superficial fluid velocity versus adsorption rate data.

This model has satisfactorily correlated adsorption data measured by this worker for the Amberlite IRA 938 - Primal E1743 system and qualitatively explained adsorption data collected for the other adsorption systems studied.

The approach used in this model can be applied to most colloid - collector systems and thus deserves further investigation.

CHAPTER 6

RECOMMENDATIONS

The work in this thesis covered the fluid dynamic and electrostatic factors expected to affect colloidal particle adsorption onto and into highly porous ion-exchange resins. Results of these investigations showed that further research into the undermentioned areas would be imformative. It is recommended that the following be carried out:

1) Further investigation into the uptake and release of colloids from the unfunctionalised precursor of Amberlite IRA 938, cation, weak cation and weak anion resins prepared from the unfunctionalised resin. Investigation by this researcher into colloid adsorption to the unfunctionalised resin and cation resin prepared from the latter is inconclusive as the unfunctionalised precursor bead was covered by a polymer layer. This resin therefore, did not have the same pore structure as the Amberlite IRA 938 resin supplied by Rohm and Haas.

2) Further investigation into the effect of surface roughness on mass transfer efficiencies of colloidal particles to the resin surface, by the manufacture of resins with intermediate porosity between Amberlite IRA 938 and Amberlite IRA 904. This study could lead to improved estimates of hydrodynamic boundary layer thickness surrounding both gel and macroporous ion-exchange resins.

3) Characterisation of (resin) surface roughness using fractal dimensions derived from microscopic measurements. The use of an image analyser or electron micrographs may be of advantage. Fractal dimensions and derived parameters may be useful in correlating data.

4) Investigation of colloid transport mechanisms within the resin pores. The variation of internal porosity distribution

and the ability to characterise it would be essential. Knudsen diffusion and surface "hopping" in the resin pores could be studied using ultrasonics and the measurement of colloid diffusion coefficients.

5) Investigation into the effect of organic molecules and multivalent ions on the zeta potentials and consequently the strength of surface forces between the colloids and collector surface. Also the effect of colloid loading on the zeta potential of the adsorbent.

6) Investigation into the factors determing the speed of the colloid physisorption to the resin surface. Adsorption at very high superficial velocities in a packed bed appears to be controlled by the physisorption step. Thus the rate of physisorption for various colloidal particles to a collecting surface could be measured.

The understanding of the fluid dynamic and electrostatic factors which determine colloid adsorption/deposition on charged surfaces can be applied in numerous fields and thus future reseach possibilities are almost endless. Examples of current applications and reseach are given in appendix F.

REFERENCES

1. Leather, J.B. and Kwiecinski, H.C., "Removal of colloid suspensions from natural waters". Effluent Water Treatment Journal, August, 35 (1974).

2. Kunin, R., "The role of silica in water treatment". Amberhilites, Rohm and Haas Company, Philadephia, Pensylvania. 164 (1980).

3. Morin, O.J. and Latour, S.R., "Economic comparisons of seawater reverse osmosis and multi-stage flash desalination plants". Sixth Annual Conference National Water Supply Improvement Association, Sarasota, Florida, July 16-20 (1978).

4. Du Pont Design Manual, Technical Bulletin 401, 9/1/77, Du Pont Company, Wilmington, DE.

5. Rainstrick, J.H. "Adsorptive filtration of liquids". Filtration and separation, March/April, 149 (1981).

6. Brunelle, M.T., "Colloidal Fouling of reverse osmosis membranes". Seventh Annual Conference Natural Water Supply Improvement Association, New Orleans, Louisianna. Sept 16-20, (1979).

7. Sienko, M.J. and Plane, R.A., Chemical Principles and Properties. 2nd Ed., McGraw-Hill, New York. p 249 (1974).

8. Gregory, J., " Stability and flocculation of colloidal particles". Part 1. Effluent and Water Treatment Journal, Oct, 516 (1977).

9. Rajagopalan, R. and Tien, C. in Progress in Filtration and Separation. Wakeman, R.J. (editor), Elsevier, Amsterdam, 1, p 189, 213 (1979).

10. Edwards, D.M. and Monke, E.S. "Electrokinetic studies of slow sand filtration". Journal of American Water Works Assoc., 59, 1310 (1967).

11. Kim, J.S. and Rajagopalan R. "A comprehensive equation for the rate of adsorption of colloidal particles and for stability ratios". Colloids and Surfaces, 4, 17, (1982).

12. Tilsley, G.M., "Interaction of organic matter with anion resins". Chemistry and Industry, 3 March, 147 (1979).

13. Kunin, R., "Two decades of macroreticular ion-exchange resin". Amberhilites, Rohm and Haas Company, Philadephia, Pensylvania., 161 (1979).

14. Kunin, R., "Pore structure of macroreticular ion-exchange resins". Conference, Imperial College of Science and Technology London, S.W.7. July 16-18 (1969).

15. Kunin, R., "The role of Organics in water treatment Part 2". Amberhilites, Rohm and Haas Company, Philadephia, Pensylvania., 168 (1981)

16. Mottershead, T., "High-purity water for semi-conductor technology". Effluent and Water Treatment Journal, July, 356 (1972).

17. AMF Cuno booklet ZP 20-1-E, "Zeta plus microfiltration".

18. Physical Chemistry Series 1, Volume 6, Electrochemistry. Brockris, J. O'M. (editor), MTP International Review of Chemistry. p 290-292 (1973).

19. Winfield, B.A. "A study of the factors affecting the rate of fouling of reverse osmosis membrane treating secondary sewage effluents". Water Research, 13, 565 (1979).

20. Sugahara, M. et al. "Effect of properties of feed solution on transport of inorganic solutes in reverse osmosis". Int. Chemical Eng., 19, 322 (1979).

21. Burton, J.D., and Leatherland, T.M., "The reactivity of dissolved silica in some natural waters". Limnology and Oceanography, 15, 3, 473 (1970).

22. Dean, R.B. et al. "An electronmicroscope study of colloids in waste water". Environmental Science and Technology, 1, 2, 147 (1967).

23. Stumm, W and Morgan, J.J., "Chemical aspects of coagulation", Journal of American Water Works Association, August, 971, (1962).

24. Rajagopalan, R. and Tien, C. in Progress in Filtration and Separation. Wakeman, R.J. (editor), Elsevier, Amsterdam, 1, p 189 (1979).

25. Crittenden, J. and Weber, W. "Predictive model for design of fixed bed adsorbers: Parameter estimatiom and model development". Journal of Enviromental Engineering Division, American Society of Civil Engineers, 104, EE2, 185 (1978).

26. Yao, Kuan-Mu et al. "Water and waste water filtration: Concepts and applications". Enviromental Science and Technology, 5, 11, 1105 (1971).

27. Thompson, G. et al. "Particle adhesion and removal in model systems - viii". Chemical Engineering Science, 38, 11, 1901 (1983).

28. Levich, V.G. Physicochemical Hydrodynamics. Prentice Hall, Englewood Cliffs, N.J. p 41 (1962).

29. Helfferich, F. Ion Exchange. McGraw-Hill, New York, p 253 (1962).

30. Schlegelmilch, W.Z. "Physics of the Nerst diffusion layer". Physik. Chem., 214, 165 (1960).

31. Vielstich, W.Z. "Relation between Nerst diffusion layer and Prandtl's stream boundary layer". Electrochem., 57, 646 (1953).

31. Levich, V.G. Physicochemical Hydrodynamics. Prentice Hall, Englewood Cliffs, N.J. p 43 (1962).

33. Spielman, L.A. and Friedlander, S.K. "Role of the electrical double layer in particle deposition by convective diffusion". Journal of Colloid and Interface Science, 46, 1, 22 (1974).

34. Kallay, N. and Matijevic, E. "Particle adhesion and removal in model systems, vii. Haematite particles on steel at 22 and 210 C". National Association of Corrosion Engineers, 39, 1, 15 (1983).

35. Ruckenstein, E. and Prieve, D.C. in Testing and Characterization of powders and fine particles. Beddow, J.K. and Meloy, T.P. (editors), Heydon, London. p107 (1980).

36. Ruckenstein, E. "On mass transfer in a continuous phase from spherical bubbles or drops". Chemical Engineering Science, 19, 131 (1964).

37. Pfeffer, R. and Happel, J. "An analytical study of heat and mass transfer in multiparticle systems at low Reynolds numbers". American Institute of Chemical Engineers Journal, 10, 605 (1964).

38. Williamson, J.E. et al. "Liquid-phase mass transfer at low Reynolds numbers". Industrial and Engineering Chemistry Fundamentals, 2, 126 (1963)

39. Kuo, R.J. and Matijevic, E. "Particle adhesion and removal in model systems, Part ii". Journal of the Chemical Society Faraday Transactions 1, 75, 2021 (1978).

40. Ruckenstein, E. and Prieve, D.C. in Testing and Characterization of powders and fine particles. Beddow, J.K. and Meloy, T.P. (editors), Heydon London, p 10 (1980).

41. Ruckenstein, E. and Prieve, D.C. "Rate of deposition of Brownian particles under the action of London and double layer forces". Journal of the Chemical Society, Faraday Transactions ii, 69, 1522 (1973).

42. Prieve, D.C. and Ruckenstein, E., "The role of surface chemistry in particle deposition". Journal of Colloid and Interface Science, 60,337 (1977).

43. Overbeek J. "Recent developments in the understanding of colloid stability". Journal of Colloid and Interface Science 58,2 (1977).

44. Prieve, D.C. and Ruckenstein, E. "Effect of London forces upon the rate of deposition of Brownian particles". American Institute of Chemical Engineers Journal, 20, 1178 (1974).

45. Levich, V.G. Physicochemical Hydrodynamics. Prentice Hall, Englewood Cliffs, N.J. p 40 (1962).

46. Primal E1743 information sheet, supplied by Rohm and Haas, (South Africa)(Pty) Limited.

47. Amberlite and Amberlyst ion exchange resins and adsorbents, Summary chart of properties and applications., Rohm and Haas Company, 9th Summary Bulletin (1978).

48. Microsil specification sheet, supplied by Silicon Smelters (Pty) Limited.

49. Levenspiel, O. The chemical reactor omnibook. OSU Book Stores, Corvollis. p 51.4 (1979).

50. Helfferich, F. Ion Exchange. Mc Graw-Hill, New York, p 285 (1962).

51. Levich, V.G. Physicochemical Hydrodynamics. Prentice Hall, Englewood Cliffs, N.J. p 162 (1962).

52. van Vliet, B.M. and Weber, W.J. "Comparative performance of synthetic adsorbents and activated carbon for specific compound removal from wastewaters". Jour. Water Poll. Controll Fed., 53, 11 (1981).

53. Levich, V.G. Physicochemical Hydrodynamics. Prentice Hall, Englewood Cliffs, N.J. p 163, 166 (1962).

54. Johansen, P.G. and Buchanan, A.S. "An application of the microelectrophoresis method to the study of the surface properties of insoluble salts". Australian Journal of Chemistry, 10, 4, 398 (1957).

55. Mori, S., Okamoto, H., Hara, T. and Aso, K. in Fine Particles Process, Proceedings of International Symposium. Somasundoran, P. (editor), AIME, New York, N.Y., 1, p 632 (1980).

56. Visser, J. "On Hamaker constants; A comparison between Hamaker constants and Lifshitz - van der Waals contants". Advances in Colloid and Interface Science, 3, 331 (1972).

57. Weast, R.C. (editor), CRC Handbook of Chemistry and Physics, 58 th edition, CRC Press Incorporated, Florida, p E70 (1977).

58. Zeta-meter Manual, Zeta-Meter Incorporated, p 46-55 (1961).

59. Water Research Commission. Annual Report, p 9 (1983).

60. Van Robbroeck T.P. "Conventional water resources of the Western Cape". The decade ahead symposium on unconventional sources of water, Cape Town, Oct 28 (1980).

61. Gluekstern, P. and Kantor, Y. "Economic Evaluation of using small sized nuclear reactors for seawater desalination". Desalination, 22, 101 (1977).

62. Eykamp, W., "Fouling of membranes in food processing". American Institute of Chemical Engineers Symposium, Ser. no. 172, 74, 234 (1976/66).

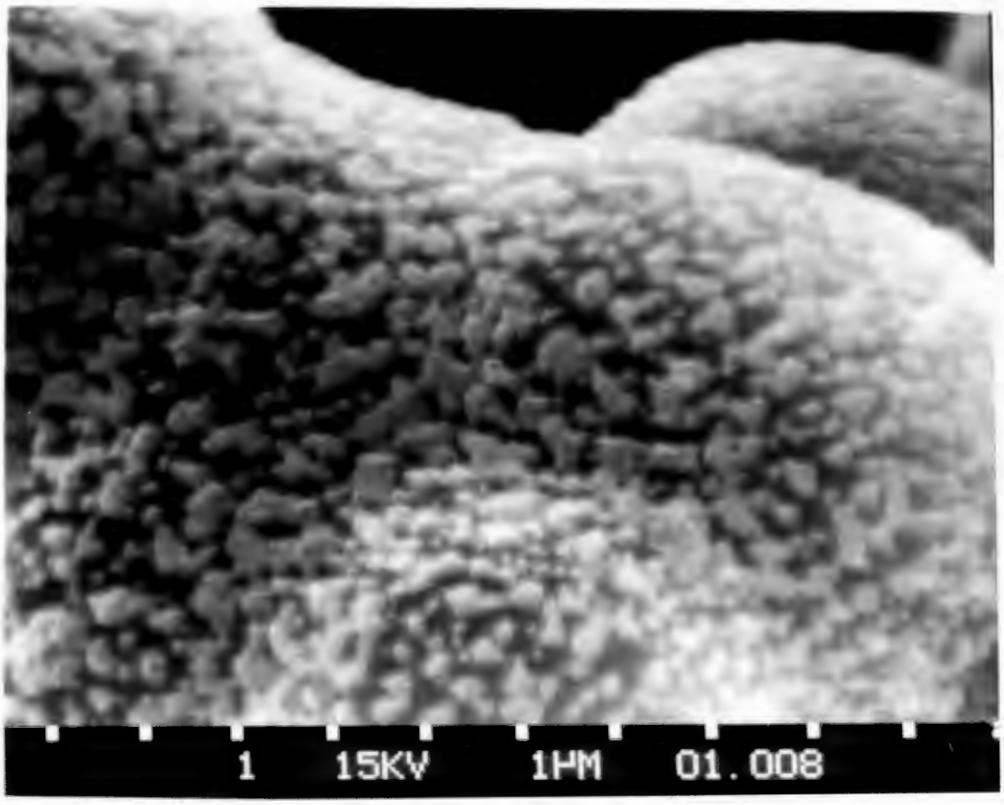

Photograph 7 AMBERLITE IRA 938 RESIN LOADED WITH NATURAL SEAWATER COLLOIDS. (× 12 700)

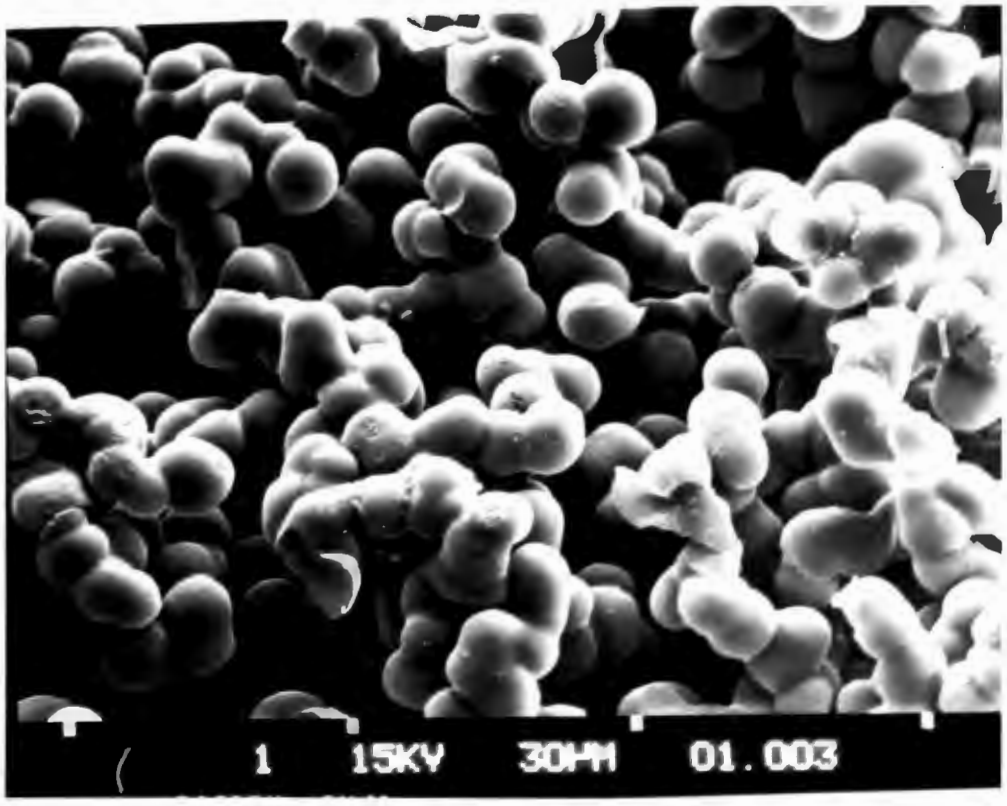

Photograph 8 AMBERLITE IRA 938 RESIN AFTER REGENERATION WITH NaOH. (× 1 300)

with less than 25mg of Primal E1743 could be at least 50% cleaned after 2 hours in the ultrasonic bath.

A further, more detailed investigation using the more powerful "Branson" ultrasonic bath confirmed the above findings. The regeneration/cleaning however was more efficient, being faster and consequently producing a more concentrated effluent. It was found that the resin is approximately 50% cleaned after 1.6 litres of distilled water was pumped through the resin bed at a flow rate of 20ml per minute during sonication. This increased to approximately 75% regeneration after a further 1.8 litres had passed through the bed (see Figure 4.4).

Studying Figure 4.4 two interesting points arise. The first is that initially a high effluent concentration leaves the bed and then the concentration slowly tapers off. A probable reason for this is that the surface adsorbed colloids are released quickly while the colloids further into the bead take a considerable time to "find their way out" of the bead. This reasoning is substantiated by an electronmicroscope study of the regenerated resin which showed that the exterior surface of the resin was almost completely clear whereas the interior surfaces were sparsely dotted with Primal E1743 spheres. These electron microscope observations were not recorded on film.

An interesting fact revealed by the electronmicroscope study was that the ultrasonic vibrations moved the colloid spheres both into and out of the resin beads. Primal E1743 spheres were found close to the centre of the bead whereas previously they were found a maximum of 50 microns into the bead. This indicates that the rate of pore diffusion and therefore the useful capacity of the resin could be increased with the use of ultrasonic vibrations.

The electronmicroscope study further showed that there is minimal damage to the resin after an approximate six hour conditioning and regeneration/cleaning cycle in the ultrasonic bath.

The second point arising from Figure 4.4 is that the position of the resin column in the bath or the power of the vibrations is

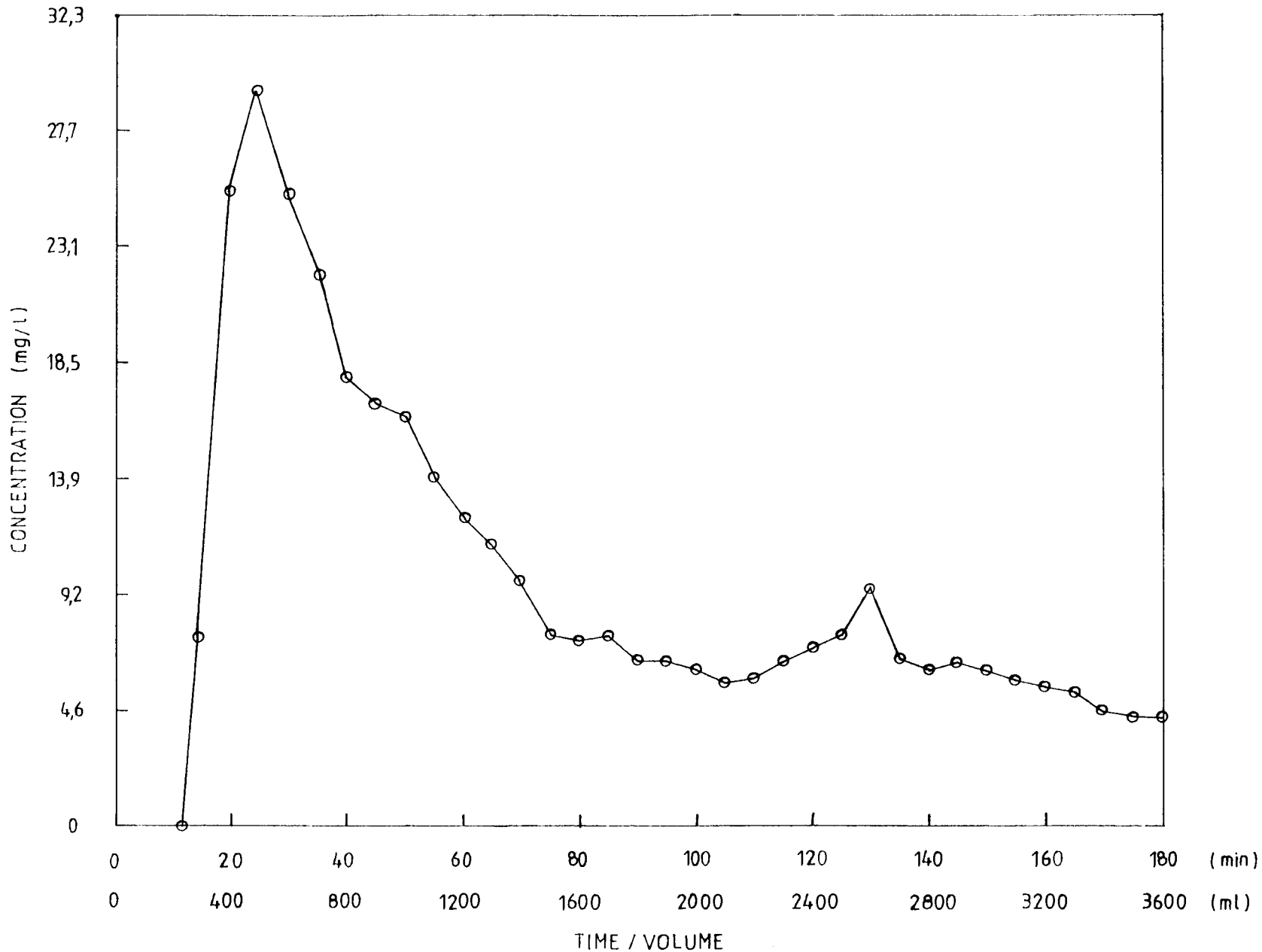

Figure 4.4 ULTRASONIC REGENERATION OF AMBERLITE IRA 938 RESIN LOADED WITH PRIMAL E1743 SPHERES.

important. This is shown by the second peak which resulted from the resin column being moved so that it was positioned directly above one of the ultrasonic transducers. (The frequency of the vibrations was not varied but may have a major effect.)

4.3.4 Summary of available regeneration techniques

From the above discussion it is apparent that the resin can be regenerated. Resin loaded with natural colloids can, in most cases, be regenerated/cleaned using sodium hydroxide. However should the colloidal particles be strongly held to the resin, as with Primal E1743, it can be adequately cleaned using ultrasonic waves and rinsing, with minimal damage to the resin structure. (The long term effects of ultrasonic waves on the resin have not been determined.)

4.4 PARAMETERS EXPECTED TO AFFECT COLLOID ADSORPTION TO RESIN

A number of parameters were studied in order to elucidate the driving forces and mechanisms of particulate adsorption to polymeric resins. The influence of each parameter will be discussed in turn and finally be bound together in an empirical model which will be presented at the end of this section.

4.4.1 Colloidal particle size

Particle size determines the transport mechanism by which a particle is brought to the collector surface (discussed in section 2.3).

The rate of adsorption of five different size colloidal particles of silica to Amberlite IRA 938 resin was measured. The data is shown in Table 4.5 and plotted in Figure 4.5.

Comparing Figure 4.5 to the results obtained by Yao et al. (See Inset) it is clear that the shape and trends shown by the two graphs are similar. Both graphs indicate that there is a

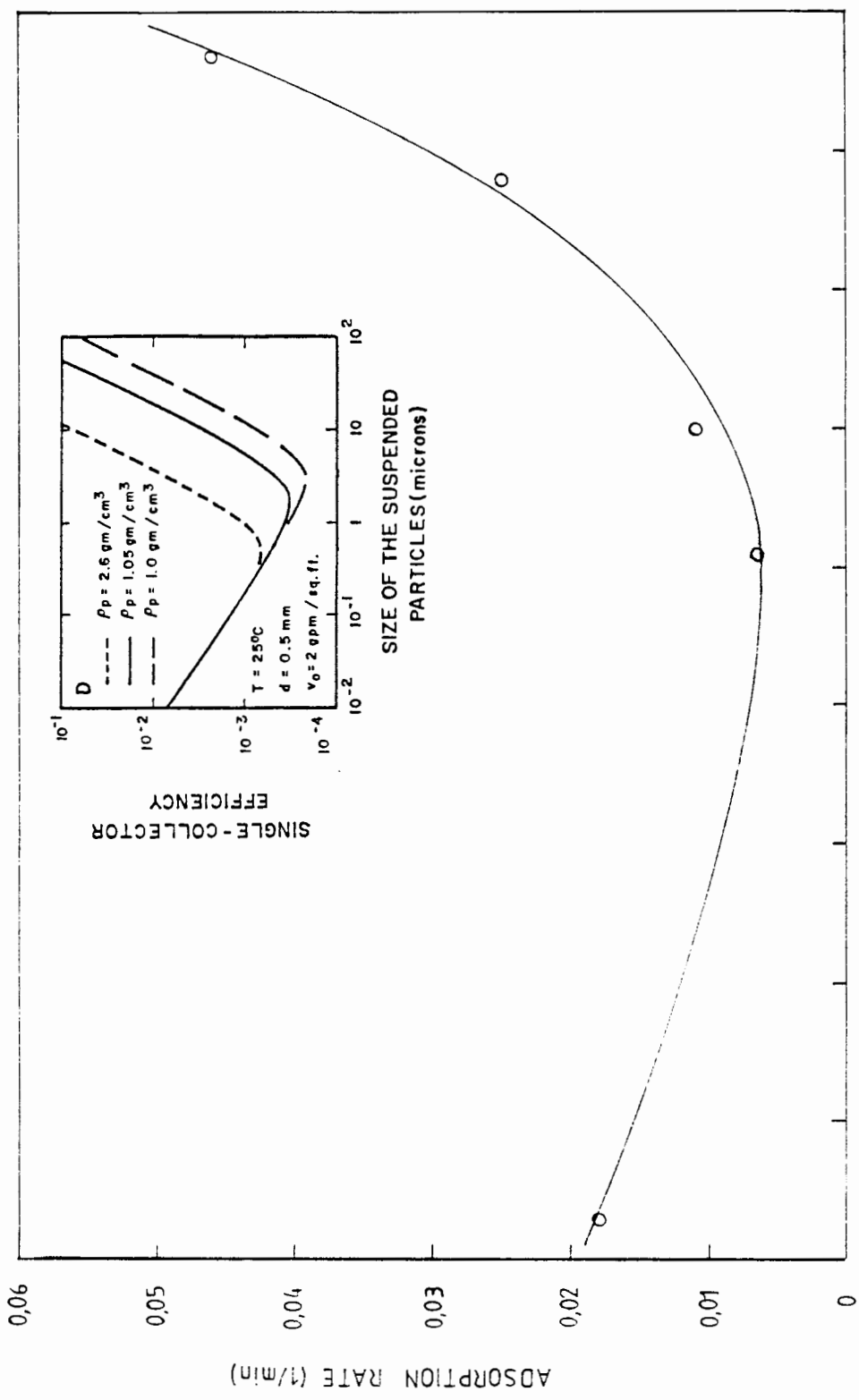

Figure 4.5 THE EFFECT OF COLLOIDAL PARTICLE SIZE ON ADSORPTION RATE. (Inset Yao et al.)(26)

particle size close to 1 micron which is least amenable to removal by adsorptive or filtration processes.

Size of Silicon Dioxide particle (microns)	Rate of Adsorption* (1/min)
0.012	0.018
0.5	0.006
1.2	0.012
4	0.025
8	0.046

TABLE 4.5 The effect of colloid particle size on adsorption rate on Amberlite IRA 938 resin.
*(flow rate 22ml/min, fluidised bed)

Particles smaller than approximately 1 micron are transported to the collector surface by Brownian diffusion. As particle size decreases the diffusion coefficients of the particles increase thus increasing the rate of transport to the collector surface and consequently the removal rate.

Larger particles have reduced diffusion coefficients and therefore the increasing removal efficiency with particle size above 1 micron indicates that factors other than Brownian diffusion begin to contribute to mass transfer. Rajagopolan et al. (24) and Yao et al. (26) both suggest that the increase in removal efficiency with particle size is due to the shifting of the transport mechanism of the particle to the collector surface, from diffusion to size (interception) and inertial (gravity, velocity) effects.

As particle size increases there is an increasing probability that particles following laminar streamlines across the surface of the collector could contact the collector surface and adsorb. Similarly, as the mass of the particles increase with increasing size, there is a growing tendency for the particles to follow a trajectory determined by inertial effects rather than the laminar streamlines.

From this investigation it is evident that particle size determines the transport mechanism by which the particles are brought to the collector surface and consequently affects the rate of adsorption to the resin. Further it is apparent that Brownian diffusion is the major transport mechanism for the smaller particles used in the kinetic experiments conducted in this work.

4.4.2 Resin bead size

The effect of resin bead size on adsorption rate can help identify the rate determining step in adsorption processes.

Typically for film diffusion control (49),

$$\text{adsorption rate} \propto (\text{particle diameter})^{(-1.5 \text{ to } -2.0)}$$

while for particle or pore diffusion control,

$$\text{adsorption rate} \propto (\text{particle diameter})^{(-2.0)}.$$

Adsorption rates were measured for five different resin size fractions (see section 3.4.2). Figures 4.6 and 4.7 are plots of the mass transfer rate constants for each resin size fraction against i) outside surface area and ii) the resin bead diameter to the power -1.66. Both are straight lines indicating that the adsorption rate is directly proportional to the resin surface area and the resin bead diameter to the power -1.66.

These results tend to support the previous proposal that the initial adsorption rate, at low resin loadings, is film diffusion controlled. This is further substantiated by the fact that the adsorption rate is directly proportional to the colloid concentration which is typical of a film diffusion controlled system.

Figures 4.6 clouds this simplistic view as the graph does not pass through the origin. This anomaly probably arises from errors in the estimated resin surface areas (a systematic error of 0.015 m^2 would suffice.)

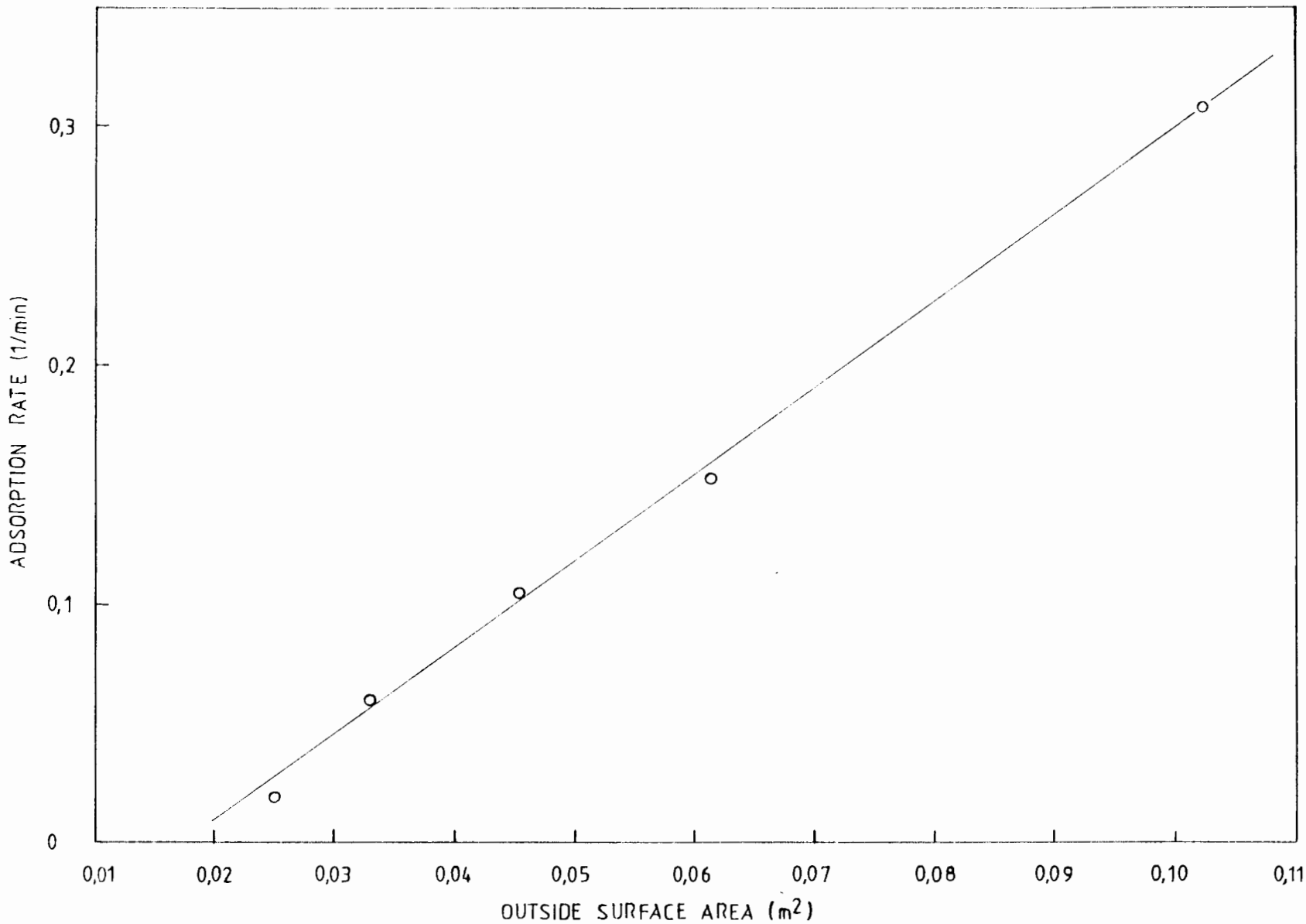

Figure 4.6 A PLOT OF RESIN OUTSIDE SURFACE AREA VERSUS ADSORPTION RATE SHOWING THE LINEAR RELATIONSHIP BETWEEN ADSORPTION RATE AND READILY AVAILABLE SURFACE AREA.

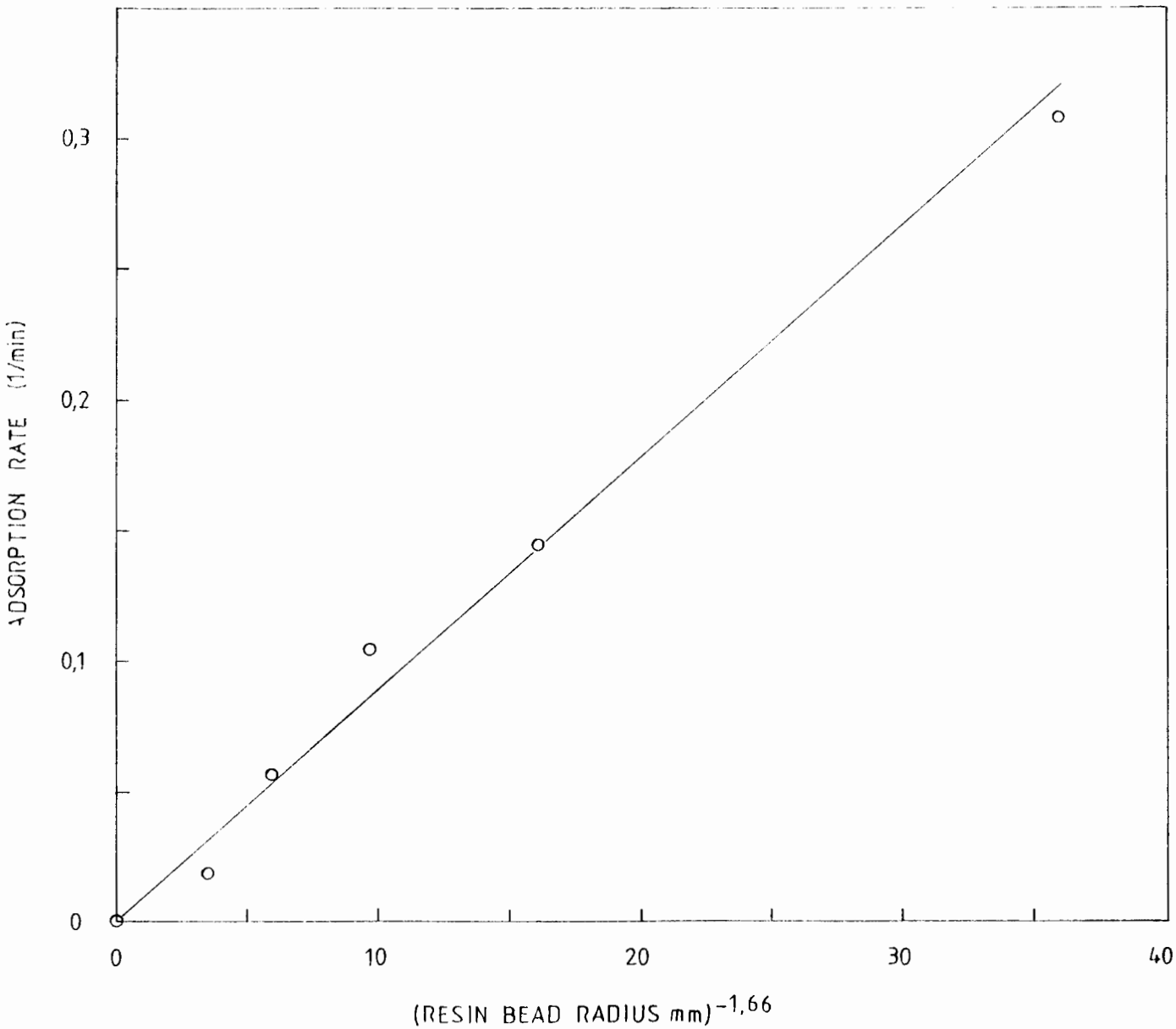

Figure 4.7 A PLOT SHOWING THE RELATIONSHIP BETWEEN RESIN BEAD SIZE AND ADSORPTION RATE.

The adsorption rate being proportional to surface area indicates that it would be advantageous to have resin beads with high surface area to volume ratios, ie small beads. The use of small diameter resin beads would lead to relatively high adsorption rates and efficient use of the resin.

4.4.3 Superficial fluid velocity in the resin bed

The adsorption rate versus flow rate data is plotted in Figure 4.8.

Simple diffusion models propose that the adsorption rate is inversely proportional to the boundary layer thickness. The above results contradict this as the dependence of adsorption rate on flow rate and therefore boundary layer thickness declines at high at high flow rates.

The majority of authors referred to have assumed that the hydrodynamic boundary layer thickness is to proportional to $U^{-1/3}$, and thus obtain the adsorption rate proportional to $U^{1/3}$. Predicted rate constants using the this assumption are also plotted on Figure 4.8 for comparison. It is clear that this assumption results in gross underestimation of the effect of flow rate on adsorption rate, for this system. There are two factors which affect the "effective" thickness of the hydrodynamic boundary layer and thus could explain this difference.

4.4.3.1 Electrostatic sub-layer within the hydrodynamic boundary layer

The electrostatic force field referred to in section 2.2 extends from the charged surface of the resin into the liquid. Thus an electrostatic sub-layer extends from the resin surface into the hydrodynamic boundary layer which surrounds the resin beads. As the movement of colloidal particles in this sub-layer is governed by electrostatic forces and consequently is very rapid, the distance across which a particle has to diffuse to reach the resin surface, is effectively reduced by the thickness of the

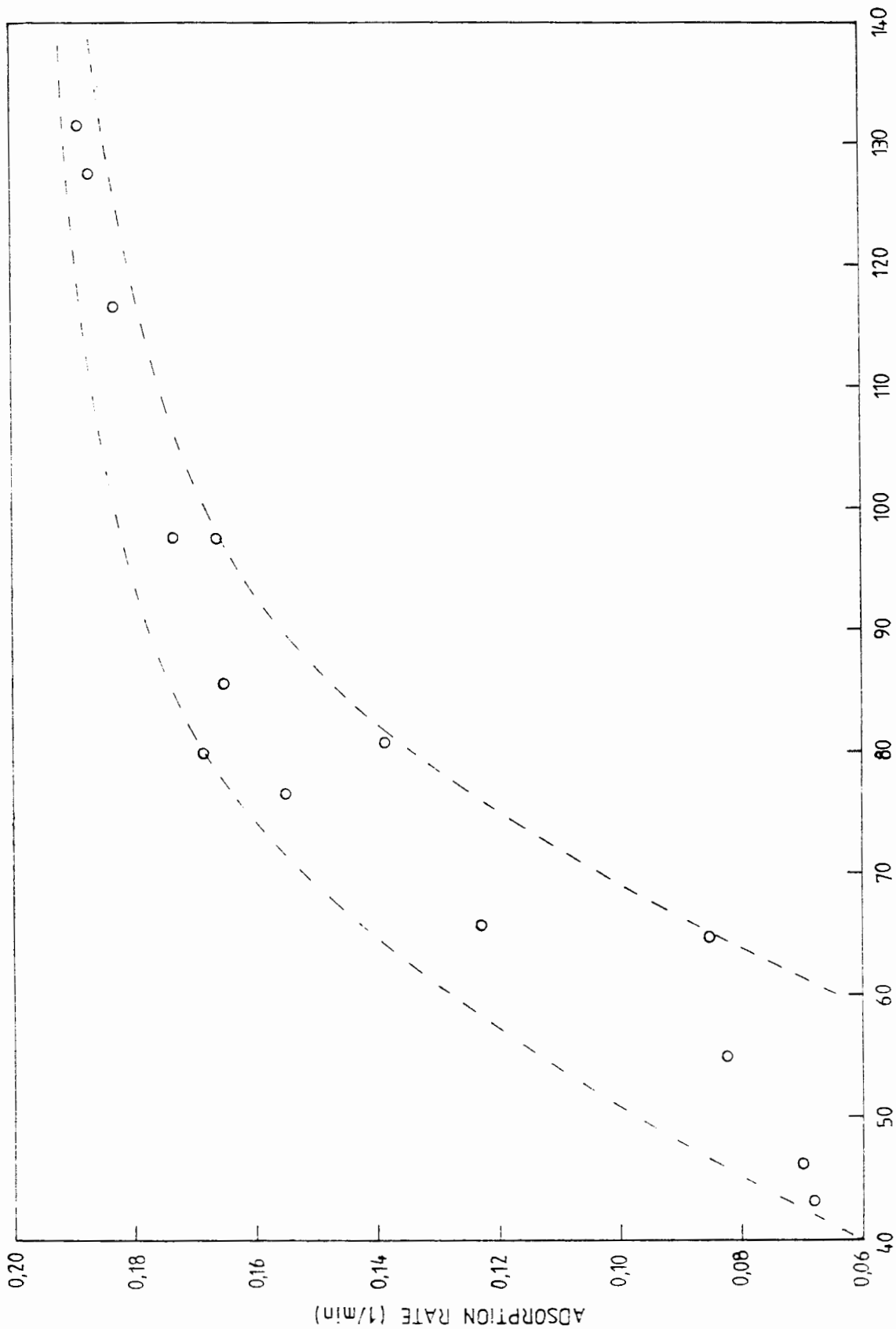

Figure 4.8 THE VARIATION OF ADSORPTION RATE WITH FLOW RATE FOR THE AMBERLITE IRA 938 RESIN - PRIMAL E1743 SYSTEM.

sub-layer. Adsorption rates are therefore often enhanced by charged collector surfaces.

4.4.3.2 Roughness of exterior resin surface

Amberlite IRA 938 resin, as discussed in section 1.2, is far from a smooth sphere. It is a highly macroporous resin, with pores ranging from 2.5 to over 25 microns in diameter and therefore has a very rough surface (see Photograph 1).

Levich explains that surface roughness changes the nature of the flow past a surface and consequently changes the diffusional flux to that surface (51). This idea is supported by van Vliet and Weber (52), who studied activated carbons, Amberlite XAD resins etc. which are less rough than Amberlite IRA 938 resin, and found that adsorbent surface roughness or topography has a marked effect on external mass transfer efficiencies.

Surface protrusions and depressions, result in local turbulence and eddies as show in Figure 4.9 (53). These effects are obviously strongly flow rate dependent. On the downstream side of a protrusion turbulence appears enhancing the mass transfer, whilst the upstream side is subject to laminar flow only.

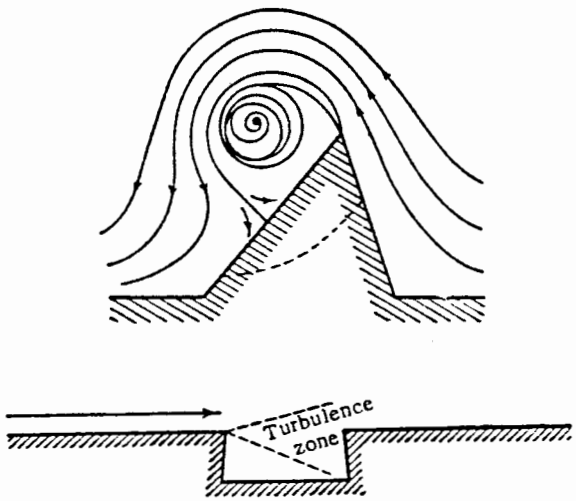

Figure 4.9 THE EFFECTS OF SURFACE ROUGHNESS ON FLOW.

Resin surface roughness therefore results in reduced hydrodynamic boundary layer thicknesses and consequently enhanced adsorption rates.

The postulates of an inner electrostatic sub-layer and of the effect of surface roughness on the real or effective thickness of the hydrodynamic boundary layer seems to offer a plausible explanation for the observed rapid increase in adsorption rate with superficial fluid velocity in the resin bed at low flow rates.

At high flow rates the hydrodynamic boundary layer is so much reduced that the electrostatic forces act over most of its thickness and therefore the resistance to mass transfer of the boundary layer becomes less significant. Adsorption rate therefore becomes insenitive to further flow increases.

Above a flow rate of about about 100 ml/min the adsorption rate approaches a maximum, which is thought to correspond to the surface reaction rate.

4.4.4 Surface reaction

In most chemical processes (eg. catalysis, chemisorption etc.) the surface reaction step is exceedingly fast and thus surface reaction control is rare. However, we are dealing here with physisorption which is a relatively slow process. Diffusion control of a colloid adsorption process therefore, can give way to surface reaction control when the hydrodynamic boundary layer surrounding the collector becomes very thin.

The outer surface adsorption process is therefore controlled by two resistances in series. The first is the thickness of the diffusion boundary layer and the second is the surface reaction rate. At low flow rates film diffusion is adsorption rate controlling and the particles arrive at the surface of the collector at a slower rate than they can be removed by physisorption. However as flow rate increases, the hydrodynamic boundary layer thickness decreases and a point arises where the rate of particle

arrival exceeds the rate of removal by physisorption. The concentration gradient across the diffusion film becomes flatter and the adsorption process becomes surface reaction rate controlled.

The movement of a colloidal particle from the bulk suspension to the adsorbed state consists of the following steps:

i) Diffusion, by a concentration gradient driving force, across the hydrodynamic boundary layer to the electrostatic sub-layer.
ii) Exponential acceleration of the particle, across the electrostatic sub-layer, towards the resin surface under the influence of coloumbic and London - van der Waals forces.
iii) Slowing of the particle, by hydrodynamic retardation as it approaches the resin surface.
iv) Physisorption of the particle to the resin surface.

An idealised velocity profile for a colloid particle crossing the various regions to reach a collecting surface in an adsorption process is shown in Figure 4.10.

4.4.5 Adsorption rate expression

The outer surface adsorption rate, assuming very low surface coverage, can still be modelled using first order kinetics, where the mass transfer rate constant now is made up of two terms.

$$-r_a = \frac{1}{V} kC_a \qquad \text{where } C_{so} \text{ is a constant, and}$$

$$k = \left[\frac{1}{k_f} + \frac{1}{k_r}\right]^{-1}$$

k_f, the film mass transfer rate constant, is determined by the thickness of the diffusion boundary layer and k_r, the reaction rate constant, is determined by the speed of the physisorption step.

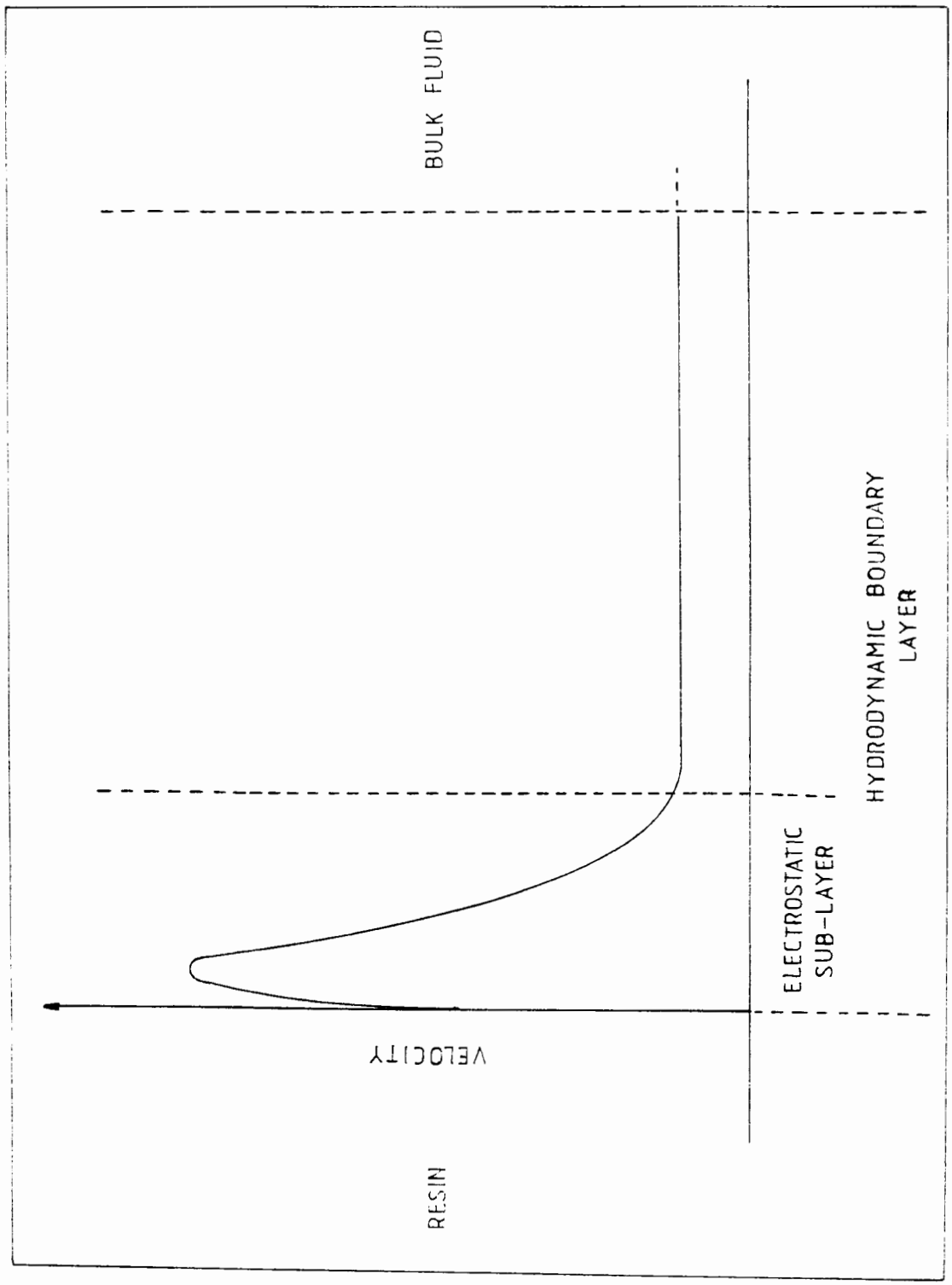

Figure 4.10 AN IDEALISED VELOCITY FROFILE FOR A PARTICLE CROSSING THE REGIONS ADJACENT TO A COLLECTING SURFACE.

4.4.6 Surface charge

To investigate the effect of surface charge on adsorption rate, adsorption rates for silicon dioxide, titanium dioxide and Primal E1743 to Amberlite IRA 938 were measured. The size and zeta potentials of the colloids and their adsorption rates to Amberlite IRA 938 resin are compared in Table 4.6. These adsorption rates, as with all previous adsorption rates, were measured at a pH of 7 +- 1.5.

Colloid Type	Size (microns)	Zeta potential (pH 7 +- 1.5)	Adsorption rate (1/min)
Primal E1743	0.5	-35 to -39 mv	0.105
Titanium Dioxide	0.4	+15 to -23 mv	0
Silicon Dioxide	0.5	-33 to -40 mv	0.097

TABLE 4.6 The adsorption rates of various colloidal particles to Amberlite IRA 938 resin.

The charge on the colloid particle determines whether adsorption will occur. Primal E1743 and silicon dioxide, having similar negative zeta potentials (-33 to -40 mv), adsorb to the positively charged resin at approximately the same rate. However titanium dioxide, the zeta potential of which varied from +15mv to -23mv over the pH range used (7+-1.5), did not adsorb to Amberlite IRA 938 resin. The pH was unfortunately not measured during the whole run but it is apparent that the pH of the colloidal titanium dioxide suspension must have been such that the particles had a positive charge and thus were repelled from the resin surface.

In order to check this, firstly the charge on the resin and secondly the charge on the colloidal particle were varied.

4.4.6.1 Variation of resin surface charge

The adsorption rate of Primal E1743 to strong anion resin Amberlite IRA 938, its unfunctionalised precursor bead and a strong cation resin prepared from the latter (Appendix D) were measured at a pH of 7+-1.5. The results are presented in Table 4.7.

Resin Type	Resin Charge	Silica Dioxide	Primal E1743	Titanium Dioxide
Amberlite IRA 938	positive	0.097	0.105	0
Cation form	negative	0	0	0
Unfunctionalised form	uncharged	0.013	0.051	0.026

TABLE 4.7 The adsorption rates of the colloids of Table 4.6 to resins of varying surface charge.

The results in Table 4.5 show that the negatively charged cation resin did not adsorb silicon dioxide, Primal E1743 or titanium dioxide at the pH of 7 +- 1.5. However at pH values below 5 titanium dioxide particles did adsorb to the cation resin. Titanium has a positive surface charge below a pH of 6 which explains the above anomaly. Further it is interesting to note that all three particles adsorbed to the uncharged bead.

Unfortunately the rate data for Amberlite IRA 938 resin cannot be directly compared with that for the cation and unfunctionalised forms as the latter resins were coated with what looked like a polymer layer (see Photographs 9&10) consequently the accessible surface area was reduced and the measured rates may therefore be expected to be lower. However, it does appear that the adsorption rates of silicon dioxide and Primal E1743 are higher on positively charged Amberlite IRA 938 resin than on uncharged resin, showing that the resin and colloid surface charge can have a major effect on adsorption rate.

Photograph 9 AN UNFUNCTIONALISED RESIN BEAD SHOWING ITS REDUCED SURFACE AREA AND POROSITY DUE TO A POLYMER COATING. (× 230)

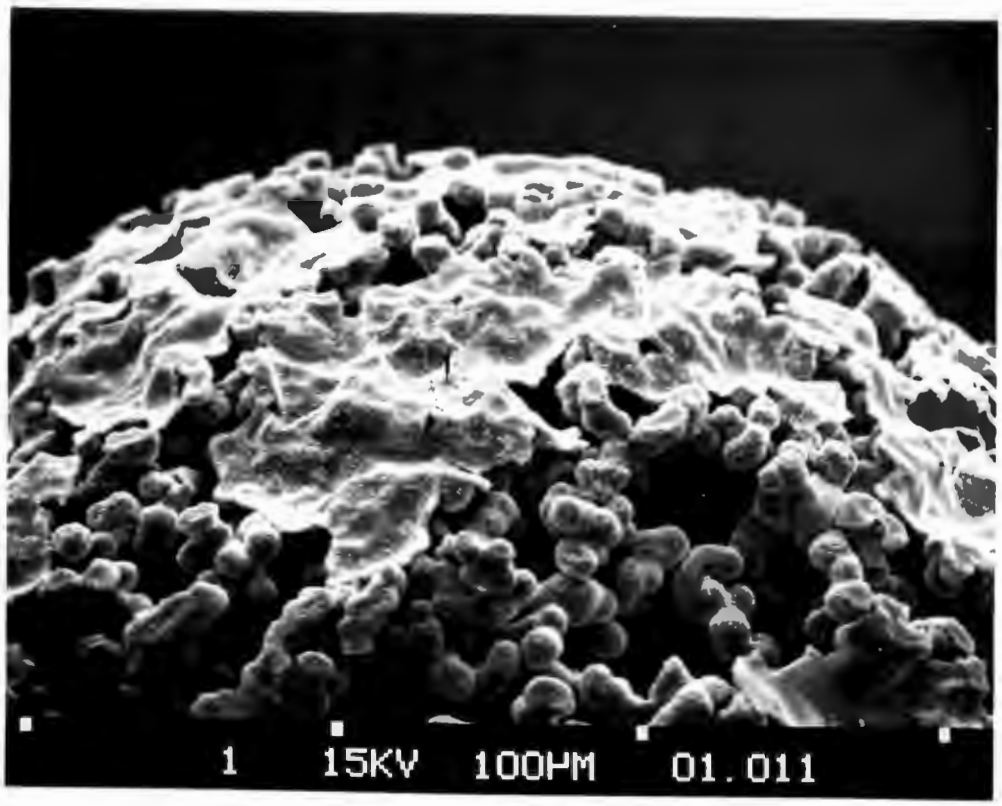

Photograph 10 A CLOSE UP PHOTOGRAPH OF A COATED RESIN BEAD SHOWING THE POLYMER LAYER BLOCKING SOME OF THE RESIN MACRO-PORES. PRIMAL E1743 SPHERES ARE ADSORBED TO BOTH THE RESIN AND POLYMER COATING. (× 400)

4.4.6.2 Variation of colloid surface charge by pH variation

In a further investigation the pH of the colloidal suspension and thus the charge on the particle (see Table 4.8) was varied. This resulted in unforseen problems as changing the pH of the colloidal suspension affected the zeta potentials of both the resin and the colloidal particles.

Substance	Zeta potential (mv)		
	pH 4	pH 7	pH 10
Amberlite IRA 938	+51	+77	+91
Primal E1743	-29	-38	-41
Silicon Dioxide	-44	-38	-53
Titanium Dioxide	+42	-16	-28

TABLE 4.8 The variation of zeta potential of the colloids and resin with pH.

The results of the investigation in Table 4.9 nevertheless confirm the proposal that the surface charges of the resin and colloidal particles determine whether adsorption will occur. At pH 10 titanium dioxide particles have a negative surface charge and consequently adsorption to the positively charged resin surface takes place. However at a pH of 4 titanium dioxide has a positive zeta potential and is therefore repelled by the positively charged surface of the resin.

Colloid Type	Adsorption rate (1/min)		
	pH 4 +- 0.2	pH 7 +- 1.5	pH 10 +- 0.2
Primal E1743	0.100	0.105	0.080
Silicon Dixoide	0	0.097	0.068
Titanium Dioxide	0	0	0.060

TABLE 4.9 Adsorption rates of colloids of varying surface charges as affected by pH variation, to Amberlite IRA 938 resin.

Table 4.9 shows that for Primal E1743 and silicon dioxide adsorption rate is greatest at neutral pH. A possible reason for the adsorption rate decreasing at low pH is that the resin had a low zeta potential. However the rate should have been enhanced at high pH because the zeta potential is greater and consequently the attractive forces between the resin and colloidal particles increased. This anomaly might be explained by the variation in the ionic strengh of the suspension with changes in pH.

The effect of ionic strength on adsorption rate was therefore investigated.

4.4.6.3 Electrolyte strength

According to the Stern model (see Section 2.2) increased ionic strength of a solution shrinks the "diffuse layer" of ions surrounding the particle and thus allows particles to approach a surface more closely without the attractive or repulsive influence of coulombic forces.

The adsorption rate of Primal E1743 to Amberlite IRA 938 resin was measured at various ionic strengths. The results are shown in Table 4.10 and plotted in Figure 4.11.

NaCl added to distilled water (ppm)	Overall ion concentration (M)	Adsorption rate (1/min)
0	3.0×10^{-5}	0.113
20	3.7×10^{-4}	0.091
250	4.3×10^{-3}	0.087
1000	1.7×10^{-2}	0.085
2500	4.3×10^{-2}	0.089
3000	5.1×10^{-2}	0.084

TABLE 4.10 The effect of ionic strength on adsorption rate.

There is a marked decrease in adsorption rate as ionic strength increases, up to about 5×10^{-3} M but further increases have a

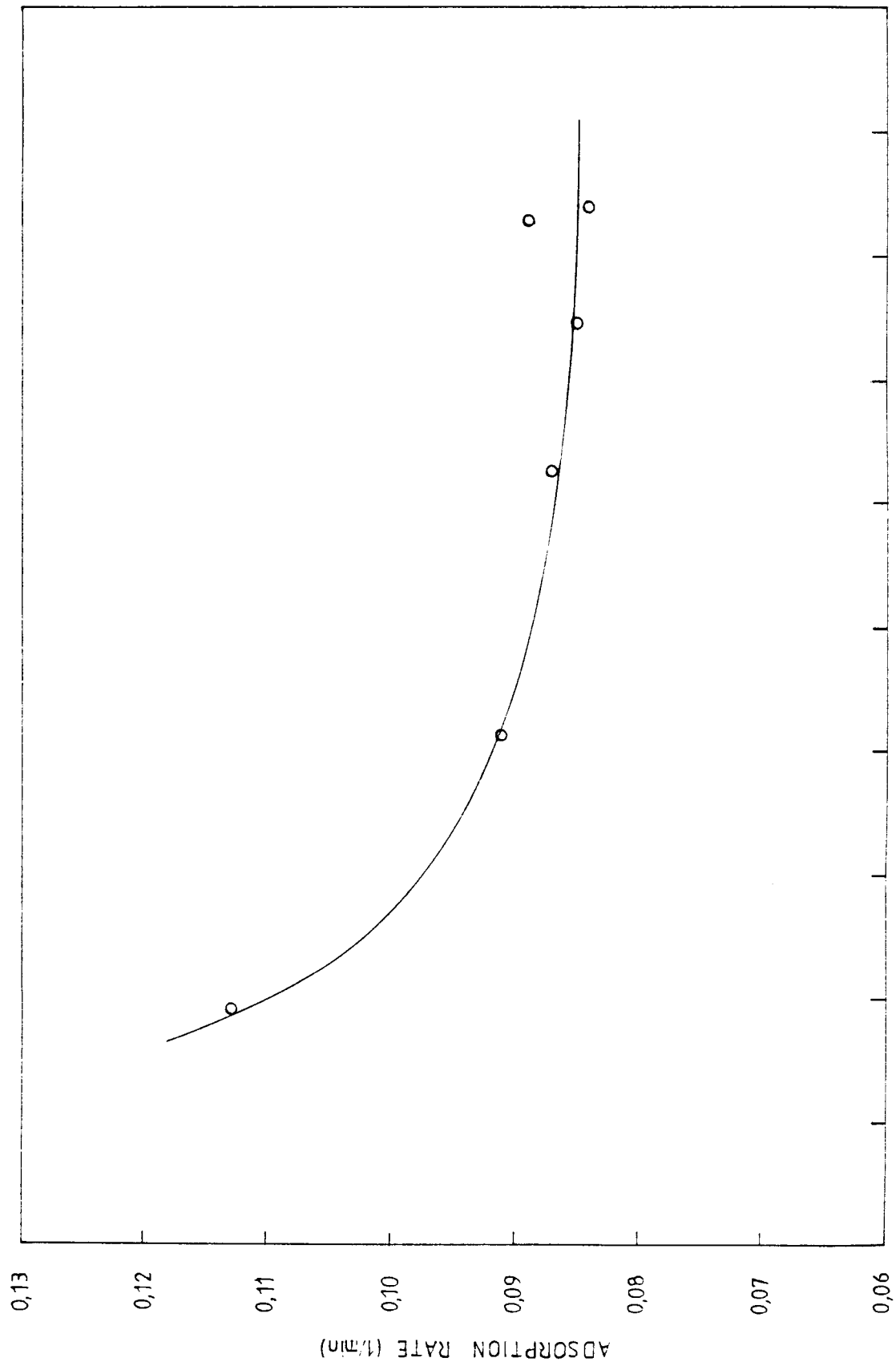

Figure 4.11 THE EFFECT OF IONIC STRENGTH ON ADSORPTION RATE FOR THE AMBERLITE IRA 938 RESIN - PRIMAL E1743 SYSTEM.

smaller effect on the rate of adsorption. This is explained in the following section.

4.4.6.4 Interaction potential energy

The explanation of the effect of ionic strength and pH on the adsorption requires calculation of the London - van der Waals and coulombic forces, at varing separation distances between the resin and colloidal particle, for the differing pH values and ionic strengths of the suspension. The theory related to London - van der Waals and electrostatic forces is presented in section 2.2 and the values of the net interaction potential energy were calculated using the procedure in Appendix D.

Figure 4.12 shows the variation of the net interaction potential energy with ionic strength for the Amberlite IRA 938 resin - Primal E1743 system. Increasing the concentration of the electrolyte compresses the thickness of the "diffuse double layer" and decreases the magnitude of the attractive energy of interaction. This effect is most pronounced at low ionic strengths.

At low ionic strengths the net attractive force between the colloid and the resin surface extends over relatively large distances and consequently enhances the diffusion rate of the particle to the resin surface. The attractive forces extend into the diffusion film surrounding the resin beads and reduce the effective thickness of this layer. The movement of colloidal particles in the zone of interaction forces is not governed by Brownian diffusion but by London - van der Waals and electrostatic forces. This explains the results shown in Figure 4.11; at low ionic strengths the coulombic attractive forces reduce the effective thickness of the diffusion film and the adsorption rate is enhanced. This effect rapidly decreased with increasing ionic strength and therefore the adsorption rate levelled off after a sodium chloride concentration of about 5×10^{-3} M.

The observed effect of a maximum adsorption rate at neutral pH (see Table 4.9) can be explained using interaction potential energy curves. Figures 4.13 and 4.14 show the interaction

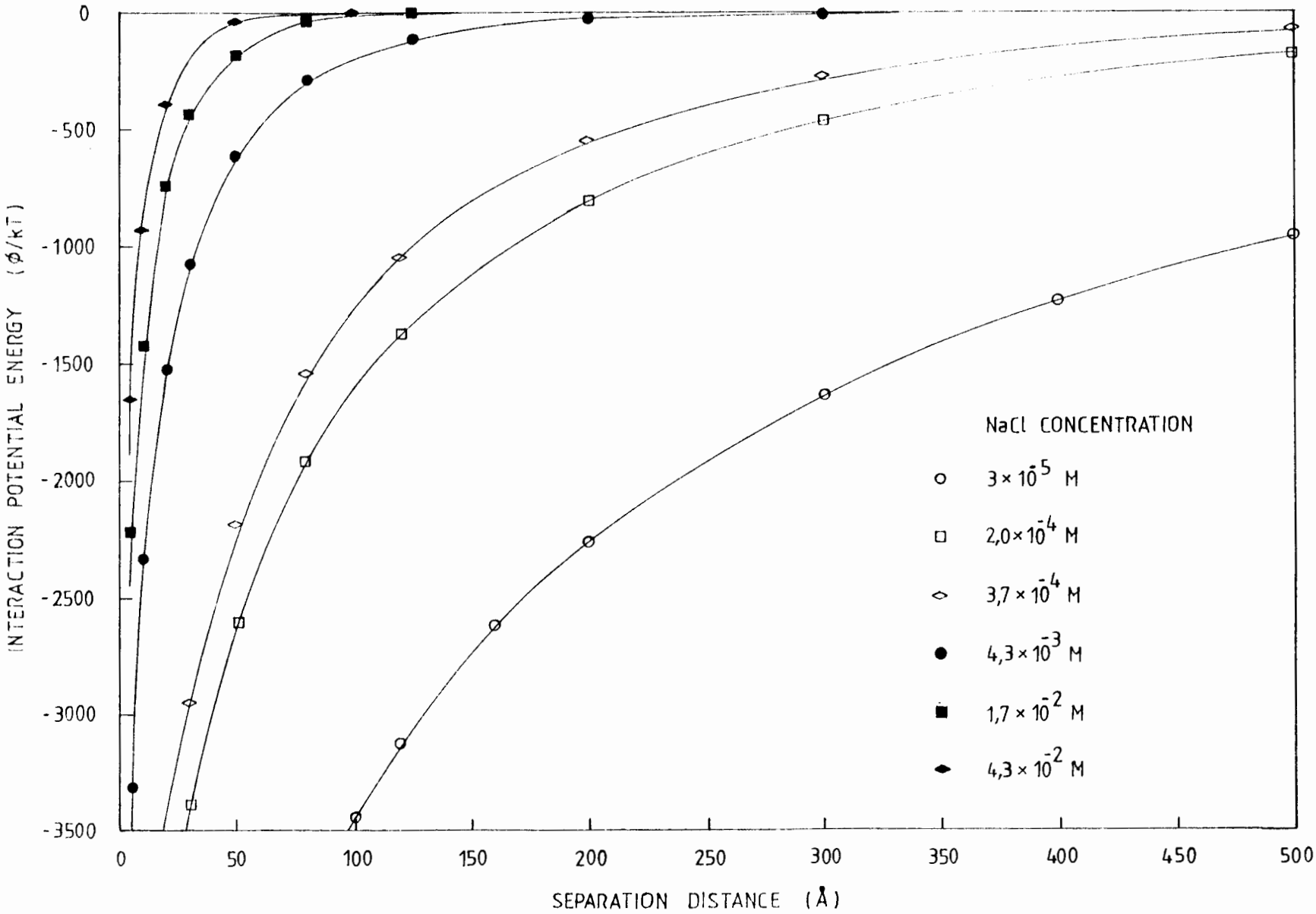

Figure 4.12 THE VARIATION OF NET INTERACTION POTENTIAL ENERGY WITH IONIC STRENGTH FOR THE AMBERLITE IRA 938 - PRIMAL E1743 SYSTEM.

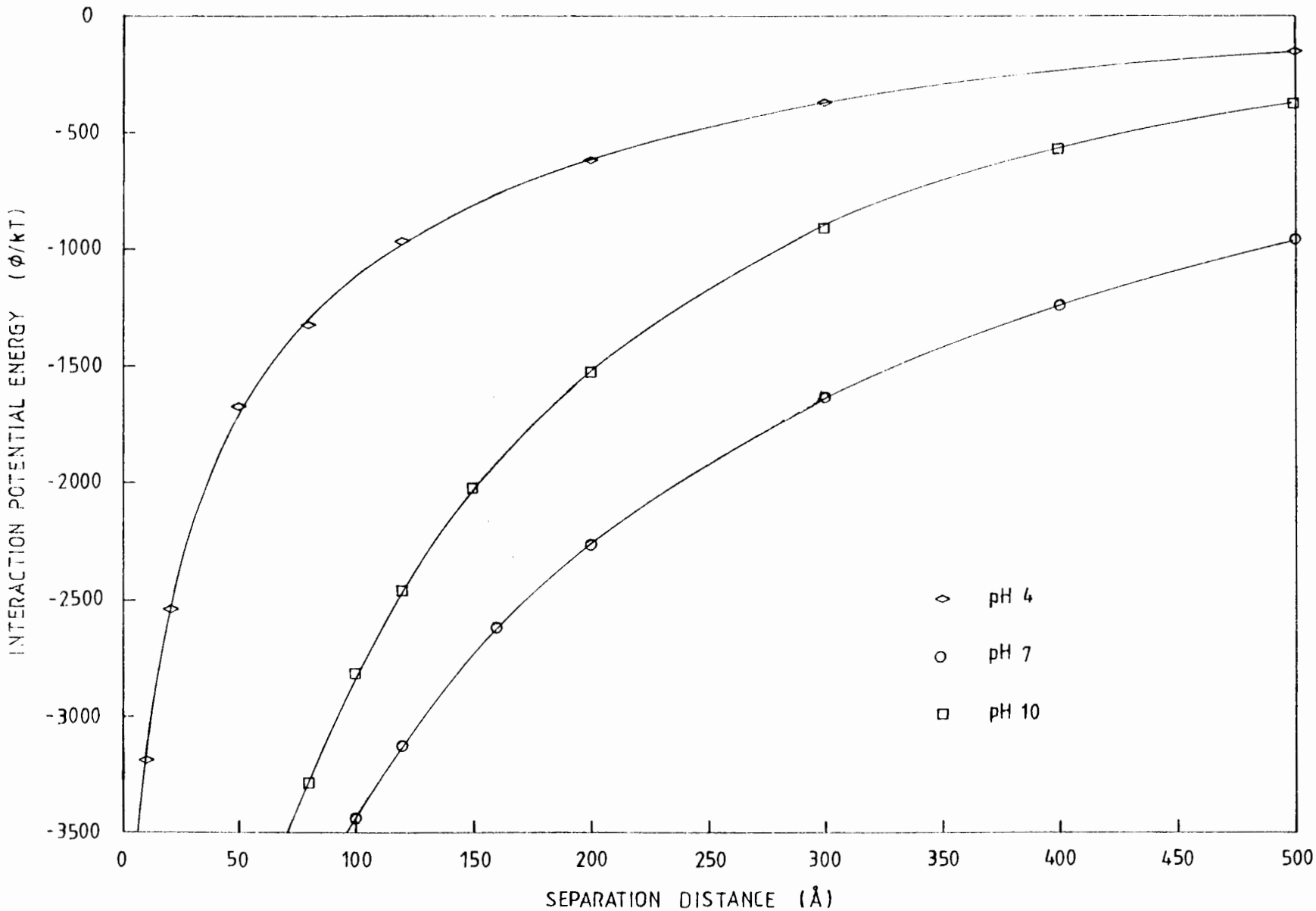

Figure 4.13 THE EFFECT OF pH ON THE INTERACTION POTENTIAL ENERGY CURVES FOR THE AMBERLITE IRA 938 RESIN - PRIMAL E1743 SYSTEM.

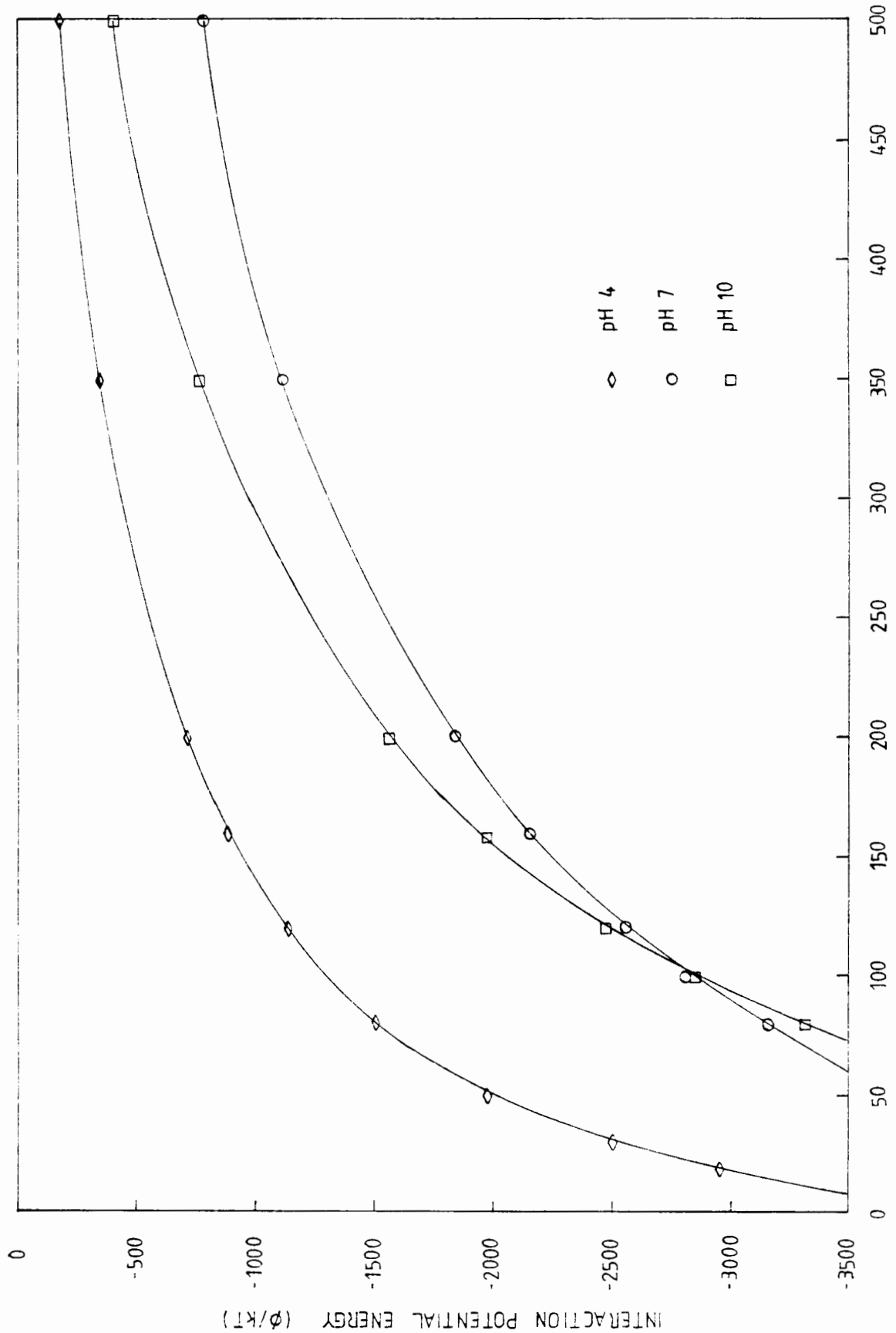

Figure 4.14 THE EFFECT OF pH ON THE INTERACTION POTENTIAL ENERGY CURVES FOR THE AMBERLITE IRA 938 RESIN - SILICON DIOXIDE SYSTEM.

liquid is observed to fall from the initial value to a value approaching what can be regarded as an equilibrium value corresponding to the conditions of the contact.

Time (days)	"Equilibrium" Concentration (mg/l)	Resin loading (mg/g dry resin)
0	322	0
20	104	76.3
40	44.3	97.2
110	0.7	112

TABLE 4.1 Adsorption isotherm results for sample No. 11

Inspection of Figure 4.1 reveals that after 20 days the samples had not yet equilibrated, as the colloid loading on the resin was still increasing with time. This is shown by the movement of the adsorption isotherm from curve A (after a 20 day contact) to curve B (after a 90 day contact).

Data in Table 4.1 indicates that the adsorption is irreversible and will continue until either of the two reacting species (Amberlite IRA 938 resin or Primal E1743) is depleted. (Adsorption reversibility of Primal E1743, and other colloids is further discussed in section 4.3.)

4.2.1 Effect of surface coverage on adsorption rate interpreted by electronmicroscopy

Electron micrographs of cross-sections through resin beads from sample 11, which had been contacted for 110 days, show that at least the outer 30 microns of the bead is fully covered (Photograph 4). Photograph 3 shows that there is a concentration profile across the bead; the readily accessible outside surfaces are covered (See close up Photograph 4) with Primal E1743 spheres while 50 microns (+- 1/10 of resin bead diameter and +- 100 colloid sphere diameters) into the bead, surfaces are completely clear.

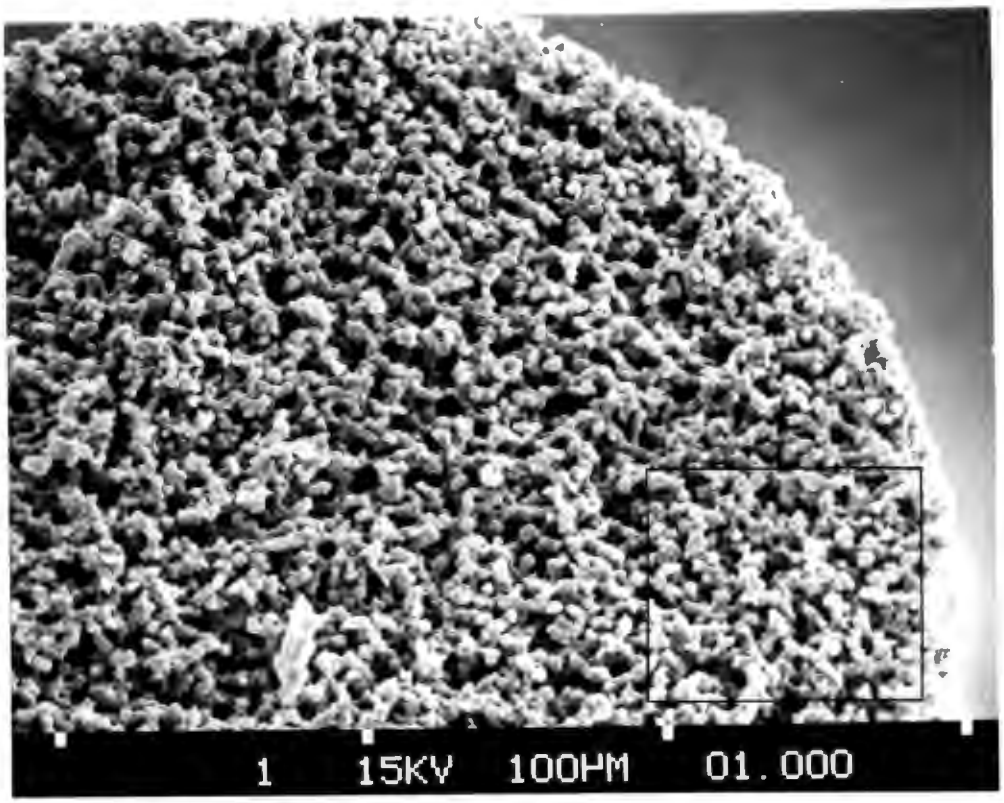

Photograph 2 A CROSS-SECTION THROUGH AN AMBERLITE IRA 938 RESIN BEAD, WHICH HAS BEEN CONTACTED WITH A PRIMAL E1743 SUSPENSION FOR 110 DAYS. THE EDGE OF THE RESIN IS COVERED WITH WHITE PRIMAL E1743 SPHERES. (× 400)

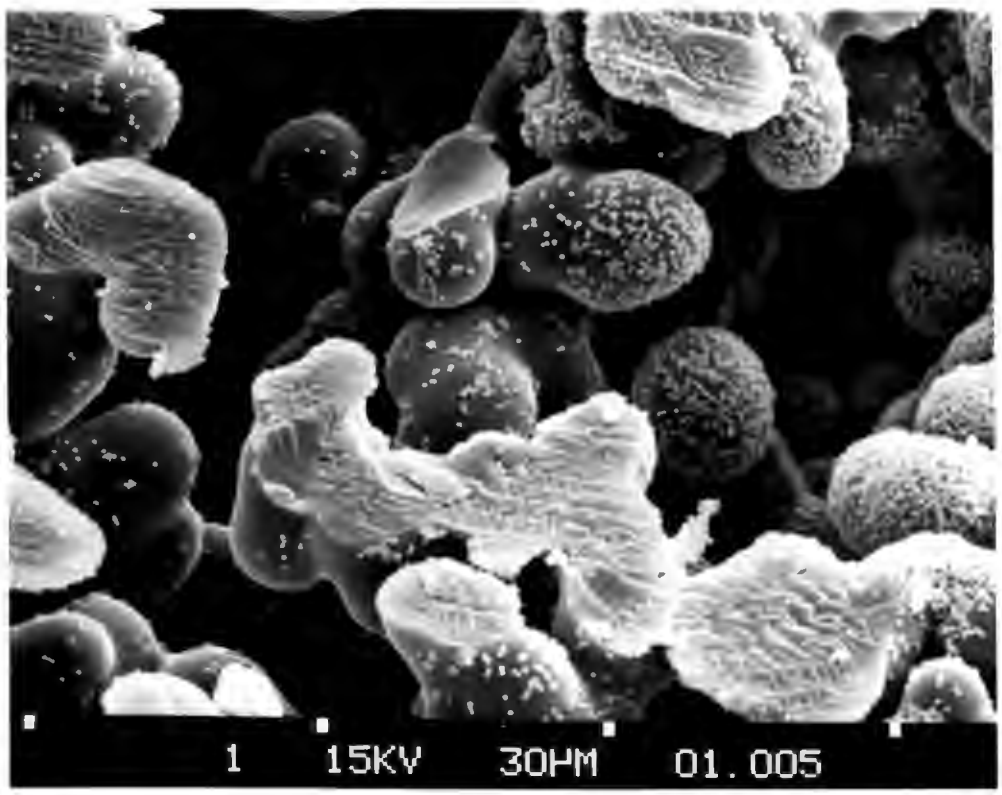

Photograph 3 A CLOSE UP OF THE AREA SHOWN IN THE ABOVE PHOTOGRAPH. NOTE THE STEEP CONCENTRATION GRADIENT OF THE ADSORBED PRIMAL E1743 SPHERES, GOING FROM LEFT TO RIGHT. (× 1 300)

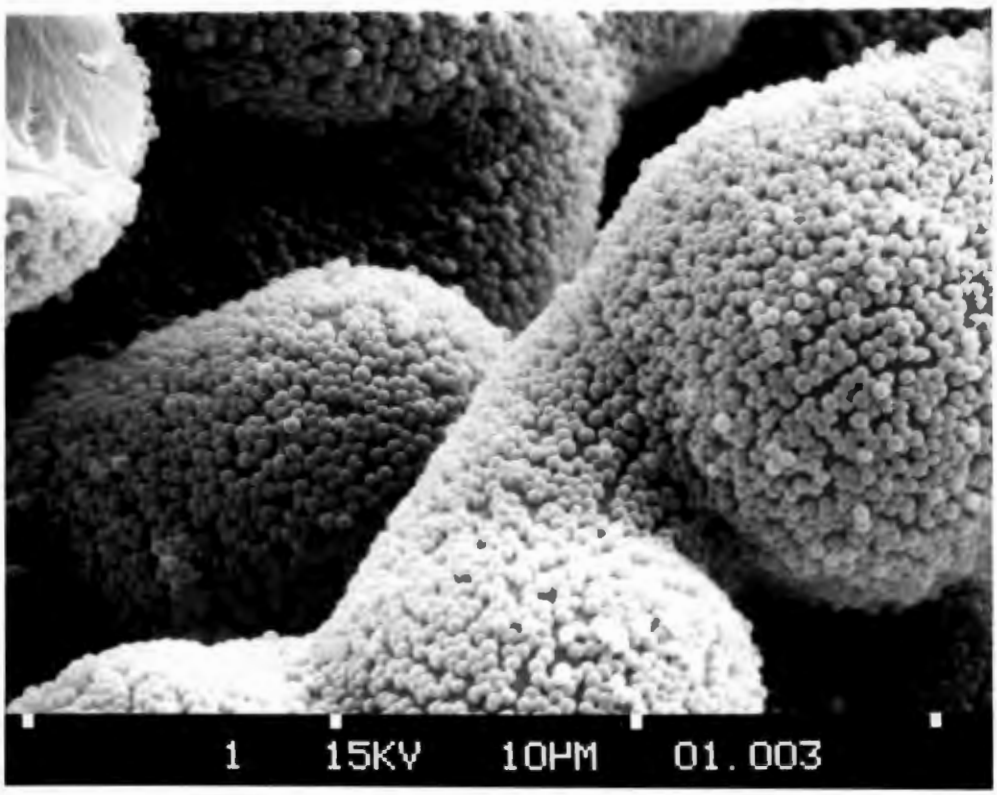

Photograph 4 A CLOSE UP OF THE OUTER EDGE OF THE RESIN BEAD. THE READILY AVAILABLE OUTSIDE AREA IS COVERED BY A MONOLAYER OF PRIMAL E1743 SPHERES. (× 4 000)

The question that arises from the above is: why is the adsorption rate so slow if only a small fraction of the total area has been covered ?

It is apparent that there is a large percentage of the total area that is not readily available for adsorption and is accessible only via the slow process of pore diffusion.

Table 4.2 shows that adsorption rate is strongly dependent on resin surface coverage, a 3.4 % decrease in surface area at low resin surface coverages resulted in a five fold decrease in the average adsorption rate. Clearly therefore adsorption to the outer surfaces of the resin (bottle 2) is faster than adsorption to the inner surfaces of the resin (bottle 8). Thus the outer surfaces of the resin have a higher availability than the inner surfaces of the resin.

Bottle No.	Resin loading time 0 (mg/g)	Surface coverage (%)	Contact time (days)	Suspension concentration (mg/l) start	end	Average adsorption rate (mg/day)
2	0	0	20	70	0	1.1
8	71	3.4	70	63	15	0.2

TABLE 4.2 Comparison of average adsorption rates at two different resin loadings/surface coverages.

The rate of adsorption therefore, is relatively fast until the outer surface of the resin is covered. It then decreases rapidly as the colloid has to penetrate further into the resin bead to "find" an available adsorption site. In a classical case the rapid slowing of the adsorption rate, as the surface reaction sites are utilised, yields information pertaining to the rate of film diffusion across the diffusion boundary layer and to the mechanisms and rate of pore diffusion.

In order to elucidate the importance of surface coverage and mechanisms of adsorption a 7 day run on the batch apparatus was

undertaken.

4.2.2 Investigation of effects of surface coverage using the Batch apparatus

In this investigation the rate of adsorption of model colloid, Primal E1743, to a one gram sample of resin, was monitored with increasing resin colloid loading but constant liquid phase concentration. Results are in Table 4.3. The flow of suspension through the resin bed and constant liquid phase concentration resulted in any given resin loading in Table 4.3 being attained in a shorter contact time than with the bottle point data presented in Table 4.2.

Time (day)	Rate Constant (1/min)	Resin Loading (mg/g)*	Surface Coverage (%)
0	0.0164	0	0
0.28	0.0066	25	1.2
0.56	0.0034	37	1.8
1.25	0.0016	55	2.7
2.15	0.0010	67	3.2
3.12	0.0009	73	3.5

TABLE 4.3 The variation of adsorption rate with resin loading. * (mg colloid/gram dry resin)

Looking at Table 4.3, it is evident that the adsorption rate decreases rapidly with resin loading. A value for surface coverage based on the manufacturers data is presented in the table. At low resin loadings, very small changes in the resin surface coverage are accompanied by large reductions in the adsorption rate. The expected first order relationship between surface coverage and adsorption rate is on indicated in this data.

Because adsorption rate is dependent on available resin surface area and only the outer shell of +- 50 microns is an active area,

effective outer and inner resin surface areas were calculated. The total surface area of the resin, given by the manufacturer, is approximately 7.3 m^2/g of dry resin. Outside surface areas for various resin particle sizes have been calculated in Appendix B12-B14. For the resin size fraction 425-600 microns, assuming the resin beads are perfect spheres, the value is 0.0455 m^2/g. Amberlite IRA 938 resin beads however are far from perfect spheres and are made up of myriads of microspheres as shown in electronmicroscope Photograph 1. The outer surface area of Amberlite IRA 938 resin beads is therefore greater than that of perfect spheres. An adjusted value for the outside surface area should therefore be calculated. The adsorption rate of Primal E1743 to Amberlite IRA 938 resin was therefore compared with the adsorption rate to a similar resin with a structure such that adsorption is an outside surface phenomenon only. Amberlite IRA 904 resin was used as it is identical to Amberlite IRA 938 resin except that its pores are much smaller so that the Primal E1743 spheres cannot penetrate the bead (see Photographs 5&6 and Table 1.1).

The two adsorption rates were compared and the adjusted outside surface area for Amberlite IRA 938 was calculated as follows:

$$\text{Area of resin} = \frac{\text{Adsorption rate for Amberlite IRA 938}}{\text{Adsorption rate for Amberlite IRA 904}} \times \text{surface area of 1g of perfect spheres } (0.0455\ m^2/g)$$

$$= 0.2\ m^2$$

Thus the two effective surface areas are,

outside surface area = 0.2 m^2/g
inner surface area = 7.1 "
total surface area = 7.3 "

The variation of adsorption rate with this modified outside surface coverage is presented in Table 4.4.

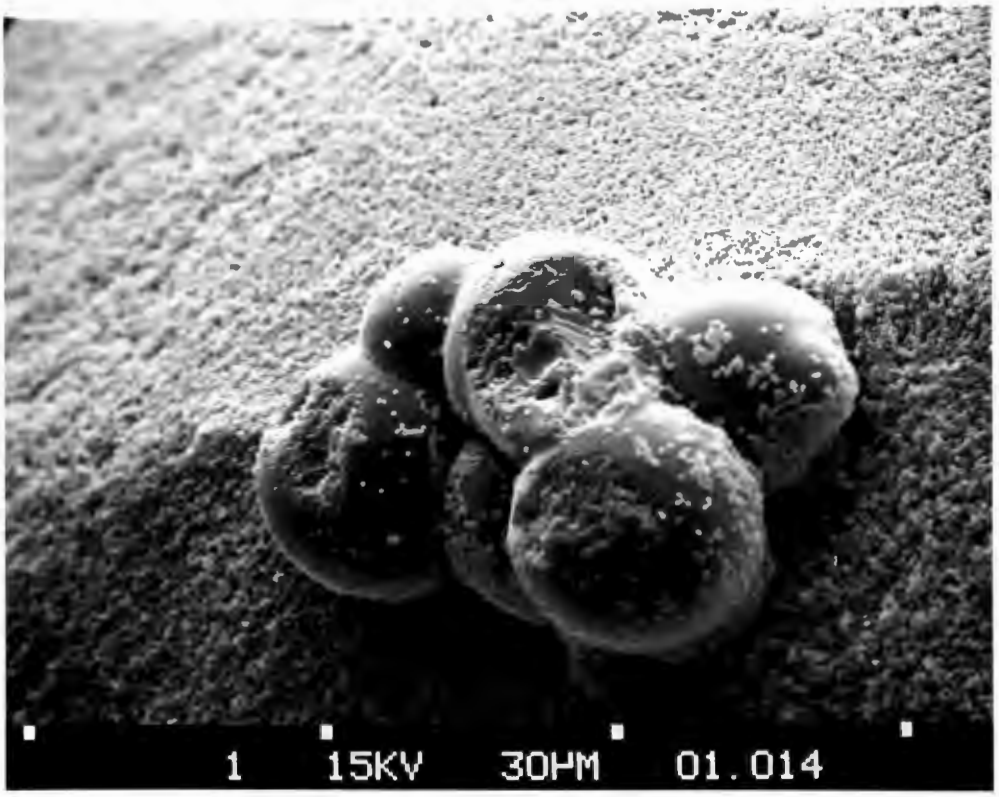

Photograph 5 A PIECE OF AMBERLITE IRA 938 RESIN RESTING ON THE SURFACE OF AN AMBERLITE IRA 904 RESIN BEAD. THE RELATIVE SIZES OF THE TWO RESINS MICROSPHERES IS WELL ILLUSTRATED. (× 1 300)

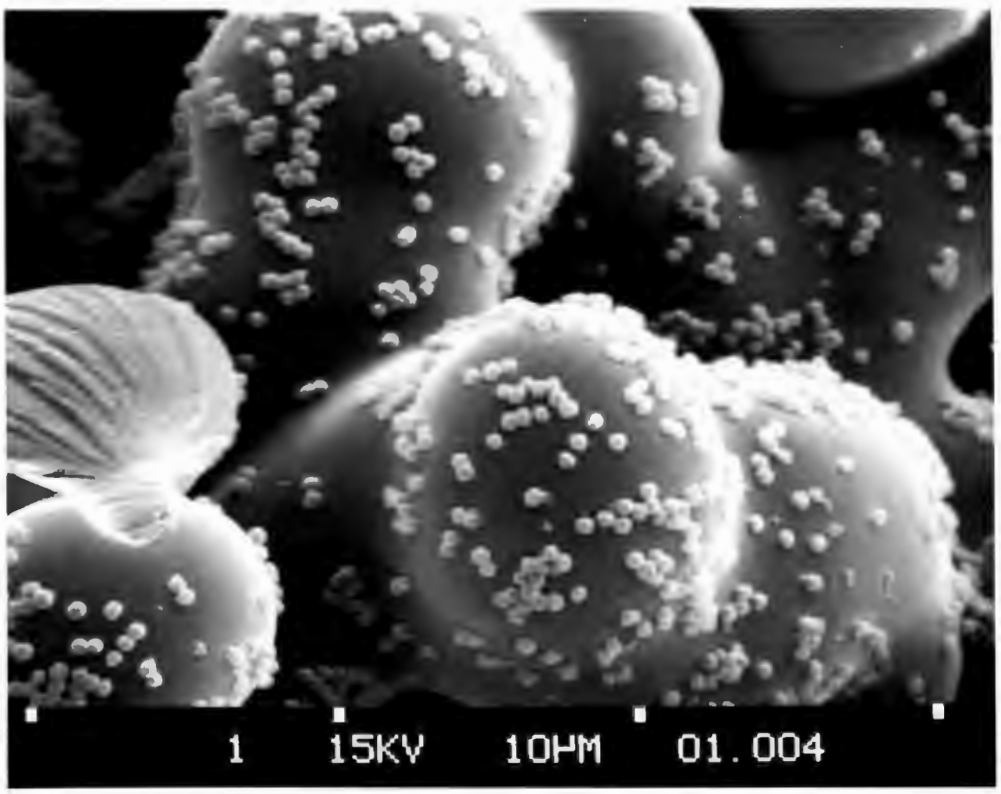

Photograph 6 PRIMAL E1743 SPHERES ADSORBED TO AMBERLITE IRA 938 RESIN SHOWING, THE RELATIVE SIZES OF THE RESIN MICROSPHERES AND PRIMAL E1743 SPHERES. (× 1 500)

Time (days)	Rate Constant (1/min)	Resin Loading (mg/g)*	Outside Surface Coverage (%)
0	0.0164	0	0
0.28	0.0066	25	44.3
0.56	0.0034	37	66.4
1.25	0.0016	55	97.8
2.15	0.0010	67	100.0
3.12	0.0009	73	100.0

TABLE 4.4 The variation of adsorption rate with resin outside surface area.
* (mg colloid/gram dry resin)

4.2.3 Rate expressions based on % modified outside surface coverage

The adsorption rates at low resin loadings show a first order dependence on the available outside surface area. This indicates that when the adsorption rate is film diffusion controlled, the rate equation could be given by,

$$-r_a = \frac{1}{V} kC_aC_{so}$$

where C_a is the colloid concentration,
C_{so} is the available outside surface area of the resin, and
k is the mass transfer reaction rate constant.

This is a typical equation for a second order irreversible process. A simplification of this model is used to interpret the data from kinetic studies, as described in section 3.3.3.2.

Whereas the above exterior surface coverage is a useful concept at low resin loadings, the slowing of the adsorption rate with increasing loading can best be explained by the shifting of the rate controlling step in the adsorption sequence. At low loadings the adsorption rate is controlled by the diffusion through the hydrodynamic boundary layer around the resin bead, however as

the outer surface of the resin becomes covered the adsorption becomes increasingly pore diffusion controlled.

The above situation, of shifting rate controlling steps and decreasing rates due to particles having to diffuse further into the resin bead, is analagous to the "Shrinking core model" used to explain certain solid catalysed reactions.

4.2.4 Shrinking core model

In this model the reaction occurs first at the outer skin of the particle. The zone of reaction then moves into the solid, and leaves behind completely converted material, an inert solid. Thus at any time there exists an unreacted core of material which shrinks in size during reaction as shown in Figure 4.2. Film diffusion gives way to pore diffusion, as the rate controlling step, when the reaction zone moves from the outer surface skin to the interior of the particle.

4.2.5 Colloid transport within the adsorbent

The question as to why the adsorption is such a slow process, may now be rephrased to read: why is penetration of the colloidal particles into the bead so slow ?

There are two possible mechanisms for particle diffusion along a pore. Both these transport mechanisms are slow processes. The first is bulk diffusion in the macropores (called Knudsen diffusion for gaseous systems). In the Amberlite IRA 938 resin - Primal E1743 system the particles being adsorbed are so large that their diffusion coefficients are at least 1000 times lower than those of small ions, thus their diffusion rate is exceedingly slow.

The second transport process of diffusion along the surface or pore walls may be more rapid than Knudsen diffusion (both transport processes may occur simultaneously). In a simplistic sense, an adsorbed particle is said to "hop" along the pore

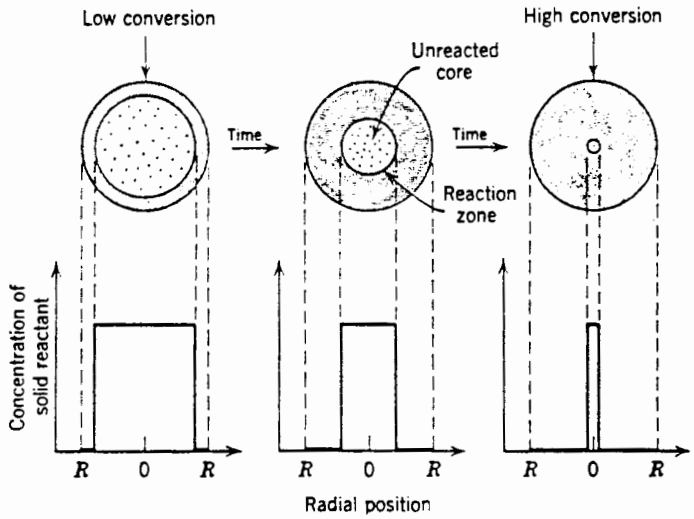

Figure 4.2a

SHRINKING CORE MODEL (Levenspiel)(73)

Figure 4.2b

REPRESENTATION OF A REACTING PARTICLE WHEN DIFFUSION THROUGH THE LIQUID FILM IS THE RATE CONTROLLING RESISTANCE. (Levenspiel)(73)

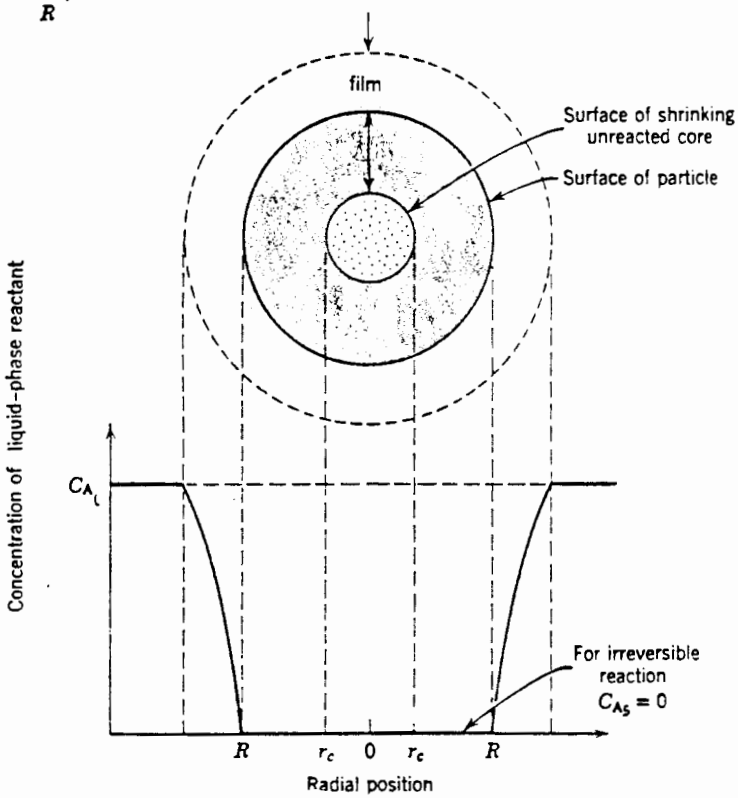

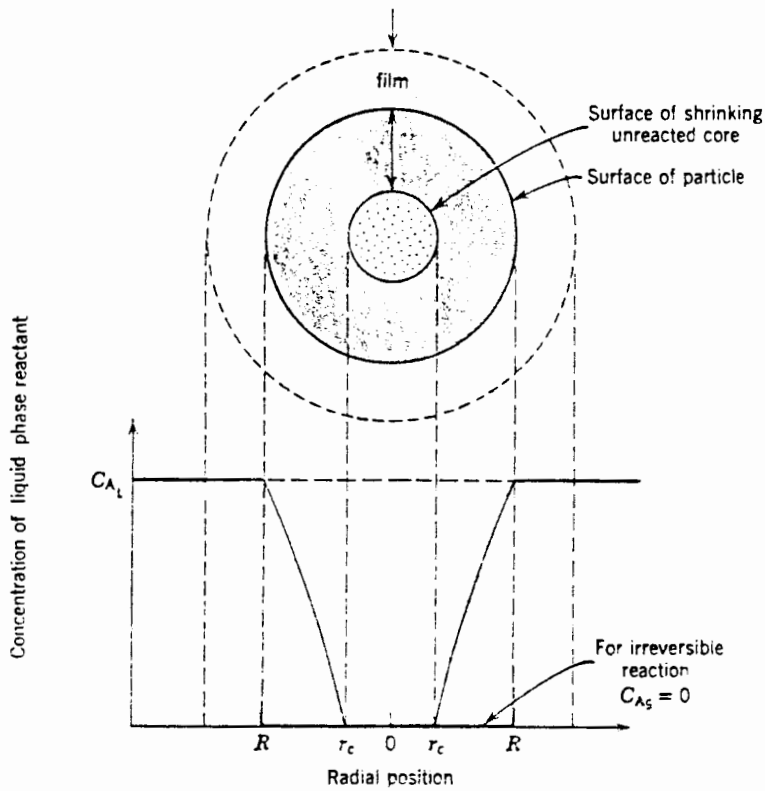

Figure 4.2c

REPRESENTATION OF A REACTING PARTICLE WHEN DIFFUSION THROUGH THE REACTED LAYER IS THE RATE CONTROLLING RESISTANCE. (Levenspiel)(73)

surface when it attains sufficient activation energy and when an adjacent adsorption site is available (25).

4.2.6 Rate expressions based on % interior and modified exterior surface coverages

From the above it is clear that there are two distinct transport steps; transport to the resin outer surface (film diffusion) and transport within the resin bead (pore diffusion), therefore an adsorption rate expression should contain two terms; a term including the modified outside surface area of the resin and a term including the interior surface area of the resin. The rate expression could therefore be of the form,

$$-r_a = \frac{1}{V}(k_1 C_a C_{so} + k_2 C_a C_{si})$$

where k_1 is the outside surface mass transfer rate constant,
k_2 is the interior surface mass transfer rate constant, and
C_{so} interior surface area of the resin.

The above expression is based on simplistic assumptions and as such ignores the following factors:

i) When the adsorption process is pore diffusion controlled, adsorption rate decreases with increasing resin coverage as the particles have to penetrate further into the resin bead to "find" an adsorption site. The "Shrinking core model" discussed in section 4.2.4 proposes that for a given size of unreacted core the adsorption rate is constant; however as the core shrinks the reacted (inert) layer becomes thicker, lowering the rate of diffusion of solute. Thus the adsorption rate should be directly proportional to $(\frac{1}{r} - \frac{1}{R})^{-1}$ where R is the radius of the particle and r is the radius of the unreacted core.

ii) Adsorption rate is thought to be insensitive to solute concentration when pore diffusion is adsorption rate controlling (50). Thus the colloid concentration C_a in the

interior surface reaction term should perhaps be raised to a power less than one. ie C_a^n where $n<1$.

Although the above is a simple rate expression it covers a wide range of adsorption situations and therefore can be very useful.

For example at low resin loadings the term incorporating k_2 may be assumed zero ($k_2 << k_1$) and the expression reverts two the second order irreversible adsorption expression based on percentage modified outside surface coverage. A further simplifying assumption, of minimal change in the modified outside surface coverage during adsorption, reduces the equation further to the typical first order (first order with respect to colloid concentration) adsorption equations found in the literature (27,34) and used in data interpretation in this work.

4.3 RESIN REGENERATION AND ADSORPTION REVERSIBILITY

Removal of the colloidal particles from the resin is of the utmost importance as regeneration/cleaning and re-use of the resin is essential if this adsorption process is to be useful in purifying water.

4.3.1 Desorption in hot water

This was tried first because the capacity of an adsorbent for a dissolved species is usually adversely affected by increasing temperature, and often an increase in temperature of 15 to 25° C is sufficient to halve the capacity of the adsorbent. The regeneration/cleaning technique attempted therefore consisted of passing hot water through a bed of resin loaded with 25 mg/g of Primal E1743. The result however was negative. Even at a temperature of 50° C, 15° C above the resin manufacturers suggested maximum operating temperature for the resin, there was no significant release of the colloid.

Attempts at higher temperature regeneration were abandoned as the high temperatures cracked the flow cell used in the spectophoto-

meter and were expected to have minimal effect on the release of colloid from resin.

4.3.2 Chemical regeneration/cleaning

The use of both 1N sodium hydroxide and ethanol proved ineffectual, as negligible quantities of Primal E1743 were removed from the resin.

The harsh regeneration conditions of hot hydrochloric acid followed by hot sodium hydroxide, recommended by Rohm and Haas for extreme regeneration problems, were more successful. Data may be found in Figure 4.3. After twenty hours of pumping 1N sodium hydroxide at 50° C through the resin bed, the regeneration was 35% complete. (Note that it took about 7 hours to load this resin to 25mg/g see Table 4.3).

Regeneration using this technique is exceedingly slow and the regeneration rate decreases as the resin loading decreases. Thus the time and the harsh chemical conditions required make this resin regeneration/cleaning technique unacceptable.

The partial success of this regeneration/cleaning method is thought to arise from the combined effects of the increased temperature of the regenerant chemicals and the changes in zeta potentials of the resin and colloidal particles. The increased ionic strength and change in the pH of the solution surrounding the resin affects the surface charges of the resin and colloidal particles and thus can drastically change the strength of the adsorptive forces (see Section 4.4.5 for discussion of the effects of pH and ionic strength on the adsorptive forces). The increased temperature of the regenerant solution, increases the "random bombardment" of the adsorbed particles by the molecules in the solution and thus increases the probability of a particle being dislodged from the resin surface. (Note that without the effect of chemicals on the adsorptive forces the increased temperature was ineffective.)

Having attempted all the conventional regeneration/cleaning tech-

niques it was decided that the adsorption of Primal E1743 to the resin for all practical purposes can be assumed irreversible. This was in direct contrast to the natural colloids adsorbed from seawater samples which were successfully removed from the resin by rinsing the resin with sodium hydroxide.

Electron micrographs of resin loaded with seawater colloids and subsequently regenerated resin (see Photographs 7&8) show that the resin can be completely regenerated/cleaned using 0.1N sodium hydroxide.

Thus it can be concluded that Primal E1743 from the point of view of the strength of the adsorbtive forces and therefore ease of regeneration of the resin is not a good model for natural colloids in this system. However it remains a good colloidal material to use for kinetic and other studies of the characteristics of resin - colloidal particle adsorption systems and possibly for studying resin bead structures.

4.3.3 Ultrasonic regeneration/cleaning

At this stage a different approach to the resin regeneration /cleaning problem was adopted. It was reasoned,that if a particle was able to diffuse along the surface of the resin by "hopping" to an available adsorption site, should it attain sufficient energy, then should it acquire enough energy, it would "hop" continuously and not re-adsorb to the resin surface. This idea was followed through and the necessary energy was applied using an ultra-sonic bath (see section 3.3.4 for experimental methods).

This technique proved to be highly successful but detrimental to the resin structure. Initial studies, using a small "Son-Blaster" ultrasonic bath (65 watt), showed that there was a rapid breakdown of the resin structure, with all the weak extremities of the resin being sheared off by the vibration. However, after a period of 5 to 6 hours, a stable core of resin remained which seemed impervious to further breakdown by the ultrasonic waves.

The initial investigation showed that a 1g resin sample loaded

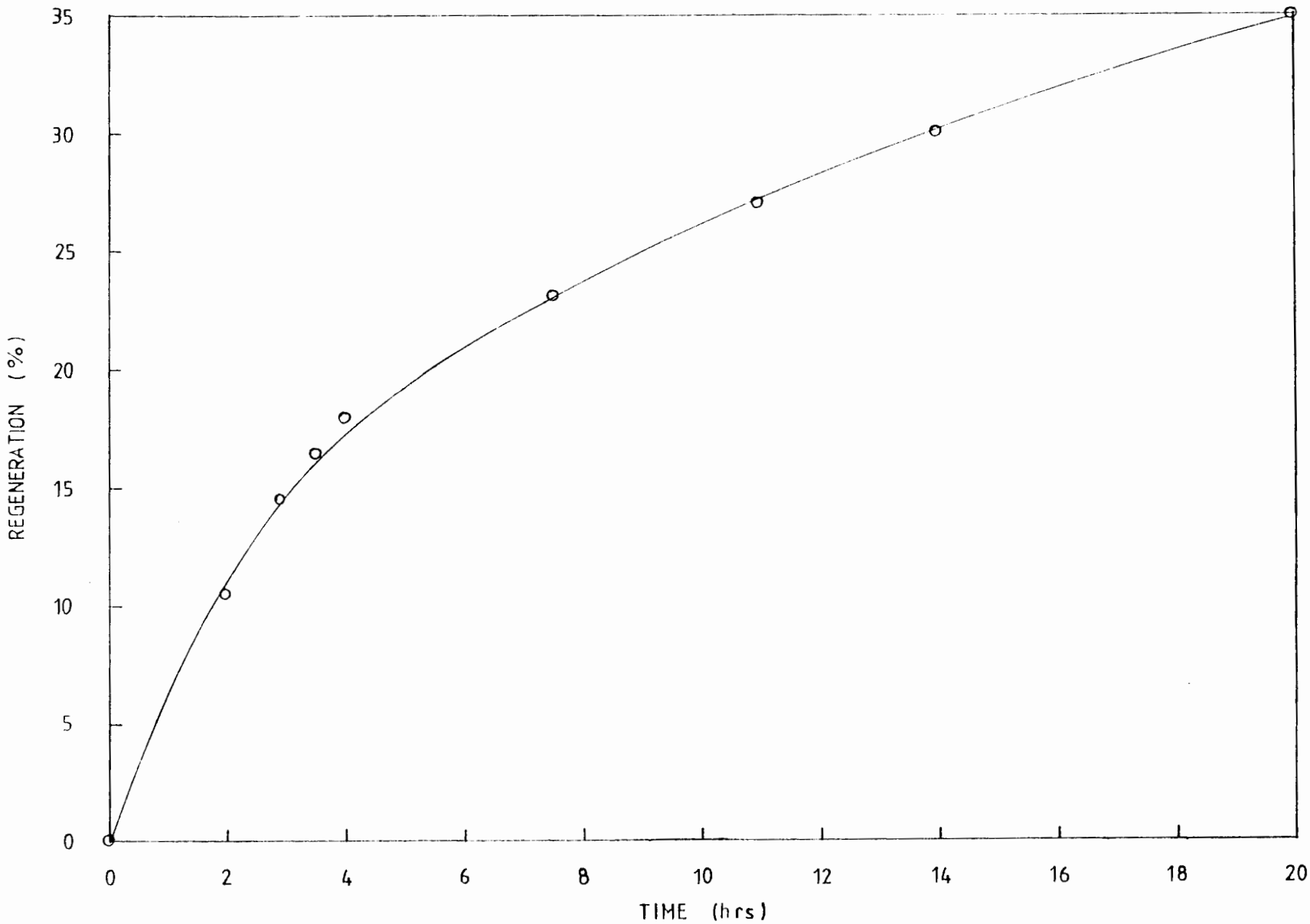

Figure 4.3 CHEMICAL REGENERATION OF AMBERLITE IRA 938 RESIN LOADED WITH PRIMAL E1743 SPHERES.

by Rohm and Haas. Amberlite IRA 938 resin has been used for the removal of both organic and inorganic colloidal matter from liquid streams (13).

A brief summary of the important properties of Amberlite IRA 938 follows (14)(detailed specifications can be found in Appendix D):

Appearance	light yellow
Functional group	$-N-(CH)_3$
Moisture content	72 - 78%
Pore diameter range	25 000 - 250 000 A*
Surface area	7.3 m^2/g
Anion exchange capacity	3.8 meq/g (chloride form)

* This is the pore diameter size range given by Rohm and Haas in reference 14. Other references (13, 47) give slightly different pore size ranges.

3.2.3 Other colloidal materials

Colloidal titanium dioxide and silicon dioxide were also used, as they had different zeta potentials and colloidal silica was available in a number of particle sizes.

Colloidal titanium dioxide, a sample of which was obtained from South African Nylon Spinners, has the following properties:

Chemical formula	TiO_2 > 99.5%
Particle size	0.4 microns*
Particle density	4.17 (SG)
Zeta potential (pH 7)	-16mv (measured value)

* This is an average particle size. However more than 99% of the particles are believed to be less than 1 micron in size.

The colloidal silicon dioxide was a Samancor product named "Microsil". Its specifications are as follows (48):

Chemical formula	SiO_2	> 92.0%
Particle size	95%	< 40 microns
	87%	< 10
	75%	< 3
	70.5%	< 1.5
Particle density	2.6 (SG)	
Zeta potential (pH 7)	-38mv (measured value)	

The colloidal silicon dioxide was separated into five size fractions (see section 3.4.1) using a Beckmann TG 6 centrifuge. The particle size of of each size fraction was checked on a Coulter Counter (Model TA II with population accessory) with a 30 micron orifice tube.

A four week period was devoted to measuring colloidal particle sizes on this instrument. This work showed that this particle sizing technique is useful down to a particle size of about 0.5 microns, below this particle size background noise becomes significant and this results in erroneous particle size distribution data. The electronmicroscope was therefore used to size smaller particles.

3.2.4 Other resins

The unfunctionalised precursor of Amberlite IRA 938 resin (supplied by Rohm and Haas on request) and a cation form prepared from the latter were used.

The cation resin was prepared using the procedure in Appendix D. The unfunctionalised resin beads and cation resin have the same specifications as Amberlite IRA 938 resin, except for the following specifications:

Unfunctionalised resin	
Appearance	white
Functional group	none
Ion exchange capacity	zero

Cation resin	
Appearance	light brown
Functional group	$-SO_3$
Cation exchange capacity	0.30 meq/g (hydrogen form)

3.3 EXPERIMENTAL PROCEDURES AND APPARATUS

3.3.1 Resin Preparation

3.3.1.1 Screening

Resin kinetics are usually sensitive to resin bead size and thus in order to obtain comparable kinetic results the resins were wet screened into the following size fractions:

1000 - 850 microns
850 - 600
600 - 425
425 - 300
300 - 150

In all experiments except the experiments investigating the effects of resin bead size, the 600 - 425 micron size fraction was used.

The resin was soaked in distilled water for 24 hours (to ensure that it was fully water-swollen). A 500 ml sample was then placed in the Endecotts test sieve shaker and sieved for one hour. The resin retained on each sieve was then saved.

3.3.1.2 Resin sample preparation and loading

The resin was then dried at 100°C for 24 hours, before being weighed out into 1 gram samples which were put into sealed sample bottles containing distilled water.

When the resin sample was required it was loaded into the required ionic form by a series of four 100 ml batch contacts

with approximately 1N solutions of the required chemical. The resin was then put into a column and rinsed with 500 bed volumes of distilled water, followed by 250 bed volumes of the solution to be used in the experiment.

The ionic form in which the resin was used depended upon the pH at which the experiment was to be run. At a pH of 4 +- 0.2 the resin was used in the chloride form. For experiments carried out at pH values of 7 +- 1.5 and 10 +- 0.2 the resin was used in the hydroxide forms.

It was found that the use of the hydroxide form at neutral and high pH values resulted in smaller variations in the total ionic strength of the suspension than the chloride form. The use of the hydroxide form for experiments carried out at neutral pH, did not cause significant increases in the pH of the suspension as the solutions contained very low concentrations of exchangable anions (distilled water). It was considered acceptable if the pH varied by +- 1.5 pH units for experiments carried out at the stated pH of 7.

3.3.2 Adsorption Isotherms

One gram resin samples were placed into bottles containing 300 ml of distilled water. Varying amounts of the model colloid (Primal E1743) were then added to each bottle. The range of concentrations prepared were 35 to 350 mg/l. The bottles were sealed and placed on a tumbler wheel which was rotated at 6 rpm so that the resin continuously fell through the colloidal suspension.

The concentration of the colloidal suspension in each bottle was checked after 20, 40 and 70 days using a Varian Superscan UV/VIS spectrophotometer. The spectrophotometer was calibrated at a wavelength of 380nm using known concentrations of the colloid suspension.

3.3.3 Batch Studies

3.3.3.1 Apparatus

Most of the experiments in this work were performed using a batch system, a recycle reactor system with an infinite recycle ratio.

The system consisted of the following apparatus:

Variable speed Watson-Marlow peristaltic pump
Varian Superscan UV/VIS Spectrophotometer with chart recorder and flow cell
1 litre glass reservoir and stirrer
Resin column (reactor)
Temperature controlled water bath
Interconnecting silicon rubber tubing

1 Gram resin samples were loaded into the resin column (19 mm in diameter, 30 mm in length). The colloid suspension was pumped from the stirred reservoir through the resin column, through the spectrophotometer, which monitored the colloidal particle concentration, back to the reservoir. The spectrophotometer was set to record the change in absorbance, (at wavelength 380nm) of the colloid suspension passing through the flow cell (path length 4 cm), with time. The temperature controlled water bath was used to control the temperature of the colloidal suspension in the reservoir while the stirrer kept its composition uniform.

3.3.3.2 Method of interpretation of batch data

The rate of particle adsorption in a packed bed can be modelled using first order kinetics, provided there is minimal change in the available collection surface area during measurement of the rate (discussed in sections 2.5 and 4.2.2). The rate equation is given by:

$$-r_a = -\frac{\partial C_a}{\partial t} = kC_a$$

k - incorporates the suspension volume and collector surface area.

The measured adsorption rates using the batch system were found

to follow this classical first order model(see figure 3.1).

The mass transfer rate constant, k , could therefore be used to quantitfy adsorption rates. Separating and integrating the above expression yields:

$$- \int_{c_o}^{c} \frac{\partial C_a}{C_a} = k \int_{o}^{t} \partial t$$

Thus the slope of a $-\ln(C/C_o)$ vs t plot gives the value of the mass transfer rate constant, k .

3.3.4 Resin regeneration and adsorption reversibility.

The regeneration studies were undertaken using the batch system.

One gram resin samples each loaded with between 25 and 45 mg of model colloid (Primal E1743), were used in the three different regeneration techniques studied.

3.3.4.1 Hot water

The first technique tried was desorption in hot water as the capacity of an adsorbent for a dissolved species is usually adversely affected by increasing temperature.

This involved cycling 200 ml of water at 35 and subsequently 50°C through the loaded resin bed, at a flow rate of approximately 45 ml/min and monitoring the increase in the colloid concentration with time.

3.3.4.2 Chemical regeneration

The second technique was chemical regeneration. Changing the ionic strength and pH of the suspension affects the adsorptive forces holding the colloid particles and thus the colloids may be released.

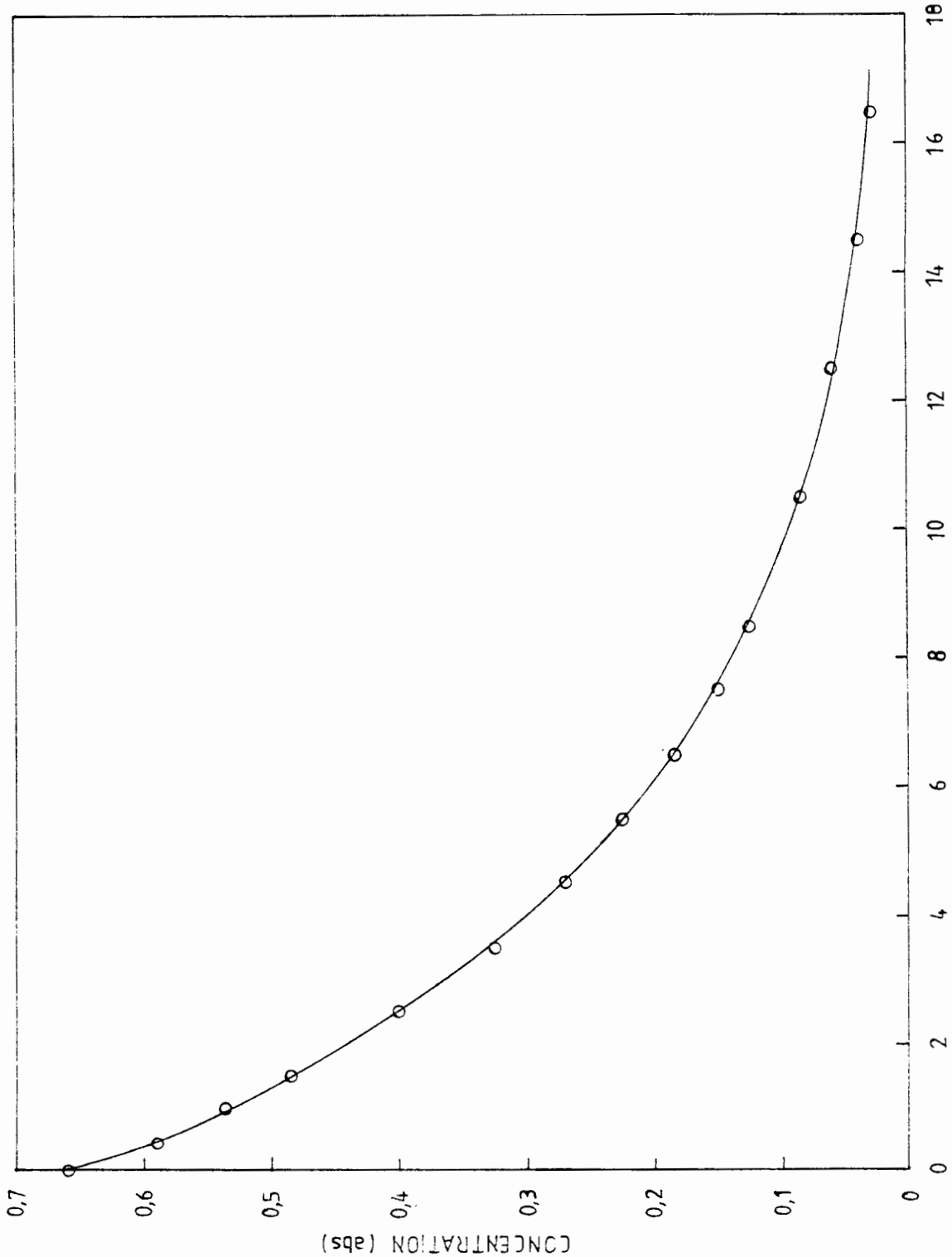

Figure 3.1 CONCENTRATION TIME - CURVE SHOWING THE CLASSICAL FIRST ORDER REACTION RATE OF THE AMBERLITE IRA 938 - PRIMAL E1743 SYSTEM.

The procedure was the same as for the hot water desorption, except that regenerant chemical replaced the hot water.

The three sets of regenerating chemicals tried were:

i) 1N NaOH at 35°C
ii) Ethanol at 20°C
iii) 1N HCl at 50°C for five minutes followed by
1N NaOH at 50°C

Regeneration at low ionic strength was not tried as Amberlite IRA 938 resin and model colloid (Primal E1743) have opposite charges and thus high ionic strength reduces the attractive coulombic forces betweem them. However, regeneration at low ionic strength may be advantageous if the particles and collector have similar charges.

3.3.4.3 Ultrasonic cleaning

The third regeneration method studied was ultrasonic cleaning of the resin. This method involved bombarding the resin and colloids with high frequency sound and thus the colloids were vibrated off the resin surface.

This technique involved a slight modification of the batch system described in section 3.3.3; the resin column was submerged in a temperature controlled 960 watt 'Branson' ultrasonic bath which operated at a frequency of 40 kHz.

Distilled water was pumped through the resin bed and the colloidal particle concentration in the effluent water was recorded using the spectrophotometer.

3.4 PARAMETERS AFFECTING THE KINETICS OF COLLOID PARTICLE ADSORPTION

3.4.1 Colloidal Particle Size

The effect of particle size on adsorption rate is of great significance, as it may determine the transport mechanism by

which a particle is brought to the collector surface.

Typically particles larger than about 1 micron are transported to the collector surface by settling and interception while smaller particles are transported by Brownian diffusion (26).

The colloidal particle used to investigate the effect of colloidal particle size on adsorption rate was silicon dioxide as model colloid Primal E1743 was not available in different sizes.

The rate of adsorption of five different size colloidal silicon dioxide particles (0.012, 0.5, 1.2, 4.0, 8.0 microns) to Amberlite IRA 938 resin was measured.

These experiments were carried out using a modified batch system. Colloidal silicon dioxide does not show sufficient absorbance on the spectrophotometer and therefore the more sensitive Hach Turbidimeter 2100 had to be used.

Discrete samples were taken from the system, their concentration measured on the turbidimeter and returned to the reservoir. Samples were taken every 1 to 2 minutes.

To prevent filtration effects of the larger particles in the resin bed, a fluidised bed system with a flow rate of approximately 22ml/min was used.

The suspensions of silicon dioxide were made up using 0.22 micron filtered distilled water. Typically the filtered distilled water had a turbidity of 0.005 NTU while the silicon dioxide suspension had a turbidity of approximately 0.12 NTU. The turbidimeter is very sensitive to particulate contamination and therefore the system was flushed with 2 litres of filtered distilled water (the resin bed included), prior to the circulation of the suspension through the system, by-passing the resin bed, to allow the colloid concentration to stabilise.

3.4.2 Resin Bead Size

The effect of resin bead size on adsorption rate can help identify the rate determining step in the adsorption process.

Typically for film diffusion control (49):

$$\text{adsorption rate} \propto (\text{resin bead diameter})^{(-1.5 \text{ to } -2.0)}$$

while for pore or particle diffusion control;

$$\text{adsorption rate} \propto (\text{resin bead diameter})^{(-2.0)}$$

The adsorption rates of Primal E1743 to five different resin size fractions were measured.

In each size fraction 1 gram resin samples were loaded into the resin column and the colloid suspension was pumped through the resin bed as described in section 3.3.3.

The colloid suspension was pumped through the system at approximately 45 ml/min (6.4 BV/min). Prior to the initiation of the experiment, the colloid suspension was pumped through the system, by-passing the resin column, for 5 minutes to allow the concentration of the suspension to become uniform throughout the system.

The experiment was then started and the chart recorder monitored the change in absorbance with time (chart recorder was usually set to record for 100 minutes).

3.4.3 Resin surface coverage

The effect of surface coverage on adsorption rate can provide useful information on the rate of film and rate and mechanisms of pore diffusion.

The surface coverage investigation was accomplished using a prolonged batch study (7 days), using the batch system.

500 ml of Primal E1743 suspension was cycled through the system at approximately 45 ml/min. The rate of adsorption was measured after 0, 25, 37, 55, 67 and 73 mg of colloid had been adsorbed to

the resin. The rates of adsorption were measured over short periods (25, 35, 70, 100, 200 and 200 minutes respectively) so that there was minimal change in the available surface area during measurement of the adsorption rate.

The concentration of the colloid suspension was kept close to 20mg/l by the injection of Primal E1743 into the reservoir when the concentration fell below 10 mg/l.

3.4.4 Superficial fluid velocity in the resin bed.

Adsorption to the outer surface of the resin is thought to be film diffusion controlled and thus dependent on the thickness of the hydrodynamic boundary layer. As the hydrodynamic boundary layer is determined by the superficial fluid velocity in the resin bed, it was decided to vary the flow rate of colloid suspension through the resin bed and measure the resulting adsorption rates.

The experiments were carried out using the batch apparatus and the range of flow rates used were 45 to 135 ml/min (6.4 to 19.3 BV/min).

The remainder of the experimental procedure is identical to that outlined in section 3.4.2.

3.4.5 Resin charge

Adsorption of colloidal particles to resin can be enhanced, retarded or prevented by the surface charge of the resin. Like charges prevent adsorption while opposite charges can enhance adsorption rates to the resin.

The effect of resin charge on colloidal particle adsorption to resin was studied using strong anion Amberlite IRA 938 resin, its unfunctionalised precursor and a strong cation resin prepared from the latter (for method of preparation see Appendix D).

The anion resin (Amberlite IRA 938) was used in the hydroxide form and the cation resin in the hydrogen form. The colloid suspension was cycled through the batch system at a flow rate of 70 ml/min.

3.4.6 Charge on colloidal particles

The charge on colloidal particles as with resin surface charge can affect the adsorption rate of the colloid to the resin.

To investigate the effect of colloid surface charge on adsorption rate, adsorption rates for three colloidal particles (silicon dioxide, titanium dioxide and Primal E1743) having different zeta potentials, to Amberlite IRA 938 resin were measured.

Adsorption rates of the Primal E1743 and the titanium dioxide to the resin were measured using the batch system. Adsorption rates of silicon dioxide to the resin were measured using the modified batch system described in section 3.4.1.

The experimental procedure used for the titanium dioxide was the same as that outlined in section 3.4.2, except that the titanium dioxide particles were prevented from flocculating by placing the reservoir in the Branson ultrasonic bath.

These experiments were undertaken at a flow rate of 70ml/min.

3.4.7 Suspension pH

Suspension pH affects the zeta potentials of both the colloidal particles and resin and thus can have a marked effect on colloidal particle adsorption rates to the resin.

The effect of pH on the kinetics of adsorption of colloidal particles to the resin was studied using the batch system.

The rate of adsorption of the colloidal particle to the resin was

studied at three pH values 4 +- 0.2, 7 +- 1.5 and 10 +- 0.2. The pH of the colloidal suspension was adjusted using dilute NaOH and HCl. The resin was used in both of its ionic forms; the chloride form at pH 4 and the hydroxide form at pH 7 and 10 (see section 3.3.1.2).

The experimental procedure used in this investigation was the same as that described in section 3.4.2, except that the colloid suspension was cycled through the system at a flow rate of 70ml/min (10.0 BV/min).

3.4.8 Ionic strength of the suspension

The ionic strength of a suspension affects the distance over which coulombic forces are effective, thus ionic strength can have a marked effect on adsorption rate.

The effect of ionic strength on adsorption rate was carried out using the batch system.

The ionic strength of the suspension was adjusted using NaCl. The six ionic strengths used were - 0, 20, 250, 1000, 2500 and 3000 mg/l NaCl. The resin was used in the chloride form and the suspension was cycled through the systen at 70 ml/min.

3.4.9 Combined effect of certain parameters

After the initial investigations the combined effect of a number of parameters was studied.

i) The ability of the cationic and unfunctionalised resin to adsorb each of the three colloidal particles (Primal E1743, titanium dioxide and silica dioxide) was studied. The experimental procedure and apparatus used can be found in sections 3.4.5 and 3.4.6.

ii) The ability of the anion resin to adsorb each of the

colloidal particles at the three pH values of 4, 7 and 10 was studied. The experimental procedure is located in sections 3.4.6 and 3.4.7.

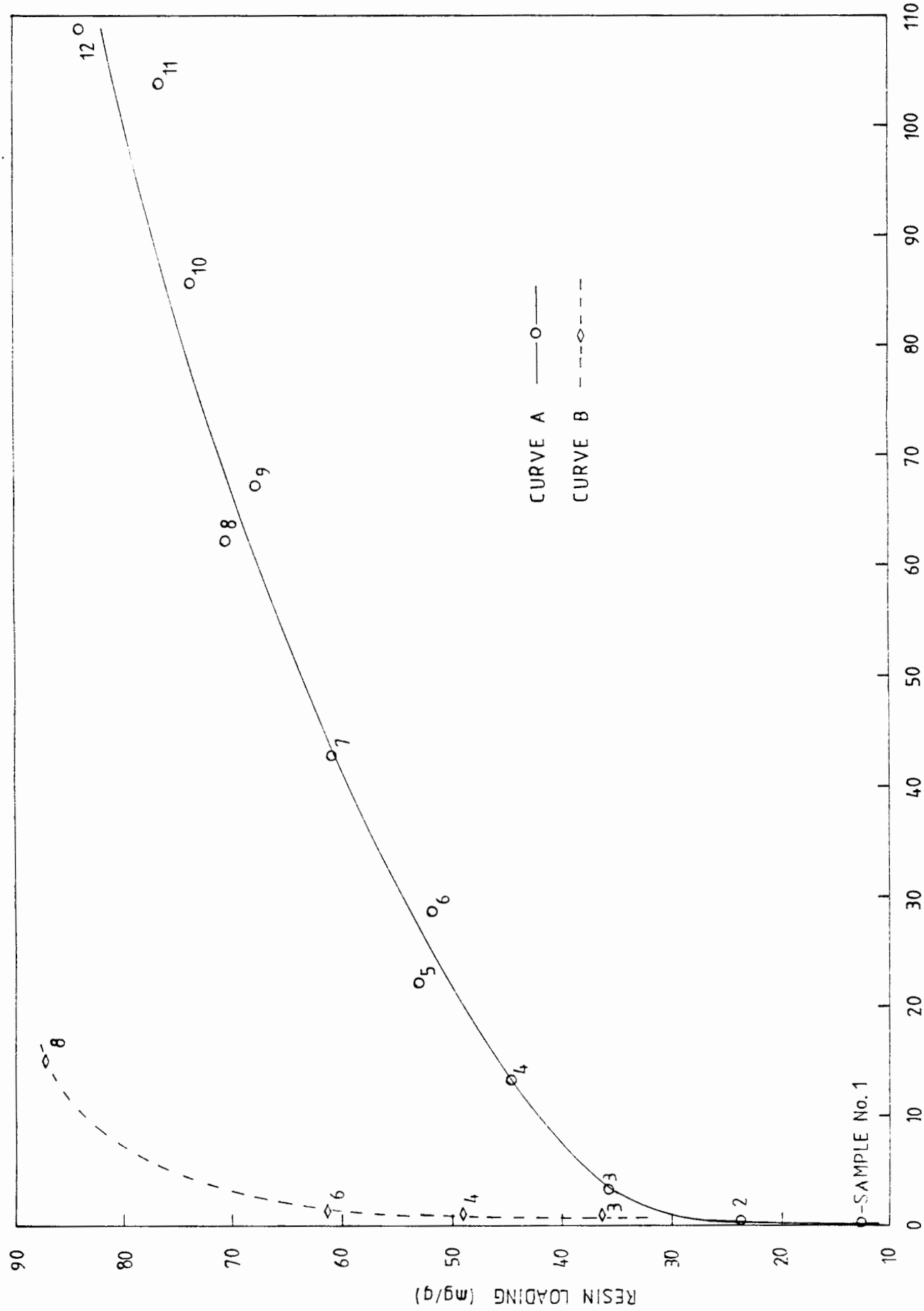

Figure 4.1 ADSORPTION ISOTHERMS FOR THE AMBERLITE IRA 938 RESIN - PRIMAL E1743 SYSTEM.

CHAPTER 4

RESULTS AND DISCUSSION

4.1 INTRODUCTION

The suitability of a solid sorbent for treating a liquid feed depends largely on two factors:

i) The useful capacity of the sorbent for the solute (capacity used under process conditions), which is usually less than the ultimate capacity.
ii) The adsorption/desorption rates, and the mechanisms and resistances controlling these rates.

Thus the main areas of investigation to be discussed are:

i) Equilibrium resin capacity.
ii) Kinetics and mechanisms of adsorption.
iii) Resin regeneration and adsorption reversibility.
iv) Systematic study of important parameters in order to elucidate the driving forces of particulate adsorption to resin.
   a) Colloidal particle size.
   b) Resin bead size.
   c) Superficial fluid velocity in the resin bed.
   d) Adsorbent and colloid surface charge.
v) Qualitative and Numerical models developed for the system.

4.2 RESIN CAPACITY

Adsorption isotherms measured for the Amberlite IRA 938 - Primal E1743 system studied are presented in Figure 4.1. Detailed results for one of the point determinations (bottle 11, the concentration of which was monitored over a longer period than the other point determinations), are in Table 4.1.

In these experiments colloidal particle concentration in the

coagulated and aggregated) but can be removed by adsorptive filtration.

In adsorptive filtration particles are transported to and held to the filter media surface by attractive forces. London - van der Waals and electrostatic forces are the major factors which determine whether or not particles adhere to the surfaces of a filter (5,9,10).

London - van der Waals forces are attractive irrespective of the nature of the surface or particle. Electrical double layer forces are attractive if the surfaces have opposite charges and repulsive if the surfaces have the same charge. The degree to which the surface forces influence filtration has been found to be related to the ionic strength and pH of the liquid (11).

For high efficiency, an adsorptive filter must also have a high internal surface area so that there is a very low probability that any particle will pass through the filter without contacting or being attracted to a surface to which it can adhere. In contrast, the design of surface and depth straining filters is dominated by the need for interstices which are smaller than the particles to be removed.

From the above it is clear that the efficiency of an adsorptive filter is dependent on two criteria:

i) The strength of the forces between the colloidal matter and filter media surface.

ii) The available filter surface area.

The available surface may include a significant amount of internal surface of a porous particle depending on the rate of diffusion of the colloids into these pores.

The use of a synthetic adsorbent, such as a highly porous ion-exchange resin, would be advantageous as it would permit variation and selection of the adsorbent surface charge, pore size distribution and surface area (Figure 1.1d). Thus the properties of the particular colloid or suspension to be treated could be accommodated.

There is at present only limited application of ion-exchange resins as adsorbents for the removal of particulate material from liquid streams. One reason may be that little is known or published about the migration of colloidal particles into the interior of highly porous solids. Most published work has dealt with impervious solid filter media such as sand, steel etc.

1.2 ADSORPTIVE FILTRATION USING ION-EXCHANGE RESINS

Removal of particulates from liquids by ion-exchange resins only became practical in the mid 1960`s with the development of highly macroporous ion exchange resins by Rohm & Haas (12). Ion-exchange resins available prior to this date were of the gel-type. Although gel-type ion-exchange resins are capable of adsorbing colloids on their surfaces, their effective surface area in the typical resin particle size range (0.3 to 1.2 mm) is quite small: less than 0,1 m^2/g, hence their capacity for adsorbing viruses, proteins, bacteria and other colloids present in water is limited (13).

In contrast, the highly macroreticular resins Amberlite IRA 938 and Amberlite IRA 904 have high surface areas and porosities as shown in Table 1.1 (13, 14) and electron micrograph 1.

Resin name and type	Surface area m^2/g(dry)	Pore size range A	Moisture content %
Amberlite IRA 400 gel	<0.1	None	45
Amberlite IRA 900 macroreticular	18.0	140 - 220	60
Amberlite IRA 904 macroreticular	46.9	210 - 1200	57
Amberlite IRA 938 highly porous	7.3	25000 - 250000	73

TABLE 1.1 Comparison of porosity and surface area data for highly porous and gel ion-exchange resins.

The resin surface areas in Table 1.1 were measured using nitrogen adsorption, thus only a small fraction of the surface area reported for Amberlite IRA 400, 900 and 904 resin is available

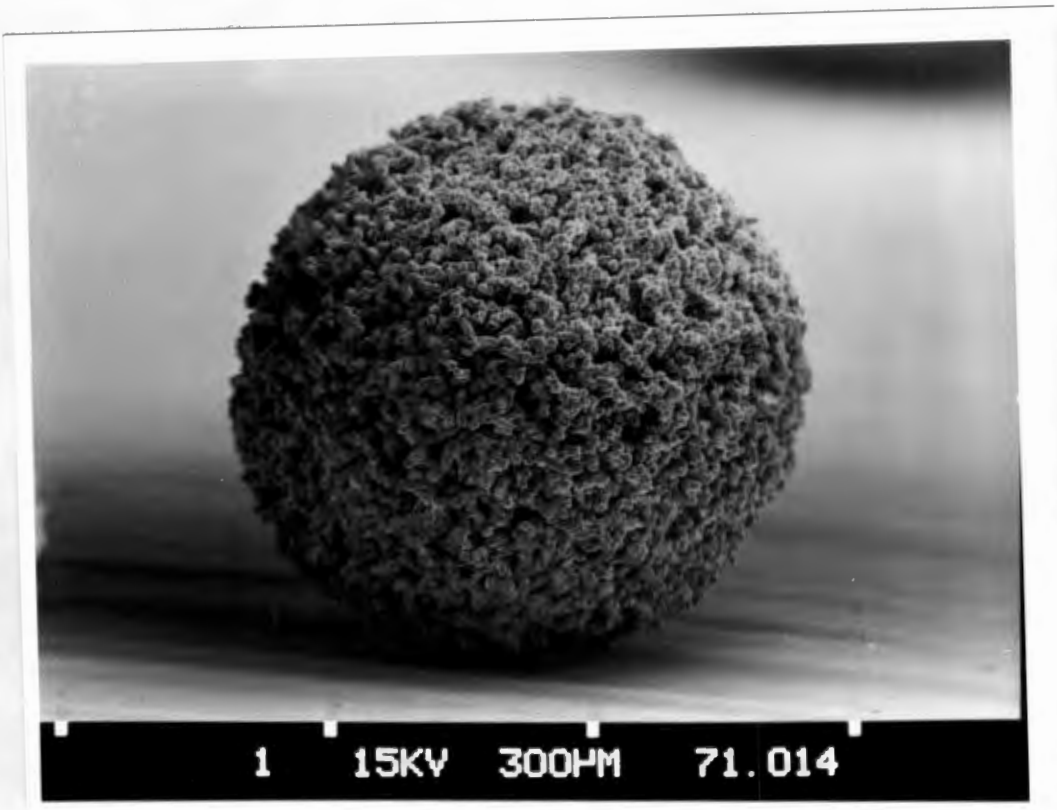

Photograph 1 A SCANNING ELECTRON MICROGRAPH OF AN AMBERLITE IRA RESIN BEAD SHOWING ITS HIGH POROSITY. (× 120)

to colloidal particles, as the colloids are occluded from the resin internal surface area by the resin's small pore size.

The effectiveness of highly macroporous ion-exchange resins in the removal of organic and inorganic colloids was shown in early laboratory trials reported by Tilsley (12).

River	Influent (ppm)		Effluent (ppm)		Removal %	
	SiO_2	Fe	SiO_2	Fe	SiO_2	Fe
Wabash Terre Haute, Indiana	0.0001	7.1	0.00008	0.085	20.0	98.0
James Big Island, Virginia	0.000049	1.7	0.000043	0.050	12.2	97.1
Savannah Augusta, Georgia	0.20	2.1	0.00012	0.045	99.9	97.9
Ohio Brookport, Illinois	0.43	1.8	0.095	0.015	78.0	99.2
Mississippi Helena, Arkansas	0.39	0.8	0.053	0.042	86.4	94.7
Tennessee Calvert City, Kentucky	0.031	2.7	0.000076	0.050	99.7	98.1

TABLE 2.2 Effectiveness of Amberlite IRA 938 for inorganic colloid removal. (Tilsley 1979)(12)

Subsequent research has shown that highly macro-porous resins can

be used effectively for removing non-reactive silica, high molecular weight humic matter, radioactive "crud", and for rendering water sterile and pyrogen free (13,15,16).

Other successful applications are reviewed in Appendix F.

1.3 OBJECTIVES AND MOTIVATIONS

The primary objective of the present study is to determine the fluid dynamic and electrostatic factors which affect colloidal particle diffusion across the ion-exchange resin-liquid boundary, with particular reference to the highly porous outer surface of Amberlite IRA 938 resin and similar materials, and thus appraise the adsorptive filtration process as an alternative pretreatment process for seawater desalination by reverse osmosis.

However, understanding of fluid dynamic and electrostatic factors which determine colloidal particle adsorption/deposition on charged surfaces can also be applied in other fields.

For example, fouling of membranes by adsorption/deposition of colloidal particles on the membrane surface can be described and thus possibly prevented. The significance of surface charge in membrane processes has already been acknowledged by certain membrane manufacturers who are producing charged membranes in an attempt to limit particulate fouling (17).

In the medical field a charged coating on the wall of an artifical organ might be used to repel similarly charged platelets in flowing blood, thus preventing their damage (18).

In filtration it would be advantageous to have filtration media which attract colloidal particles and thus increase filtration efficiency. Adsorptive filtration is thought to account for the removal of most of the micro-particles from liquids. A relatively new application of adsorptive filtration is the use of ion-exchange resins to recover or remove virus, bacteria and colloidal silica from aqueous solutions.

Information concerning the transport of colloidal particles within the porous resin bead, will shed light on process problems such as the use of anion exchangers for mining effluent desalination where current practice avoids high pH in the belief that metal hydroxide precipitation will cause resin fouling. The general problem of particulate fouling of resins and membranes will be further understood.

Finally it is significant that fundamental relationships for diffusivity of molecular species are accepted as analogous with the diffusivity of colloidal species. The behaviour of large organic molecules, which often have varying charge and polarity, is therefore likely to be similar to that of colloidal particles as regards electrostatic and chemical interactions. Thus insight into the adsorption and fouling of resin by large organic molecules can be obtained by the study of the adsorption of colloidal particles to resins. The use of well defined stable colloidal particles to study the interior characteristics of porous adsorbents eg. as "probes" may also be considered as a useful research tool arising from the study reported here.

CHAPTER 2

THEORETICAL BACKGROUND TO COLLOID DIFFUSION, INTER-PARTICLE ATTRACTION/REPLUSION AND ADSORPTIVE FILTRATION

2.1 INTRODUCTION

Colloids are intermediate in size between true solutions and suspended matter (6,7). Although there is no clear cut definition as to the size of colloidal particles, the term is generally applied to any particle larger than 10 angstroms and less than 1 micron (7,8).

In this study emphasis has been placed on small particles present in natural waters, which cause fouling of reverse osmosis membrane surfaces. Two independent reseachers have determined, relatively conclusively, that large particles do not contribute significantly to reverse osmosis fouling. Winfield (19) found that particles larger than 5 microns do not cause reverse osmosis fouling and speculates that these particles are swept away in the bulk liquid flow, due to shear forces. Sugahare et al.(20) examined the effect of smaller particles on reverse osmosis fouling and concluded that particles smaller than 0.45 microns, generally classed as colloidal particles, contribute more to fouling than particles larger than 0.45 microns.

Most colloidal particles are sufficiently small and stable to pass though reverse osmosis pretreatment systems (6), but are concentrated, destabilised and deposited on the reverse osmosis membrane surface.

Colloidal foulants are generally difficult to characterise as they vary widely in composition and size. In practice however most colloidal particles found in natural waters fall into one of the following three groups:(6,21,22)

i) Aluminium silicate clays - products of natural weathering.

ii) Colloidal silica - includes silicon dioxide, bisilicate

and polymerised silica.

iii) Amorphous organic debris, cell walls, cellular fragments and organisms such as bacteria and viruses.

In order to understand the behaviour of colloidal foulants and colloid removal by adsorptive filtration, a basic understanding of colloidal systems is required.

2.2 COLLOIDS AND THE STABILITY OF COLLOIDAL SYSTEMS

A brief summary of this and the following sections can be found at the end of the chapter (section 2.7).

It has long been observed that solid particles in a colloidal dispersion can move in an electric field, indicating that these particles carry an electric charge. Solid phases (eg. clays, silica, bacteria, etc.) take on a net electrostatic charge which may be either negative or positive; most colloids in natural waters develop a net negative surface charge.

Colloidal particles have large surface area to weight ratios; consequently their behaviour is governed by their surface properties the most important of which is surface charge.

Three distinct processes can produce a surface charge on a solid colloid particle (23).

i) Many colloids contain functional groups which are readily ionisable (eg. hydroxyl, carbonyl, amino). The charge on these particles is dependent upon the extent to which these surface groups dissociate; particle charge therefore depends upon the pH of the solution.

ii) Surface charge could be caused by lattice imperfections at the solid surface. For example, if in an array of solid silicon dioxide tetrahedra a silicon atom is replaced by an aluminium atom, a negatively charged framework as shown in Figure 2.1 is established.

iii) The surface charge on a colloidal particle may arise from the preferential adsorption of certain ions from solution. This specific adsorption of ions arises from hydrogen bonding and/or London - van der Waals forces.

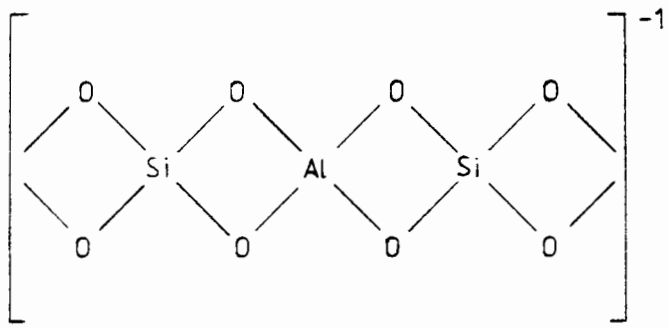

Figure 2.1 AN ALUMINIUM ATOM SUBSITUTED INTO A SILICON TETRAOXIDE LATTICE, SHOWING THE RESULTING NET NEGATIVE CHARGE.

The surface charge of a colloidal particle influences the distribution of nearby ions in the liquid, ions of opposite charge (counter-ions) are attracted towards the surface and ions of like charge (co-ions) are repelled from the surface.

Two models have been developed to explain the distribution of ions around a charged colloid. The older of the two models developed by Gouy and Chapman (8), proposes that the electrical double layer surrounding a colloid consists of the charged colloid surface and a diffuse region of ions around the surface. The counter-ions near the charged surface screen those further away from the full electrostatic field, causing their concentration to fall off rapidly with increasing distance from the solid/solution interface. This concentration profile causes back diffusion of the ions to the bulk solution so that a steady state dynamic equilibrium distribution of ions and charge develops.

The Stern model (6,8) proposes that the electrical double layer consists of a compact (Stern) layer and a diffuse layer of ions. The compact Stern layer is composed of counter-ions which are strongly held to the surface by electrostatic or van der Waals forces. The diffuse layer is composed of both co- and counter-ions in a concentration profile as in the Gouy-Chapman model.

When two similarly charged colloidal particles approach each other, their diffuse ion atmospheres begin to interact and both the replusive forces due to their surface charges and the attractive forces due to London - van der Waals forces are effective.

Similar interactions can be expected between a colloid particle and surface such as a flat plate collector or the surface of an adsorptive filter which may be charged for similar reasons as the colloid.

London - van der Waals forces are attractive forces between matter, and are inversely proportional to the sixth power of the separation distance. Coulombic/double layer forces arise from surface charge and consequently can be either repulsive or attractive. Coulombic forces, although strongly affected by electrolyte strength, are typically inversely proportional to the square of the separation distance and thus, at low ionic strengths, act over greater distances than the London - van der Waal forces. Figure 2.2 shows the variation of London - van der Waals and double layer forces with separation distance.

It is customary to describe the interaction between colloidal particles in terms of interaction potential energies. Repulsive forces give rise to positive potential energies while attractive forces result in negative potential energies. The summation of the two interaction potential energies, London - van der Waals and coulombic potential energies, is represented using a graph describing the variation of the net interaction potential energy as a function of the separating distance between the colloids. Figures 2.3a and 2.3b show typical interaction potential energy curves for two similarly charged and oppositely charged colloidal particles.

From Figure 2.3a it is apparent that for similarly charged particles only particles having sufficient kinetic energy can penetrate the energy barrier and unite to form a secondary particle. Thus a stable colloidal suspension can be destabilised by increasing the kinetic energy of its particles; this energy usually results in increased Brownian motion causing perikinetic

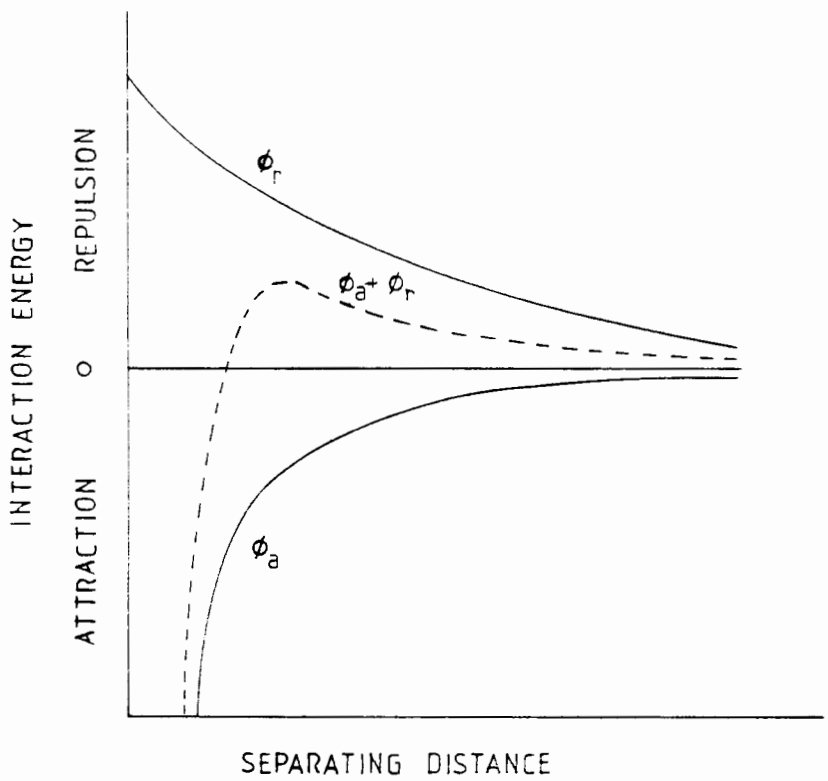

Figure 2.2 THE VARIATION OF LONDON - VAN DER WAALS AND COULOMBIC FORCES AS A FUNCTION OF THE SEPARATING DISTANCE BETWEEN TWO SIMILARLY CHARGED PARTICLES.

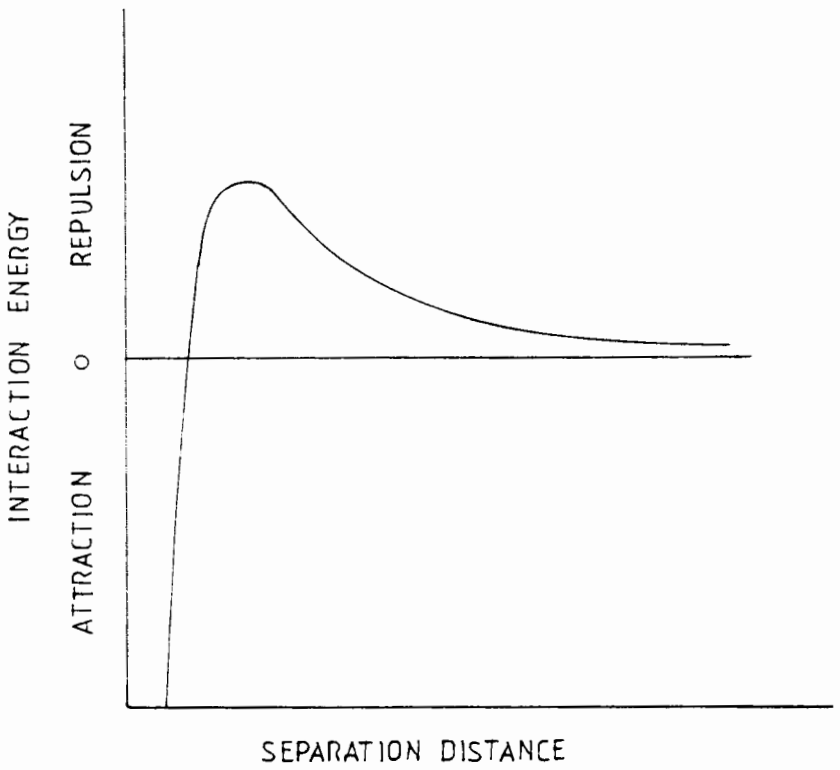

Figure 2.3a INTERACTION POTENTIAL ENERGY CURVE FOR SIMILARLY CHARGED PARTICLES.

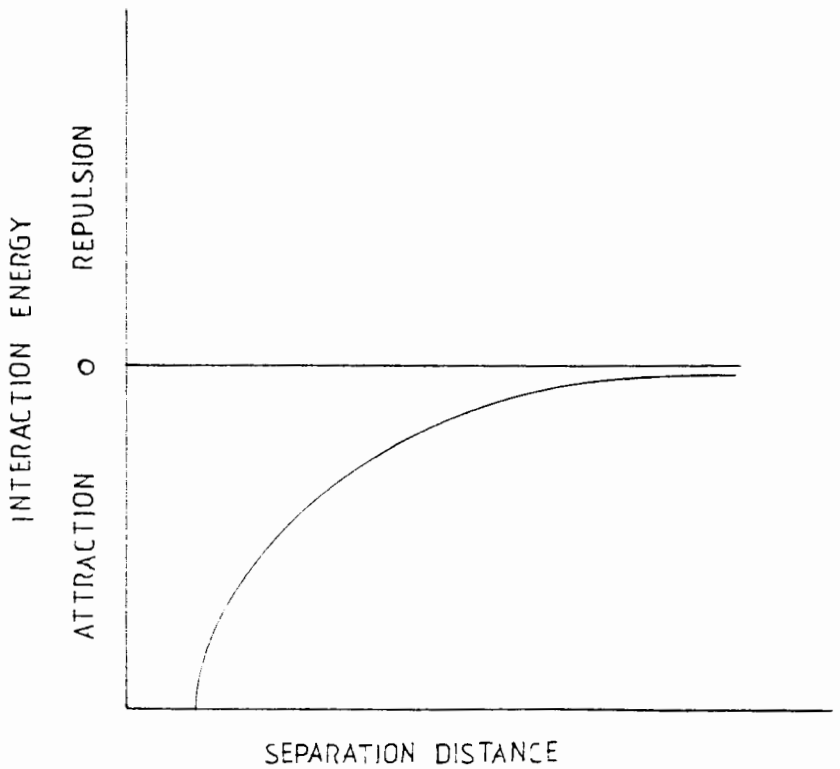

Figure 2.3b INTERACTION POTENTIAL ENERGY CURVE FOR OPPOSITELY CHARGED PARTICLES.

flocculation and/or increased motion and shear forces in the liquid causing orthokinetic flocculation. Colloids can also be destabilised by the addition of or an increase in, electrolyte strength. Increasing the concentration of electrolyte compresses the thickness of the diffuse boundary layer, surrounding the particle, decreases the distance over which the repulsive forces are effective and therefore substantially reduces the potential energy barrier as shown in Figure 2.4.

2.3 THE MECHANISMS OF ADSORPTIVE FILTRATION IN PACKED BEDS

Deep bed filtration is an engineering practice of long standing and is used primarly for the removal of suspended particles from fluid streams. The removal is accomplished by passing the suspension through beds consisting of granular or fibrous materials.

A fundamental analysis of filtration involves the study of particle adsorption/deposition on a collecting surface.

In packed beds particulate suspensions flow past the surface of the packing (filtration media), particles in the suspension are therefore transported toward (or away from) the collecting surface. Adsorption/depostion of these particles on the packing depends on two main events (24):

i) transport to the collector surface, and
ii) attachment to the collector surface.

As the attachment step, in most cases, is relatively fast assuming the surface charges are favourable, the rate limiting step is the transport to the collector surface (25).

The transport of particles from the bulk suspension to or from the collector surface is the result of the combined action of numerous forces acting on the particles. The most important are:

i) Fluid motion (convection) - responsible for interception: a suspended particle following a streamline of flow may come into contact with the collector by virtue of its own size.
ii) Inertia (sedimentation, velocity) - causes impaction: if

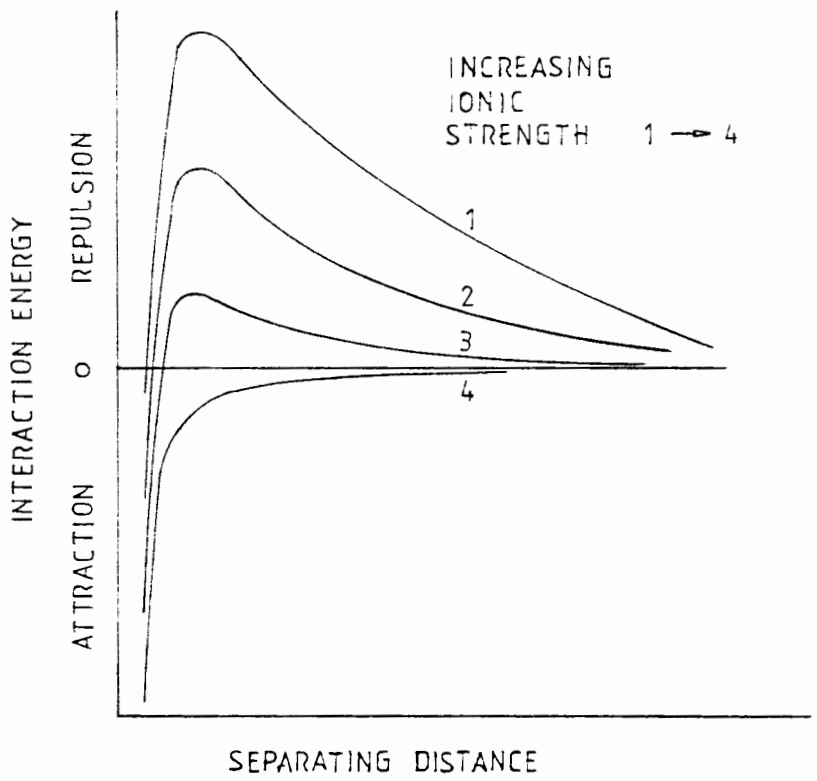

Figure 2.4 THE EFFECT OF IONIC STRENGTH ON INTERACTION POTENTIAL ENERGY CURVES RESULTING FROM TWO SIMILARLY CHARGED PARTICLES.

the density of a suspended particle is greater than that of the suspending liquid the particle will follow a trajectory influenced by gravity and its own momemtum.

iii) Brownian motion - causes Brownian diffusion: particles in a suspension are subject to random bombardment by molecules of the suspending medium resulting in Brownian movement of the particles.

iv) Surface interactions - London - van der Waals and electrostatic forces, may attract particles to or repel particles from a collector surface.

The transport mechanisms of fluid motion, inertia and Brownian motion are illustrated in Figure 2.5.

The relative importance of these forces depends on a number of factors, the most important being particle size. As particle size decreases the significance of gravity and gravity induced forces and interception decreases, while the strength of surface related forces and Brownian motion increases, as illustrated in Figure 2.6. This occurs because the surface to mass ratio of the particle increases dramatically as the particle size decreases (eg. surface to mass ratio increases by a factor of a million for a decrease in size from 100 to 0.1 microns).

The effect of hydrodynamic retardation, which like surface forces and Brownian motion becomes more significant as particle size and mass decrease, is to slow the particle as the resin surface is approached. The reduction in particle velocity results from increased drag forces which are caused by additional friction between the fluid, particle and collector surface.

Typically particles larger than about 1 micron are transported to the collector surface by settling and interception while smaller particles are transported by Brownian diffusion (26). The particle size at which Brownian diffusion becomes the major transport mechanism is largely determined by the density of the particle. It has been found that Brownian diffusion becomes adsorption rate controlling below a particle size of about 0.7 microns for particles of specific gravity 2.6. For particles of specific gravity 1.0 Brownian diffusion is adsorption rate

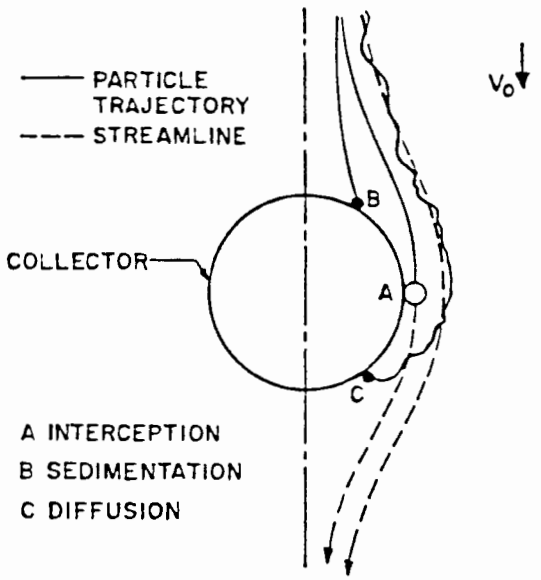

Figure 2.5 PARTICLE TRANSPORT MECHANISMS TO A SPHERICAL COLLECTOR. (Yao et al.)(26)

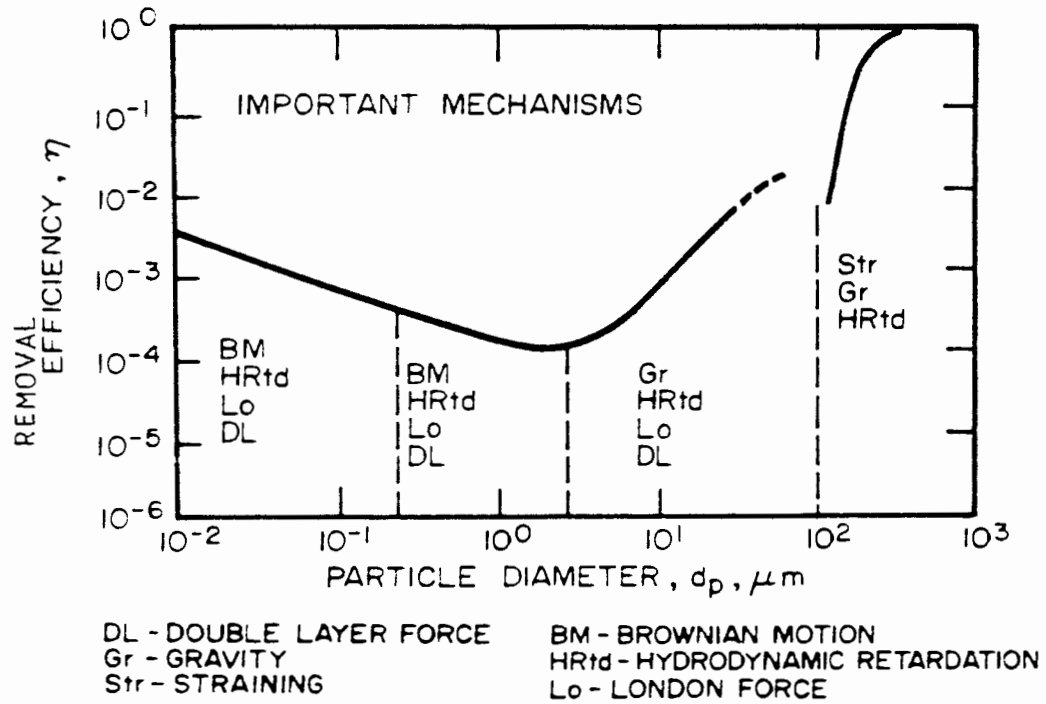

Figure 2.6 THE VARIATION OF PARTICLE ADSORPTION MECHANISMS WITH PARTICLE SIZE. (Rajagopalan and Tien)(9)

controlling below a particle size of about 3 microns (26). (A discussion of the above effects follows in section 4.4.1.)

The rate of adsorption/depositon for colloidal particles is determined largely by diffusion (Brownian motion) and surface forces (24,27).

The mass transfer rate (flux) of colloidal particles to a collector surface in a packed bed is expected to be dependent on diffusion processes, as London - van der Waals and double layer forces usually act over very short distances (+- 100 nm).

2.4 CLASSICAL DIFFUSION FILM THEORY

Diffusion controlled adsorption to the surface of a collector, is according to Nernst theory (28) dependent on three parameters:

i) The thickness of the hydrodynamic boundary layer adjacent to the collecting surface,
ii) The concentration gradient across the boundary layer,
iii) The diffusion coefficient of the colloidal particles.

The concept of a thin layer of static liquid immediately adjacent to the surface of a solid body through which diffusion of a reacting/adsorbing species takes place (see Figure 2.7 on page 28), was first proposed by Nernst. This theory however, involves a gross simplification of the real situation, as convection of a solution by turbulent or laminar flow recedes continuously from the bulk solution to the solid surface. Despite this drastic simplification the Nernst model describes diffusion phenomena at solid interfaces fairly accurately. This has been shown by both experimental evidence and more detailed theoretical approaches (30,31).

The "film thickness" is a fictitious quantity and therefore cannot be measured directly. Levich (32) points out that the diffusion layer has been found to be a function of the diffusion coefficient of the particles and the degree of agitation in the bulk fluid. This indicates that, under given experimental cond-

itions, there is a diffusion layer thickness corresponding to each particle or ion diffusing in the solution (ie. a diffusion film thickness is not necessarly equal to the hydrodynamic boundary layer thickness). This emphasizes the empirical nature of the Nernst theory.

Acknowledging the non-theoretical nature of the Nernst theory for the convective diffusion situation, it was nevertheless decided to use this approach for its ease of understanding and success in describing diffusion phenomena at solid surfaces.

For the simple case of diffusion controlled adsorption to a flat plate (the radius of the collector is usually orders of magnitude larger than the size of the colloidal particle and therefore the adsorbing surface can be approximated by a flat plate) the adsorption rate may be described by the following expression (28):

$$- r_a = \frac{D\,(C_a - C_c)\,S}{\delta}$$

where D is the diffusion coefficient of the particles,
S is the area of the plate,
δ is the boundary layer thickness,
C_a is the colloid concentration in the bulk, and
C_c is the colloid concentration at the collector surface.

The collector surface in most adsorption processes can be approximated by a perfect sink, as the attachment step in most cases is extremely rapid, thus the concentration of the colloid in the liquid adjacent to the surface can be considered to be zero at all times. The concentration gradient therefore, with its one point fixed at zero concentration, is a function of the thickness of the boundary layer. The rate of adsorption is therefore largely dependent on the boundary layer thickness.

Levich proposed that the hydrodynamic boundary layer thickness in a packed bed could be approximated by the following expression (33):

$$\delta_D \cong a\,(D/Ua)^{\frac{1}{3}} \qquad \text{---- 1}$$

where U is the superficial fluid velocity in the bed, and
a is the radius of collector particles in the bed.

Thus the adsorption rate should be proportional to $U^{\frac{1}{3}}$, keeping other parameters constant.

2.5 CORRELATIONS FOR DIFFUSION CONTROLLED ADSORPTIVE FILTRATION

The rate of particle adsorption/deposition in a packed bed, can be evaluated using first order kinetics as follows (27,34):

$$-r_a = -\frac{\partial C}{\partial t} = \frac{S}{V} kC_a \qquad \text{----- 2}$$

where k is the mass transfer rate constant,
C_a is the particle concentration in the liquid,
S the surface area of the collector, and
V the volume of liquid dispersion.

Ruckenstein and Prieve (35) using the Levich proposal that the adsorption rate should be proportional to $U^{\frac{1}{3}}$, developed the following correlation for the mass transfer rate constant:

$$k = 0{,}624\, D^{\frac{2}{3}} a^{-\frac{2}{3}} U^{\frac{1}{3}} \qquad \text{---- 3}$$

where U is the velocity of liquid flow relative to the collector,
a is the radius of the collector beads, and
D is the diffusion coefficient and is given by:

$$D = k_B T/6\pi n a_h \qquad \text{---- 4}$$

where k_B is the Boltzman constant,
T the absolute temperature,
n the viscosity of the liquid, and

a_h the radius of the particles in the suspension.

Equation 3 gives the rate constant, k, for single collector beads and makes no correction for close packing in a bed. Ruckenstein, Pfeffer and Happel (36,37) included a porosity term into this equation which takes into consideration a collection of beads rather than a single sphere.

$$k = 0{,}624\ D^{\frac{2}{3}} a^{-\frac{2}{3}} (\beta U)^{\frac{1}{3}} \qquad \text{----} \quad 5$$

where U is the superficial flow velocity, and
β is given by the following relation:

$$\beta = 2(1 - \gamma^5)/(2 - 3\gamma + 3\gamma^5 - 2\gamma^6) \qquad \text{----} \quad 5a$$

and γ is given by,

$$\gamma = 1 - \varepsilon \qquad \text{----} \quad 5b$$

where ε is the void fraction in the packed bed.

The mass transfer correlation for dissolved species proposed by Williamson, Bazaire and Geankoplis (38) is of a similar form to equations 3 and 5.

$$k = 2{,}40\ Re^{-0{,}66} Sc^{-0{,}58} \qquad \text{----} \quad 6$$

where the Reynolds number given by:

$$Re = \frac{\rho a U}{\varepsilon \eta} \qquad \text{----} \quad 6a$$

where ρ is the density of the liquid,
ε the bed void fraction,
D_ℓ the liquid diffusivity *

and Sc is the Schmidt number given by:

$$Sc = \frac{\eta}{\rho D_\ell} \qquad \text{----} \quad 6b$$

* The liquid diffusivity must be replaced by the diffusion

coefficient of the particles being used (equation 3 can be used to calculate this coefficient).

2.5.1 Limitations of the proposed correlations

The correlations discussed above assume that the surface forces acting between the particles and collector are negligible. This limits their usefulness. Experimental evidence has clearly shown that the rate of adsorption/deposition of sufficiently small particles, although governed by diffusion can be enhanced or retarded by London - van der Waals and coulombic forces (27,39). This is illustrated in Table 2.1 which compares experimental and predicted mass transfer rate constants obtained by this author for various colloidal particles to postively charged Amberlite IRA 938 resin.

Colloid Type	Size (microns)	Zeta Potential (pH 7 +- 1.5)	Adsorption Rate $\times 10^{-7}$ (m/s) measured	predicted**
Primal E1743	0.5	-35 to -39 mv	17.6	7.23
Titanium dioxide	0.4	+15 to -23 mv	0	8.39
Silicon dioxide	0.5	-33 to -40 mv	16.3	7.23

TABLE 2.1 A comparison of predicted and measured adsorption rates for various colloidal particles to postively charged Amberlite IRA 938 resin.

** predicted adsorption rates were calculated using equation 5.

2.6 CORRELATIONS FOR ADSORPTIVE FILTRATION WHICH INCORPORATE INTERACTION FORCES

The rate of diffusion of colloidal particles may be greater or lessor under the influence of interaction forces existing near the surface of the collector, than under the influence only of diffusion due to concentration gradients further away from the surface, where interaction forces have diminished to negligible values.

The dependence of adsorption rate on London - van der Waals and double layer potentials has been investigated by Prieve and Ruckenstein (40,41). When the diffusion boundary layer is thick compared with the interaction force boundary layer (which is usually the case), the mass transfer rate constant, k, is given by:

$$k = (1/k_i + 1/k_d) \qquad \text{----} \quad 7$$

where k equals k_d in the absence of interaction forces, and is k_i related to the total interaction potential through the following expression:

$$k_i = D(\omega/2\pi k_B T)^{\frac{1}{2}} e^{(-V_{max}/k_B T)} \qquad \text{----} \quad 8$$

where V_{max} is the maximum interaction potential (see Figure 2.3a) and is given by:

$$\omega = -\frac{\partial^2 V}{\partial x^2} \qquad \text{----} \quad 8a$$

where x is the distance of separation between the collecting surface and particle.

2.6.1 Evaluation of the total interaction potentials

The total interaction potential, Φ, between a particle and collector, as a function of distance, x, in an ionic medium is due to London - van der Waals potential, $\Phi_A(x)$, and electrical double layer potential, $\Phi_R(x)$, (39)

$$\Phi(x) = \Phi_A(x) + \Phi_R(x) \qquad \text{----} \quad 9$$

The London - van der Waals potential can be calculated using Hamaker constants. The Hamaker constant of a substance is a function of the number of atoms per unit volume and the polarisability of that material. The London - van der Waals potential is calculated as follows:

$$\Phi_A(x) = \frac{A_{132}}{6}\left[\ln\frac{(x+2a_h)}{x} - \frac{2a_h(x+a_h)}{x(x+2a_h)}\right] \qquad \text{----} \quad 10$$

where a_h is the particle radius,

A_{132} is the overall Hamaker constant which is approximated as follows:

$$A_{132} = (\sqrt{A_{11}} - \sqrt{A_{33}})\,(\sqrt{A_{22}} - \sqrt{A_{33}}) \qquad \text{----} \quad 11$$

where A_{11}, A_{22}, A_{33} are individual Hamaker constants for the collector, particle and medium.

Equation 10 assumes that the particles are adsorbed/deposited on a flat plate; this approximation, as explained previously is acceptable as the diameter of the collector, such as a resin bead, is usually orders of magnitude larger than the diameter of the colloidal particle.

The electrical double layer potential, $\Phi_R(x)$, can be calculated using the linearised solution of the Poisson - Boltzmann equation (42):

$$\Phi(x) = \pm\frac{\xi a_h}{4}\left[(\Psi_1+\Psi_2)^2\ln(1 \pm e^{-\kappa x}) + (\Psi_1-\Psi_2)^2\ln(1 \mp e^{-\kappa x})\right] \qquad \text{----} \quad 12$$

where ξ is the dielectric constant of the medium, and

Ψ_1, Ψ_2 are the surface potentials of the collector and particle.

κ, the Debye-Huckel reciprocal length, describes the maximum separation at which a given electron will be influenced by the electric field of a given positive ion, and is given by (41):

$$\kappa = \sqrt{\frac{4\pi}{\xi k_B T} \sum_i n_i e_i^2} \qquad \text{---- 13}$$

where n_i is the number of ions of species i per unit volume,
e_i is the charge of species i
k_B is the Boltzmann constant, and
T the absolute temperature.

The electrical double layer potentials can be evaluated at two different sets of boundary conditions, called modes. These are the conditions of constant charge density and constant surface potential. The upper signs in equation 11 are for the condition of constant surface potential and the lower signs for the condition of constant charge density.

The physical significance of the modes is explained by Overbeek (43). The surface potential of a colloidal particle is determined by the activity of the potential determining ions adsorbed to its surface. If during an interaction the adsorption equilibrium of the ions is maintained the interaction is said to occur at constant surface charge. If the equilibrium is disturbed the interaction may occur at constant charge density or at some situation intermediate between the two modes.

Using the above equations the total interaction potential as a function of the separation distance between particles or collector and particle can be calculated. These values are then plotted to give surface interaction energy profiles (Figure 2.2), which can be used to explain the rate of adsorption/deposition of particles.

An energy barrier, as shown in Figure 2.3a, will retard or prevent adsorption of particles to a collector. The potential energy profile shown in Figure 2.3b will enhance adsorption of colloidal particles to a collector, and consequently the adsorption rate will be faster than for a pure diffusion controlled system.

The maximum interaction potential, V_{max}, from the plot together with the equations proposed by Ruckenstein and Prieve(equations 7

and 8) allows the prediction of the rate of adsorption/deposition of particulates.

2.6.2 Interpretation of the total interaction potential energy profiles by Kim and Rajagopalan

Kim and Rajagopalan (11) studied the relationship between the shape of interaction potential energy curves and the corresponding adsorption rates and derived a correlating equation which can be used for predicting adsorption rates of particles to various substrates.

They proposed that the surface interaction potentials can be characterised by two or three terms and that individual physicochemical properties or the double layer interaction mode need not be directly represented in the correlation for adsorption rate. This approach can be explained with the help of net interaction energy profiles shown in Figure 2.8. These potential profiles represent the sum of coulombic and London - van der Waals interaction energies between two surfaces.

Curve 1 has a large potential energy barrier (V_{max}) and a negligible secondary minimum. In this case the rate of adsorption/deposition is determined by the height of the potential barrier (V_{max}), the magnitude of the London-van der Waals force ($N\ell_o$) and the amount of convection (Pe, Peclet number), if a significant velocity component perpendicular to the surface exists.

Curve 2 in addition to having a large potential energy barrier (V_{max}), has a large secondary minimum. Thus particles accumulate close to the secondary minimum (V_{smin}) which increases convective transfer of particles parallel to the substrate if the velocity component in that direction is significant. The rate of adsorption/deposition of particles in this case is a function of four parameters, namely V_{max}, V_{smin}, $N\ell_o$ and Pe. An increase in convection (Pe) in this case generally leads to a decrease in the adsorption/deposition rate.

Curve 3 displays a negligible potential energy barrier (V_{max}) and

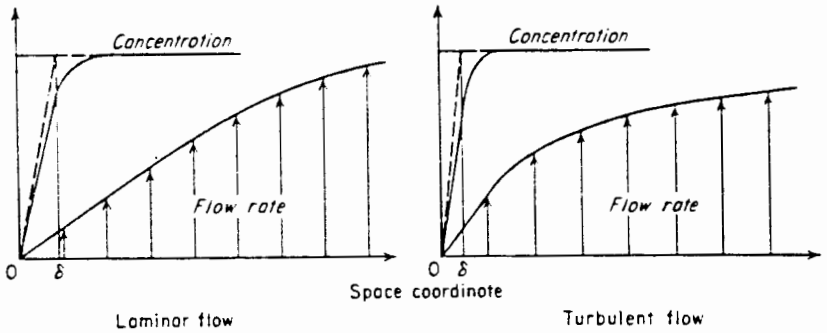

Figure 2.7 NERNST DIFFUSION LAYER. (Helfferich)(29)

The diagrams show the actual and idealised concentration profiles (solid and broken lines respectively) of a species which reacts instantaneously at a solid surface. The idealised profile is the tangent of the actual profile at the surface. In addition the actual flow rates of the solutions are shown.

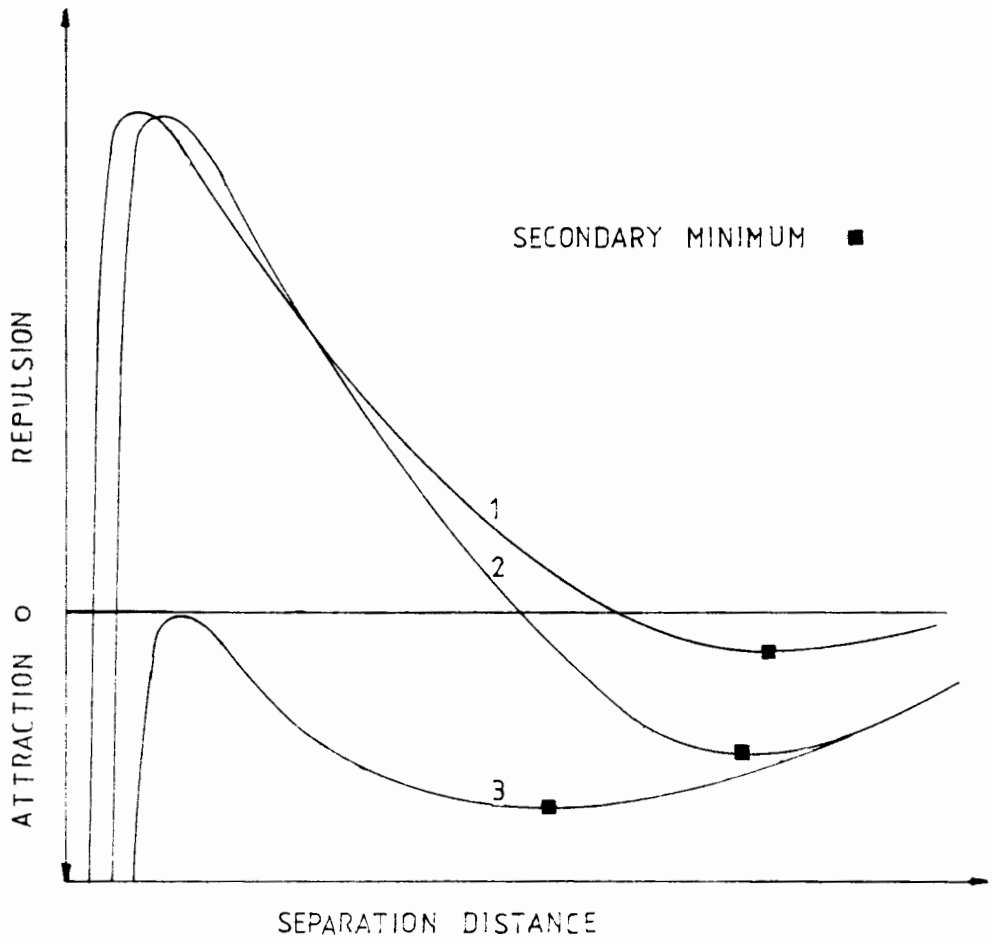

Figure 2.8 CLASSIFICATION OF SURFACE INTERACTION ENERGY PROFILES. (Kim and Rajagopalan)(11)

a large secondary minimum (V_{smin}). This causes competition between normal and tangential mass transfer. The adsorption/deposition rate therefore first increases and then decreases as convection increases (Pe).

Kim and Rajagopalan based their correlation for prediction of adsorption/deposition rates in packed beds on Curve 1. The correlating equation is presented below:

$$Sh^{cd}/Sh^{t} = f(N\ell_o, Pe, Q^{-1}) + 0{,}5Sh^{cd}Q^{-1}Be^{0{,}96}V_{max} \qquad ---- \quad 14$$

where Sh is the Sherwood number; superscript cd denotes value based on convective - diffusion alone, superscript t denotes actual numerical calculation.

$$Sh^{cd} = 0.997\beta^{\frac{1}{3}}Pe^{\frac{1}{3}} \qquad ---- \quad 15$$

This equation is similar to both the previously presented diffusion equations proposed by Ruckenstein et al. (36,37) and Williamson, Bazaire and Geankoplis (38).

Q is the aspect ratio and is the ratio of the particle and collector radii.

$$Q = a/a_h \qquad a \geq a_h \qquad ---- \quad 16$$

The Peclet number is given by:

$$Pe = U(2a)/D \qquad ---- \quad 17$$

where U is the approach velocity of the fluid,
D the diffusion coefficient for particles in the bulk

B is defined as:

$$B = N\ell_o^{-0{,}22} + 0{,}05N\ell_o^{2{,}7} \qquad ----- \quad 18$$

and the London group is given by:

$$N\ell_o = A/6k_BT \qquad ----- \quad 19$$

where A is the overall Hamaker constant given by equation 11
k_B is the Boltzman constant and
T is the absolute temperature.

Finally the function ($N\ell o$, Pe, Q^{-1}) which represents an adsorption /deposition rate in the absence of double layer forces can be approximated using Figure 6 in reference number 45.

The Kim and Rajagopalan approach using equation 14 can be used for predicting adsorption rates for colloidal particles in packed beds under a wide range of double layer interactions, the only limit being the depth of the secondary minimum in the interaction energy profile which must be $\leq 0{,}5k_BT$ (11).

2.6.3 The advantages and limitations of the presented expressions

2.6.3.1 Advantages

The prime advantage of all the correlations and expressions presented is that they are closed-form expressions for the adsorption rate constant and consequently computation of the adsorption rate can be accomplised without recourse to numerical methods and/or simplifying assumptions of ordinary or partial differential equations.

The correlating equation presented by Kim and Rajagopalan has the further advantage that it can be used to determine an effective activation energy for adsorption from experimental measurements of adsorption rates. The actual activation energy depends on the mode of the double layer interaction which is difficult to specify (11).

2.6.3.2 Limitations

For the purpose of this study the shortfall of the presented equations is that none adequately covers the situation of enhanced adsorption rates when the collecting surface and colloidal

particles have opposite charge (Figure 3.3b). Equations which account for interaction forces, (equation 8 by Ruckenstein and Prieve and Equation 14 by Kim and Rajagopalan) revert to forms of the diffusion controlled adsorption equations, as the term V_{max} becomes meaningless.

Further all the equations presented thus far assume that the transport of the colloid to the collector surface is the rate limiting step, as attachment to the collector surface is assumed to be almost instantaneous. Spielman and Friedlander (33) point out that if the transport to the surface is very rapid physisorption may be slow in comparison and thus can be rate limiting. In section 4.4.4 this case is discussed further.

2.7 SUMMARY OF THEORY

2.7.1 Colloids and colloidal systems

Colloids, generally defined as particles larger than 10 angstroms and smaller than 1 micron (see section 2.1), take on a net electrostatic charge (usually negative in natural waters). This surface charge influences the distribution of nearby ions in the liquid and thus an electrical double layer develops around the particle.

When two colloids approach, their diffuse ion atmospheres interact and similarly charged colloids are repelled while oppositely charged colloids attract.

It is customary to describe the interaction between colloids in terms of interaction potential energies. Interaction potential energies arise from London - van der Waals forces (attractive forces) and coulombic forces (either attractive or repulsive in nature).

A stable colloidal suspension can be destabilised or flocculated by increasing the kinetic energy of its particles and thus increasing the number of particles with enough energy to overcome the potential energy barrier between the particles. Also the

electrolyte strength of the suspending liquid can be increased thus shrinking the thickness of the electrical double layer around the particles and reducing the repulsive forces between the particles. This applies equally to flocculation/aggregation and to collection.

2.7.2 Mechanisms of adsorptive filtration in packed beds

Adsorption of particles to a collector surface consists of two main events: transport to the collector surface and attachment to the surface (24).

Transport to the surface is generally regarded as the rate limiting step (25). It results from the combined action of various forces, the most important being; fluid motion (convection), inertia (sedimentation, velocity), Brownian motion and the surface interactions described above.

The relative importance of these forces depends largely on the size and density of the particle: typically particles larger than about 1 micron are transported to the surface by settling and interception while smaller particles are transported by Brownian diffusion and surface forces (26).

Adsorption of colloidal particles to a collecting surface is usually governed by diffusion processes (24,27). The rate of adsorption, according to classical diffusion theory, is therefore largely dependent on the thickness of the hydrodynamic boundary layer adjacent to the collecting surface (45).

Levich proposed that the thickness of the boundary layer in a packed bed is proportional to the superficial fluid velocity in the bed (32).

2.7.3 Correlations and limitations for diffusion controlled adsorptive filtration

The rate of particle adsorption/deposition in a packed bed, has

been found to follow first order kinetics (27,34).

Ruckenstein and Prieve (35) and others (36,37,38), developed correlations for the mass transfer rate constant, to be used in conjunction with the first order kinetic model of the system. These correlations are based on the the Levich proposal that the hydrodynamic boundary layer and therefore the adsorption rate is related to the superficial fluid velocity in the bed.

These correlations however are limited by the assumption that the surface forces acting between the particles and collecting substrate are negligible.

2.7.4 Correlations for adsorptive filtration which incorporate interaction forces

Experimental evidence has clearly shown that the rate of adsorption of sufficiently small particles, although governed by diffusion can be enhanced by London - van der Waals and enhanced or retarded by coulombic forces (27,39).

Prieve and Ruckenstein (40,41) suggest calculating the interaction potential energies between the particles and collector and incorporating these in an interaction potential energy/activation energy term. This term and the adsorption rate constant predicted using diffusion controlled adsorption correlations are then summed as parallel resistances. Thus when the interaction forces are negligible the overall adsorption rate constant reverts to the diffusion controlled adsorption correlation.

Kim and Rajagopalan (11) interpreted interaction potential energy curves and related each curve to a corresponding adsorption rate. This led to the derivation of a correlating equation which can be used to predict adsorption rates of colloidal particles on various substrates. Typically the adsorption rate was found to be dependent on four parameters, the maximum potential energy of interaction (V_{max}), the magnitude of the London - van der Waals force ($N\ell_o$), the amount of convection (Pe, Peclet number) and the secondary minimum (V_{smin}) on the interaction potential energy

profile.

2.7.5 Limitations of the presented expressions

None of the above mentioned correlations or equations adequately covers the situation of enhanced adsorption rates for oppositely charged particles and collecting surface.

All the equations presented assume that transport of the particles to the surface is the rate determining step. Spielman and Friedlander (33) point out that physisorption is often a relatively slow process and thus if the transport to the surface is rapid the attachment step can be rate limiting.

CHAPTER 3

EXPERIMENTAL METHODS AND APPARATUS

3.1 EXPERIMENTAL PROGRAMME

The overall aim of the experimental study was to investigate and isolate the factors which influence the adsorption of colloidal particles onto and into highly porous ion-exchange resins. This entailed an investigation into fluid dynamic and electrostatic factors expected to affect colloid transport to the resin and consequently led to the following experimental programme:

i) Determination of equilibrium adsorption isotherms.
ii) Study of resin regeneration and adsorption reversibility.
iii) Study of the influence of the following parameters on the kinetics of colloidal particle adsorption to highly porous ion-exchange resins such as Amberlite IRA 938:

a) Colloidal particle size.
b) Resin bead size.
c) Superficial fluid velocity in the resin bed.
d) Charge on the resin.
e) Charge on the colloidal particle.
f) pH of the bulk solution/suspension.
g) Ionic strength of the bulk solution/suspension.

3.2 EXPERIMENTAL MATERIALS

In order to study the mechanisms and rate controlling parameters affecting the uptake and release of colloidal materials by highly porous adsorbents, it was necessary to use a well defined and characterised colloidal material.

3.2.1 Model colloid Primal E1743

Experimental Opaque Polymer Primal E1743 is such a material. It is manufactured by Rohm and Haas and was designed as substitute light scattering material for titanium dioxide in paint.

As supplied Experimental Opaque Polymer Primal E1743 is a 40% solids aqueous emulsion polymer with a particle size between 0.5 and 0.6 microns. These particles consist of a hard thermoplastic (acrylic) outer shell and a core of approximately 0.3 microns diameter which contains water (46).

Detailed specifications are as follows:

Appearance	milky white suspension.
Solids Content	40% (by mass)
	50% (by volume)
Particle size	0.5 - 0.6 microns
Density	1.032 g/cm^3 (wet)
Zeta potential (pH 7)	-38mv (measured value)

From the above it is clear that Primal E1743 is a well characterised aqueous emulsion polymer and consequently is an useful model colloid for the work reported here.

For all the kinetic experiments using model colloid Primal E1743, a 200 ml colloid suspension was prepared. The concentration of the suspension was so prepared that it gave an absorbance of about 1.0 on the spectrophotometer (approximately 6.25 micro-litres of Primal E1743 in 200 ml of distilled water). Prior calibration of the spectrophotometer with this suspension revealed that absorbance is linear with concentration up to concentration of 40 micro-litres/litre of distilled water ($\cong$ 20 mg/l).

3.2.2 Highly porous Amberlite IRA 938 resin

Most experiments carried out in this work involved the adsorption of model colloid Primal E1743 to the commercially available, highly porous, strong anion resin Amberlite IRA 938 manufactured